Journal of Energy Storage 94 (2024) 112401

Contents lists available at ScienceDirect

Journal of Energy Storage

journal homepage: www.elsevier.com/locate/est

Review article

Recent advancements in applications of encapsulated phase change materials for solar energy systems: A state of the art review

Shahin Shoeibi [a], Furqan Jamil [b], Seyed Masoud Parsa [c], Sadaf Mehdi [d], Hadi Kargarsharifabad [e], Seyed Ali Agha Mirjalily [f,*], Wenshan Guo [c], Huu Hao Ngo [c], Bing-Jie Ni [h], Mehdi Khiadani [b,g,*]

[a] Energy and Sustainable Development Research Center, Semnan Branch, Islamic Azad University, Semnan, Iran
[b] School of Engineering, Edith Cowan University, 270 Joondalup Drive, Joondalup, Perth, WA 6027, Australia
[c] Centre for Technology in Water and Wastewater, School of Civil and Environmental Engineering, University of Technology Sydney, NSW, 2007, Australia
[d] School of Mechanical Engineering, Purdue University, West Lafayette, IN 47907, USA
[e] Production and Recycling of Materials and Energy Research Center, Qom Branch, Islamic Azad University, Qom, Iran
[f] Department of Mechanical Engineering, Yazd Branch, Islamic Azad University, Yazd, Iran
[g] Mineral Recovery Research Center (MRRC), School of Engineering, Edith Cowan University, Joondalup, Perth, WA 6027, Australia
[h] Water Research Centre, School of Civil and Environmental Engineering, The University New South Wales, Sydney, NSW 2052, Australia

ARTICLE INFO

Keywords:
Phase change material
Encapsulated PCM
Nano PCM
Solar applications
SDGs

ABSTRACT

In recent decades, solar energy systems have played an increasingly important role in human societies, including support of the supply of drinking water, hot water, and electricity in arid, semi-arid and remote communities. The most challenging aspects of solar energy systems are storing energy when it is available and using it when there is a high demand for energy without access to solar energy. Encapsulating phase change materials (PCMs) or nano enhanced PCMs can serve as thermal batteries for storing solar energy, whereby it is important to consider the energy characteristics of various encapsulation methods. This includes taking into account encapsulation materials, such as diameter, enthalpy, efficiency, and heat cycling times, in order to integrate them with solar energy systems. In the present paper, production process methods, characteristics and ingredients of encapsulation are reviewed, followed by evaluation of the effect of the composition of encapsulation PCMs on the performance of solar energy applications in in Middle East and North African countries, including photovoltaic/thermal, solar desalination, solar water heater, solar power plant, solar pond, solar thermochemical reactor, and others. Further, the effects of dispersing various nano powders in PCM (encapsulated nano-enhanced PCM) to increase the thermal properties of thermal batteries are reviewed. In addition, a summary of the economic analysis of thermal batteries and evaluating sustainable development goals of solar energy applications as integrated by encapsulated PCMs/nano-enhanced PCMs are conducted and discussed. We conclude by evaluating the trade-off, synergy, future perspectives, and recommendations of encapsulation PCM used in solar energy applications.

Nomenclature and abbreviations

Al_2O_3	Alumina
DSC	Differential scanning calorimetry
MWCNT	Multi wall carbon nanotubes
NPCM	Nano phase change material
PCM	Phase change material
PMMA	Polymethyl methacrylate
PV/T	Photovoltaic/Thermal
SiO_2	Silica
Zn	Zinc

1. Introduction

Owing to their enhanced storage capacity, PCMs are widely used in various applications including HVAC systems, power batteries and residential buildings [1,2] and solar energy application [3–5]. However, direct use of PCMs is hampered by several issues including leakage, erosion, and instability. These challenges can be addressed by encapsulating PCMs in separate shells, which can be of various shapes

* Corresponding authors.
E-mail addresses: SAA_mirjalily@iauyazd.ac.ir (S.A.A. Mirjalily), m.khiadani@ecu.edu.au (M. Khiadani).

https://doi.org/10.1016/j.est.2024.112401
Received 14 March 2024; Received in revised form 15 May 2024; Accepted 31 May 2024
Available online 8 June 2024

including cylindrical, rectangular, and spherical shapes. Encapsulation history dates back to the 19th century [6], whereby PCMs are typically enclosed in a protective material. In this process, PCMs are encapsulated in a way that there is an increase in surface area, which in turn increases heat transfer and also helps to make sure a PCM is not in contact with its surroundings, which is important is specific applications where there is a need for extra precaution, like in food storage and blood transport.

Mostafaeipour et al. [7] conducted a case study for usage of solar energy in desalination systems for arid areas. They carried out study in Yazd province of Iran which was suffering from drinking water. The research targeted was to prioritize capital of counties for desalinating and for this purpose, five existing water wells from each of nine counties were ranked. The maximum capacity of the desalination equipment was 50 m^3/h and to be feasible, equipment must operate at least 2 h a day. Cunha and Pontes [8] carried out a case study in Brazil region by incorporating the Multi-Effect Distillation with solar collectors, thermal energy storage system and a biodigester for power production. The TES system provided continuous source of energy using solar energy. The results concluded that thermal desalination unit was feasible with water sales price of US$ 4.95/m^3 having capacity of 72 m3/day. Esmaeilion et al. [9] proposed case study to check feasibility for desalination in arid and semi-arid regions of Iran by using renewable energy. Their study carried out solar, wind, geothermal, and wave energies in Iran. Results depicted that an average solar radiation in Iran was 15.3 kWh/m^2/days, which includes >2800 h of radiation per year in central regions. Moreover, wind, geothermal as well as wave energy potentials are equaled to 100 × 106 MW, 200 MW, and 20 kW/m, respectively. This could bring a great potential renewable energy source for these arid regions of Iran. Similarly, more case studies have been found in the literature [10–14] which supported solar energy systems for drinking water, hot water, and electricity purposes in arid, semi-arid, and remote communities.

The use of phase change material as an energy storage material has widely been used to improve the performance of solar energy applications. The phase change material can store the thermal energy of the sun and transfer it to the system when needed. The introduction of this paper is focused on encapsulated PCM production methods and solar energy application sections using phase change material.

2. Encapsulated PCM production process

2.1. Encapsulation based on their size

Depending on the capsule size, as indicated in Fig. 1, encapsulation can be macro size (when the capsule size is larger than 1 mm in diameter), micro size (when the capsule size is in between 1 μm −1000 μm) or nano size (when the capsule size is <1 μm) [15,16].

2.1.1. Macro-encapsulation PCM

Macro encapsulated PCM can be prepared in any shape and size according to its requirements. Further, it does not require any predefined process, as in the case of micro encapsulation, which requires various methods and techniques to encapsulate PCM. Additionally, several forms of macro encapsulation have been prepared by various industries, where the most effective ones are high-density polyethylene bottles, tin-plated metal cans and mild steel cans [17]. Various manufacturers have used containers for macro encapsulation of PCM as depicted in Table 1. During the preparation of macro encapsulated PCM, the expansion due to volume change should be considered as a change in volume of PCM that occurs during phase transition. This can result in void formation, which will affect heat transfer [18].

2.1.2. Micro-encapsulation PCM

Microencapsulation is a technique that is used to cover solid or liquid material from a surrounding environment by packaging in a micro-container. The covering material is known as the shell, while the material to be covered is referred as the core material. This technique was invented by Green and Schleicher in the 1950s [19], where they were able to encapsulate dyes by coacervation of gelatin and gum, which helped to make carbonless copying paper [20]. Nowadays, this technique is used in a wide range of areas including chemical, pharmaceutical, thermal, and cosmetic industries. As noted above, due to leakage at high temperatures and environmental concerns associated with PCMs, micro-encapsulation has been preferred as a solution, whereby encapsulating PCM direct contact means that environmental and leakage issues can be avoided. Furthermore, this technique also helps to increase heat transfer area and assist the core material to be resistive to volume changes during phase change [21]. Kawaguchi et al. [22] have developed a microencapsulated PCM of Zn-Al alloy with a core of 30 % Zn by mass using microencapsulation. They obtained a phase change temperature of 437–512 °C and latent heat of 117Jg^{-1}. In another study, Kawaguchi et al. [16] prepared a mid to high range PCM by microencapsulation, adding $Al\,(OH)_3$ during solution treatment, whereby they found that PCM with 1.7 g L^{-1} of $Al\,(OH)_3$ exhibited a remarkable heat storage density of 0.48GJm^{-3} and cyclic durability of over 100 cycles. They attributed this enhancement due to the addition of $Al\,(OH)_3$. Yuto et al. [23] developed an Al-Ni based PCM having Al-5 % by weight using microencapsulation, whereby their PCM had a core of Al-Ni alloy and a

Table 1
Various manufacturers of macro encapsulation of PCM [17].

Company	Country	Type of container
Microtek Laboratories, Inc.	USA	Polymers
Rubitherm Technologies	Germany	Aluminum panels, polymer bags, pouches
Shanghai Tempered Entropy New Energy Co.	China	Polymers, aluminum tube, plastic blocks, flexible films
Teappcm	USA	Stainless steel balls, HDPE panels, aluminum panels
Winco Technologies	France	Breather membrane

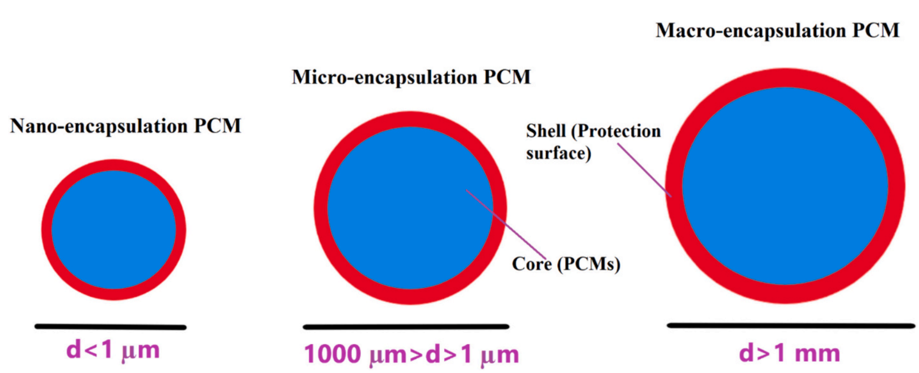

Fig. 1. The various size of encapsulation PCM.

shell of α-Al_2O_3. Their proposed PCM was able to remain in shape even after 100 cycles of melting and solidification. To address corrosion issues of PCMs, Sakai et al. [24] have developed a microencapsulated PCM with 25 %w Al-Si as a core and a shell of Al_2O_3. They were able to obtain a heat storage temperature of 577 °C and a heat capacity of 108-122Jg^{-1}. He et al. [25] have further investigated microencapsulated PCM with a core of 12.06 % by weight Al-Si and Al_2O_3 as a shell using sol-gel method. They found that the prepared PCM could only sustain 20 thermal cycles. Li et al. [26] developed a PCM using microencapsulation by catalytic oxidation with Ni nanoparticles as a catalyst. The authors prepared PCM had a shell of Al_2O_3 and a core of *Al*. They found that prepared PCM was able to sustain approximately 50 cycles. Sun et al. [27] have investigated the thermal stability of an Al-34 %-Mg-6%Zn alloy. Through differential scanning calorimeter testing, they noted an approximate 11 % decrease in latent heat of fusion after 1000 thermal cycles. Overall, PCM was found to have good thermal stability and phase transition range. Sari et al. [28] have used emulsion polymerization to prepare a microencapsulated PCM (polymethylmetracrylate) with 43 % by weight n-octacosane as a core material and shell of PMMA. They investigated the morphology and thermal stability of the PCM using SEM and differential scanning calorimetry (DSC), respectively. The measured melting point and laten heat of fusion of the PCM were 50.6 °C and 88.5 J/g, respectively. Furthermore, in 5000 thermal cycles no significant change in temperature or enthalpy was observed, confirming that microcapsules of octacosane can be a potential candidate for energy storage applications. Yang et al. [29] used in situ polymerization to prepare a PCM microcapsule slurry with polystyrene, polymethyl methacrylate and polyethyl methacrylate as encapsulation materials, respectively. They measured thermal and physical properties using DSC and investigated the impact of tetradecane concentration on latent heat and phase change temperature. Some of the microencapsulated PCMs investigated for various applications are listed in Table 1. Accordingly, it can be seen that the highest heat of fusion belonged to Octadecane microencapsulation.

2.1.3. Nano-encapsulation PCM

Rapid advancements have occurred in the development of nano-sized-optimal structures, whereby this is no longer a problem in the manufacturing industry. In this way, many researchers have sought to develop nanosized PCMs with the help of nanomaterials and advanced manufacturing, in order to address issues of low thermal conductivity of PCMs and to augment heat transfer [33]. For instance Fang et al. [34] have developed nano-sized PCM of n-tetradecane(size ~100 nm) as a core material, with urea-formaldehyde as a shell using in-situ polymerization. The authors concluded that prepared PCMs can be used for numerous energy storage applications. In another study, Qiu et al. [35] have prepared nano-encapsulated PCM by suspension-like polymerization, with 75.3 % by weight n-octadecane as a core material and methyl-methyl-acrylate(MMA) as a shell. These authors investigated thermal and structural changes with the help of DSC, thermalgravimetric analysis and hardness testing, showing that a sample with pentaerythritol tetra-acrylate as a crosslinking agent showed the highest latent heats of melting (156.4 J/g) and crystallization (182.8 J/g), as well as the highest mechanical strength as compared to the other samples.

Hu et al. [36] have prepared a nano-encapsulated PCM by using in-situ polymerization, using paraffin as a core material and carboxymethyl cellulose as a shell material. They reported a maximum phase change enthalpy of 83.46 J/g at a paraffin ratio of 63 % by weight. Park et al. [37] have prepared nano-encapsulated PCM of Mag-PCM with paraffin as a core and polyurea as a shell material. In another study, Fang et al. [38] have prepared nano-encapsulated PCMs with n-Tetradecane as a core material using in-situ polymerization for cold applications. The nano-sized PCM was able to withstand 40 freezing-thaw cycles. Their results also showed that prepared PCMs can be used for cold thermal applications. Latibari et al. [39] have prepared nano-capsules with Palmitic acid as a core and SiO_2 as a shell material using sol-gel technique, reporting their PCMs as able to withstand at least 2500 melting/freezing cycles. Their study concluded that prepared PCM has a significant potential for energy storage owing to better thermal and chemical properties. Chen et al. [40] have synthesized nano-capsules with n-dodecanol as a core and polymethyl methacrylate (PMMA) as a shell using mini-emulsion polymerization. They used DNS-86 and hexadecane as emulsifier and *co*-emulsifier respectively and investigated the effects of polymerizable emulsifiers and co-emulsifiers on PCM performance. They noted that co-emulsifiers have a significant impact on the properties of PCM. PCM with optimum performance was obtained when the mass ratio between hexadecane to n-dodecanol was 2 %. The highest noted value of latent heat was 98.8 J/g at the corresponding encapsulation efficiency of 82 %. They concluded that nano-capsules of approximately 150 nm diameter can be a good candidate for energy storage applications. In another study, Chen et al. [41] prepared nano-capsules with n-dodecanol as a core material and styrene-butyl acrylate copolymer as a shell material using mini-emulsion polymerization. They reported a maximum phase change enthalpy and phase change temperature of 109.2 J/g and 18.4 °C, respectively. Sari et al. [42] have prepared a nano-encapsulated PCM having n-Heptadecane as a core and polystyrene as a shell material using emulsion polymerization, whereby using DSC analysis they reported that the best performing PCM had a 63.3 wt% concentration of n-heptadecane. Their measured values of melting temperature and latent heat were 21.48 °C and 136.89 J/g, respectively.

Results have shown that prepared PCMs can be used in various sectors like for solar thermal, building, and medical sectors. Tumirah et al. [43] have prepared nano-encapsulated PCMs with n-Octadecane as a core material using the in-situ polymerization method. Through DSC analysis they measured an enthalpy of 107.9 J/g and melting temperature of 29.5 °C. They reported that nano-capsules were able to withstand 360 thermal cycles, which indicates that prepared PCM has good mechanical and thermal stability. They concluded that prepared PCM can be a good candidate for building other energy storage applications. Applying the direct mini-emulsion method, Zhang et al. [44] developed a nano-capsule with a core of n-octadecane and a shell of poly ethyl methacrylate (PEMA) and poly methyl methacrylate (PMMA). Nan et al. [45] have prepared a nanosized capsuled PCM having n-octadecane as a core material and PMMA as a shell material with allyl methacrylate as a *co*-polymer using in-situ polymerization. They also investigated structural and thermal properties using SEM, thermogravimetric (TGA) and DSC analysis. The results showed that nano-capsules have a stable performance and can be a competitive option for energy storage applications. Fang et al. [34] have proposed nano-capsules prepared by in-situ polymerization having n-Tetradecane as a core and urea/formaldehyde as a shell material. They obtained the best performance when the concentration of n-tetradecane was 60 % by weight. They also found that the addition of NaCl was also helpful in improving the stability of the nano-capsules. In another study, Fang et al. [46] synthesized nano-encapsulated PCM having n-Dotriacontane as a core material using mini-emulsion polymerization with an average size of 168.2 nm. They characterized the structural, thermal, and chemical performance of PCMs using transmission electron microscope, X-ray diffractometer, differential scanning calorimetry and thermogravimetric analysis. Table 2 illustrates the different studies on nano-encapsulated PCM. Their results showed that the highest phase change enthalpy of nano-encapsulated PCM belonged to n-Octadecane, which was approximately 198.5 J/g (Table 3).

2.2. Various encapsulation methods of PCM

The encapsulation methods to prepare the encapsulated PCM can be broadly classified into three major categories i.e., physical, chemical and hybrid as shown in Fig. 2. Depending on the material, various encapsulation methods can be selected using a wide range of PCM with less cost and in a shorter time.

Table 2
List of PCMs investigated for microencapsulation.

Authors	PCM	Heat of fusion (kJ/kg)	Transition point (°C)
Peippo et al. [30]	Stearic	196	64.5
Peippo et al. [30]	Capric	158	30.1
Peippo et al. [30]	Lauric-myristic	132.6	32.6
Peippo et al. [30]	Myristic-stearic	181	44
Peippo et al. [30]	Capric–stearate 86.6/13.4	160	26.8
Peippo et al. [30]	Capric–lauric 61.5/38.5	132	19.1
Koschenz and Lehmann [31]	Black paraffin	150	25–30
Koschenz and Lehmann [31]	Heptadecane	214	18
Koschenz and Lehmann [31]	Octadecane	244	22
Feldman and Banu [32]	Propyl palmitate	186	19

Table 3
List of a few studies on nano-encapsulated PCMs reported in literature.

Authors	PCM (core material)	Phase change enthalpy (J/g)	Transition point (°C)
Hu et al. [36]	Paraffin	83.46	29.2
Park et al. [37]	Paraffin	101	56
Fang et al. [38]	n-Tetradecane	98.71	4.04
Latibari et al. [39]	Palmitic Acid	180	60
Chen et al. [40]	n-dodecanol	98.8	18.2
Chen et al. [41]	n-dodecanol	109.2	18.4
Sari et al. [42]	n-Heptadecane	136.89	21.48
Tumirah et al. [43]	n-Octadecane	107.9	29.5
Zhang et al. [44]	n-Octadecane	198.5	32.7
Fang et al. [34]	n-Tetradecane	134	9
Fang et al. [46]	n-Dotriacontane	174.8	70.9

2.2.1. Hybrid encapsulation

The hybrid encapsulation processes are presented in the following sections:

2.2.1.1. Pan coating. This is one of the oldest methods, widely used in the pharmaceutical industry to make tablets. In this process, coating material is mixed with solid particles and then after heating, the coating material melts and covers the core material when the pan is rotated at high speed. Later, fully formed capsules are obtained by cooling. In another way, the core material can also be kept tumbling in a pan after which the coating material is sprayed on. This pan is usually made of stainless steel. This is a relatively simple and inexpensive process that can produce uniform and consistent coating. The process of pan coating is shown in Fig. 3.

2.2.1.2. Spray drying. In spray drying, PCM is dispersed as a fine spray in a stream of hot air that evaporates the solvent and leaves behind a solid powdered PCM encapsulated in a coating. The resulting particles are usually spherical in shape and have a porous structure, which helps to improve the stability and performance of the PCM. The coating material forms a thin layer around the PCM particles, and the solvent then becomes evaporated. In a study reported by Hawlader et al. [21], microencapsulated PCM with paraffin-wax using coacervation and spray-drying was assessed. The authors evaluated the thermal and structural performance of PCM using DSC and SEM. DSC confirmed that the storage/release capacity of the prepared encapsulated PCM to be between 145 and 240 J/g regardless of the preparation methods i.e., coacervation or spray-drying. They concluded that paraffin wax can be a good option for energy storage material. The process of spray drying is shown in Fig. 4.

2.2.1.3. Solvent evaporation. In this process the core is mixed in a solution of the shell material and later on is heated to evaporate the solvent and form a film of shell material around the core. There are several factors that affect the efficiency of this, including: coating material, vapor pressure of the solvent, rate of evaporation, properties of the coating material and properties of the shell material. The process diagram of the solvent evaporation process is shown in Fig. 5.

2.2.1.4. Centrifugal extrusion. Centrifugal extrusion was first introduced by Southwest Research Institute (SwRI) [48]. In the process, liquid of both core and shell material are used, whereby the core material runs through the inner tube while running through the outer tube, as illustrated in Fig. 6. Later, via vibration both liquids are pumped to the orifice, where spherical droplets are formed. After this process, these droplets are solidified in a bath. This generally produces capsules of a diameter between 250 μm to a few millimeters. Numerous extrusion nozzles have been used to enhance the system performance of centrifugal extraction [49].

2.2.1.5. Air suspension coating. In this technique, solid particles of core material are coated by suspending them in the air with the coating solution, where this is mostly used in pharmaceutical and food industries [50]. This process is more flexible and provides better control compared to other techniques like pan coating. The process of encapsulation using air suspension is shown below in Fig. 7.

2.2.2. Chemical encapsulation

A few of the most widely used chemical encapsulation methods are discussed below.

2.2.2.1. Interfacial polymerization. This is a widely used process to prepare micro-polymers, composites and nanomembranes. One of the first membranes prepared by interfacial polymerization was first developed by Cadotte et al. [51], whereby this has also been applied in reverse osmosis applications [52]. During interfacial polymerization, an emulsifier is mixed in water and the core is mixed with the oil. Following this, another hydrophilic monomer is added to the oil-water solution, which results in a change in temperature and pH. Later, the polymerization process was begun and then the prepared capsules were separated using various techniques like filtration and others. Cho et al. [53] were among the first to prepare microcapsules of PCMs with octadecane as a core material using interfacial polymerization. In their study, the diameter of the prepared capsule was around 1 μm. During polymerization, they used diethylenetriamine (DETA) and toluene-2,4-diisocyanate (TDI) as a monomer, both of which are soluble in water and oil, respectively. In another study by Lan et al. [54], microcapsules of PCM with n-eicosane as a core material were successfully prepared using interfacial polymerization with an encapsulation efficiency of 75 %. They used the same monomers as reported by Cho et al. [53]. Through thermogram analysis, Lan et al. found that prepared PCM can withstand temperatures up to 170 °C. In another study, Salaun et al. [55] prepared microencapsulated PCM using interfacial polymerization and systematically investigated the influence of various parameters, like stirring rate and feeding weight ratio of core/shell, on encapsulation. They showed that there is a significant impact of the weight of core/shell on the structure of the microcapsule and on encapsulation efficiency. By analyzing the impact of various parameters, they were able to obtain the optimal conditions. Yang et al. [56] prepared a microcapsule using interfacial polymerization, using lauric acid and silica as a core and shell material, respectively. Further, they added tetraethoxysilane to assist in forming mini-emulsion, where HCL was used as a catalyst to start polymerization. They examined the effect of various parameters on the

Fig. 2. The classification methods for preparation of encapsulated PCM.

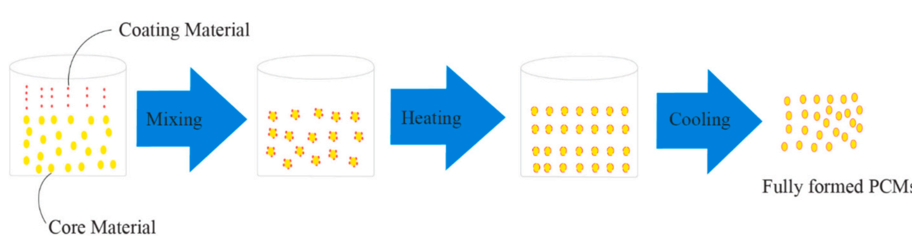

Fig. 3. Pan coating [47].

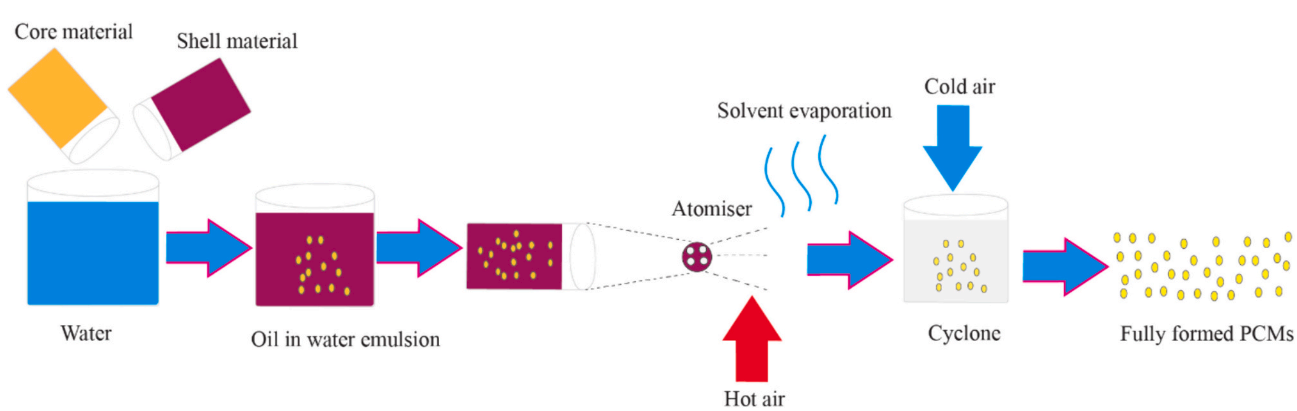

Fig. 4. Spray drying [47].

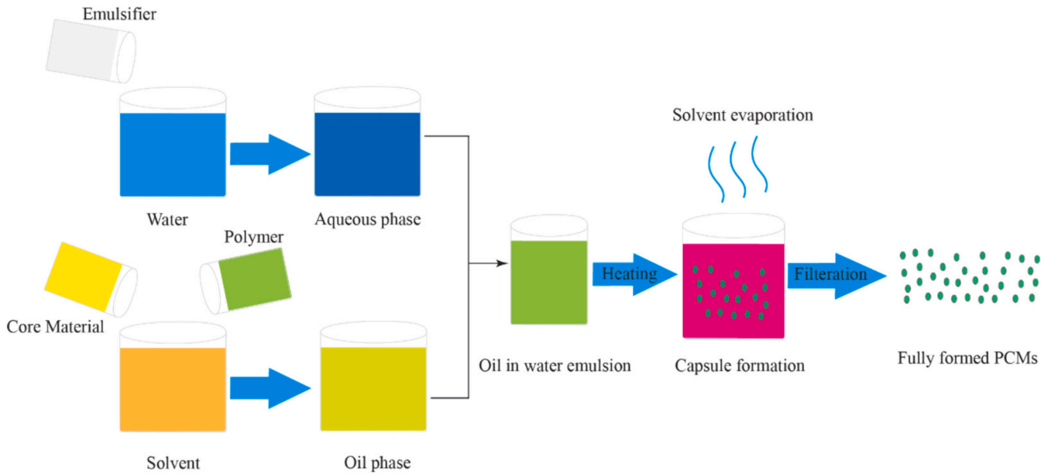

Fig. 5. Solvent evaporation [47].

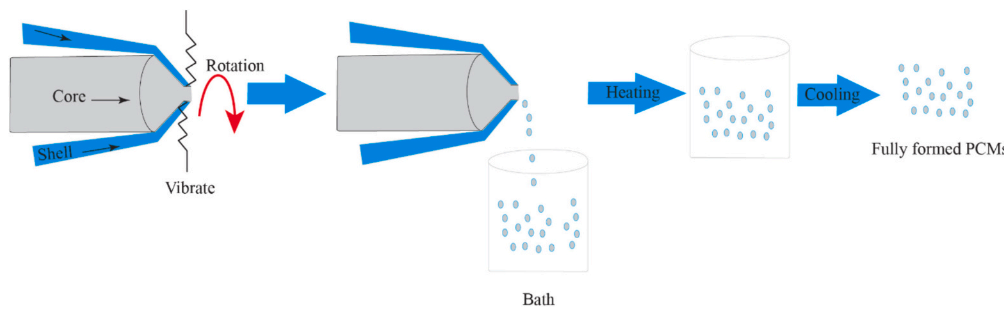

Fig. 6. Centrifugal extrusion process to made an encapsulation PCM [47].

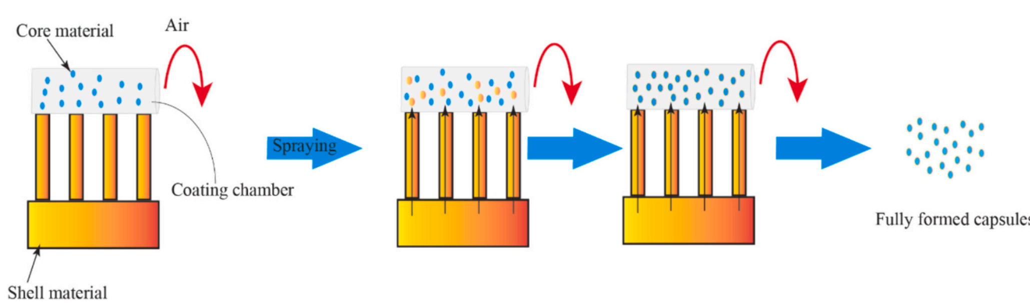

Fig. 7. Air suspension coating techniques used to produce the encapsulation PCM [47].

thermal performance of PCMs, whereby the prepared PCM exhibited a melting latent heat of 186.6 J/g and outstanding thermal stability at 60 °C under optimal operational conditions. Wang et al. [57] prepared a bifunctional micro-PCM having n-octadecane and thyme oil as a dual-core material and polyurea as a shell material through interfacial polymerization. They indicated that prepared capsules had a regular spherical shape, good structural strength, and high thermal capacity. Recently, Cai et al. [58] prepared a micro-PCM with dodecanol dodecanoate as a core and polyurea as a shell material, using interfacial polymerization but with no solvent required during polymerization. Their microcapsules had a diameter of approximately 10-40 μm. The prepared PCMs showed a latent heat of approximately 103.4–140.3 J/g and thermal stability until 234 °C. A typical flow diagram for the interfacial polymerization is shown in Fig. 8.

2.2.2.2. In-situ polymerization. This is one of the most commonly used methods because of its simplicity and the availability of mature technology. During in-situ polymerization, polymerization occurs on the surface, where there is no chemical reaction at the interface, and no need for monomers. In the process, firstly the core material is mixed in the oil and aqueous solution, with an emulsifier and aqueous solution of shell material that could be a monomer. Later, by decreasing the pH, the polymerization process begins, and the prepared capsules can be separated by filtration. Many researchers have widely investigated the development of micro/nano encapsulated PCMs. Wang et al. [59] prepared a microencapsulated PCM using in situ polymerization, using n-octadecane as a core and a poly (melamine-formaldehyde)/silicon carbide shell. Fan et al. [60] developed a microencapsulated PCM(roughly 1 μm diameter) of n-octadecane using in-situ polymerization. In another study, Fang et al. [34] developed nano-sized PCM of n-tetradecane (size ~100 nm) as a core material and urea-formaldehyde as a shell using in-situ polymerization. They concluded that the prepared PCMs can be used for numerous energy storage applications. A flow diagram of the in-situ polymerization is shown in Fig. 9.

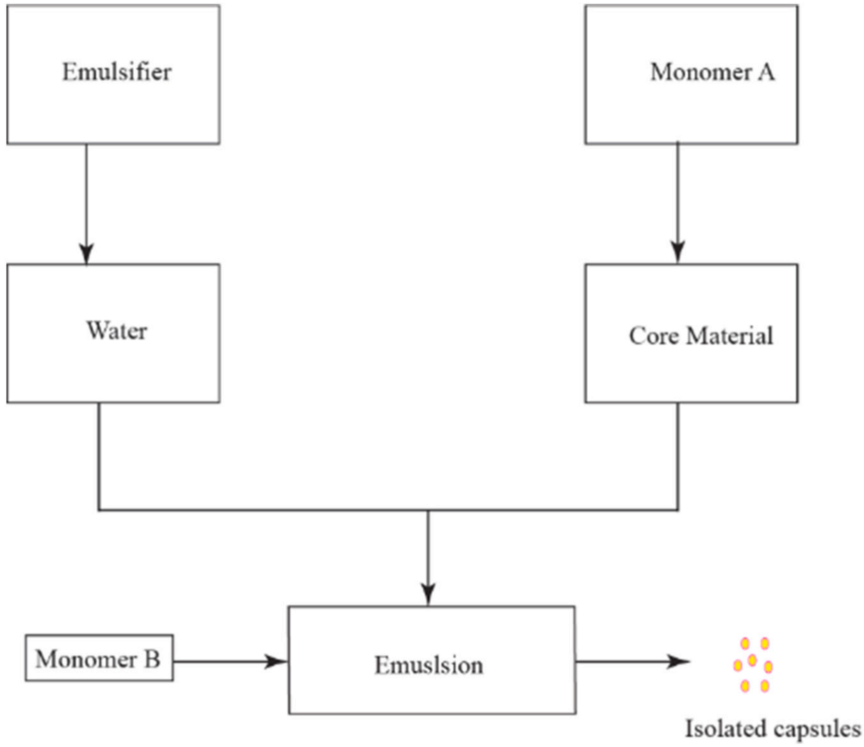

Fig. 8. Flow diagram of interfacial polymerization [47].

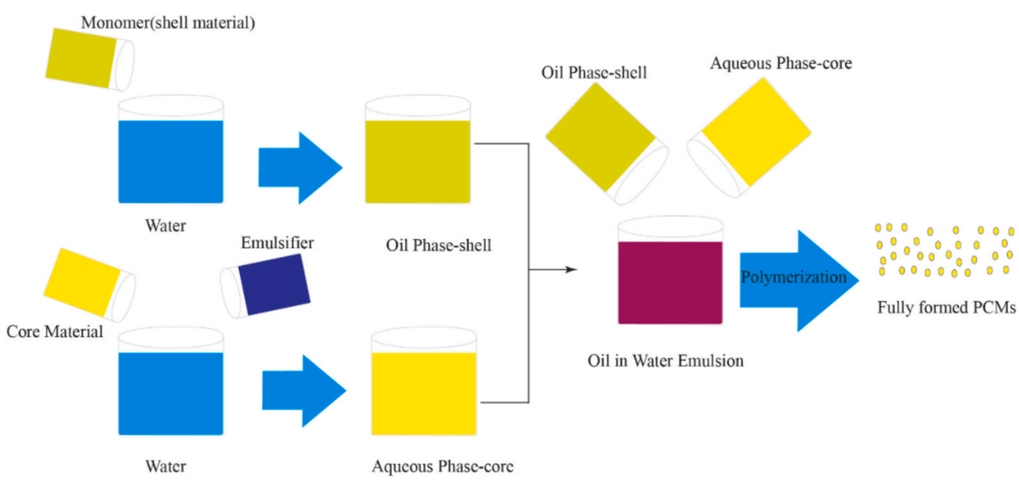

Fig. 9. Process of in-situ polymerization [47].

2.2.2.3. Suspension polymerization. In this process, firstly the core material is mixed with a monomer that has oil soluble initiators, and an emulsifier is mixed with water. Later, both solutions are mixed to form an oil-in-water emulsion. After this, the monomer gets separated and solid capsules are formed. The shape and size of the molecule depend on the monomer type and the interaction between monomers, stirring speed, suspension agent and polymers. This process is one of the widely used methods for encapsulation of PCMs. As an example of this, Sanchez et al. [61] prepared microcapsules of Repsol-YPF paraffin wax/styrene using suspension polymerization, studying the influence of various parameters on the storage capacity of the shape and microcapsules of PCM. They noted that the ratio of polyvinylpyrrolidone and styrene was the most influential parameter impacting the size of PCM capsules. They also noted that the storage capacity of the capsules increased with a corresponding increase in the ratio of Repsol-YPF paraffin wax/styrene. At optimal conditions, the PCM showed a latent heat of 102.42 J/g. The process of suspension polymerization is shown below in Fig. 10.

2.2.2.4. Emulsion polymerization. In emulsion polymerization, a monomer with a solvent is dispersed in a container with emulsifier and surfactants. Later, an initiator is added, resulting in the formation of a polymer membrane on the core material [62]. Many researchers investigated paraffins as a core and PMMA as a shell material in preparing encapsulated PCMs using emulsion polymerization [63]. Cho et al. [64] prepared a nano-capsule of n-octadecane with PS as a shell using emulsion polymerization, using styrene-*co*-acrylic acid as a surfactant and DVB as a crosslinking agent. Through dynamic light scattering, they found that the prepared PCM capsules had an average diameter of 280 nm and showed heat capacity of 110 J/g, as measured by DSC analysis. Sari et al. [65] prepared a microcapsule of n-heptadecane with a shell of

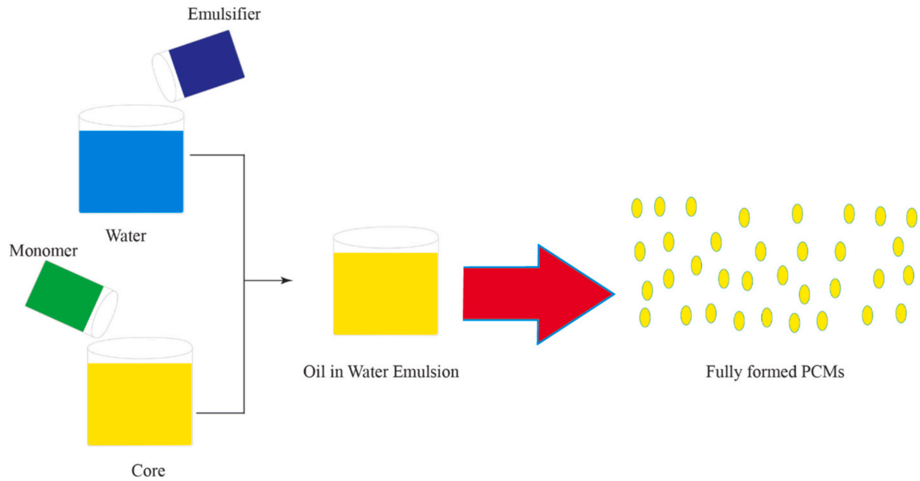

Fig. 10. Suspension polymerization [47].

Polymethylmethacrylate (PMMA) using emulsion polymerization. The average measured diameters of their PCMs were between 0.14 and 0.40 μm, when the stirring speed was 2000 rpm. These authors also reported that PCMs were able to maintain good thermal properties up to 5000 thermal cycles. They concluded that a PMMA/heptadecane microcapsule can be a competitive option for energy storage applications. Fortuniak et al. [66] fabricated microcapsules of n-eicosane having polyhydro-methylsiloxane as a shell using emulsion polymerization, using 1, 2-divinyltetramethyl disiloxane as a crosslinking agent. The process of emulsion polymerization is shown below in Fig. 11.

2.2.3. Physical encapsulation

Physical encapsulation involves the preparation of PCM without using any chemical reaction. This method is used when the encapsulated material is sensitive to chemical reactions or when it needs to retain its original properties. A few of those methods employing physical techniques are discussed below.

2.2.3.1. Coacervation. Coacervation was the first process to be used for encapsulation at an industrial scale. This process was initially defined by Bungenberg de Jong and Kruyt [67]. In this process, a homogeneous polymer is mixed with a polymer-rich phase and a coacervation medium. This process can be either simple or complex depending on how the phase separation is done, where for instance, in simple coacervation, a dissolving agent is used, while complex coacervation uses two oppositely charged polymers. Yin and Stover [68] prepared microcapsules using styrene-*alt*-maleic anhydride grafted with methoxy poly(ethylene glycol) (SMA-g-MPEG), where the styrene-*alt*-maleic anhydridewas reacted with the MPEG lithium alcoholate, resulting in the formation of complex coacervate of SMA-g-MPEG and poly diallyldimethylammonium chloride. They used chitosan and polyethylenimine as a cross-linking agent. Coacervate microspheres swell due to the interruption of electrostatic associations of complexed polyelectrolytes with the addition of salts. In another study, Huang et al. [69] prepared microcapsules of gelation and gelatin gum using coacervation, investigating the number of factors influencing encapsulation, for instance, the impact of surfactant concentration, gelatin and crosslinking agent. They noted that glycerol was a suitable crosslinking agent for a pH of 4 but did not work well for pH above 7. Their findings showed that microcapsules with shikonin can be successfully prepared using gelatin/acacia as a crosslinking agent. Uddin et al. [70] prepared a microencapsulated PCM of paraffin using the coacervation technique, evaluating its structural and thermal performance using SEM, FTIR and DSC. They obtained a plausible storage and release capacity of 56–58 J/g, whereby no significant change in structure was observed even after 1000 thermal cycles. Ozonur et al. [71] prepared a microcapsule (diameter around 1 mm) of coco fatty acid for thermal storage applications using the coacervation technique, evaluating PCMs according to morphology, thermal and chemical stability. They noted that samples were able to maintain their profiles even after the 50 thermal cycles, while the measured melting and freezing temperature were in the range of 22 to 348 °C. The process of coacervation is shown below in Fig. 12.

2.2.3.2. Ionic gelation. This is one of the widely used methods of

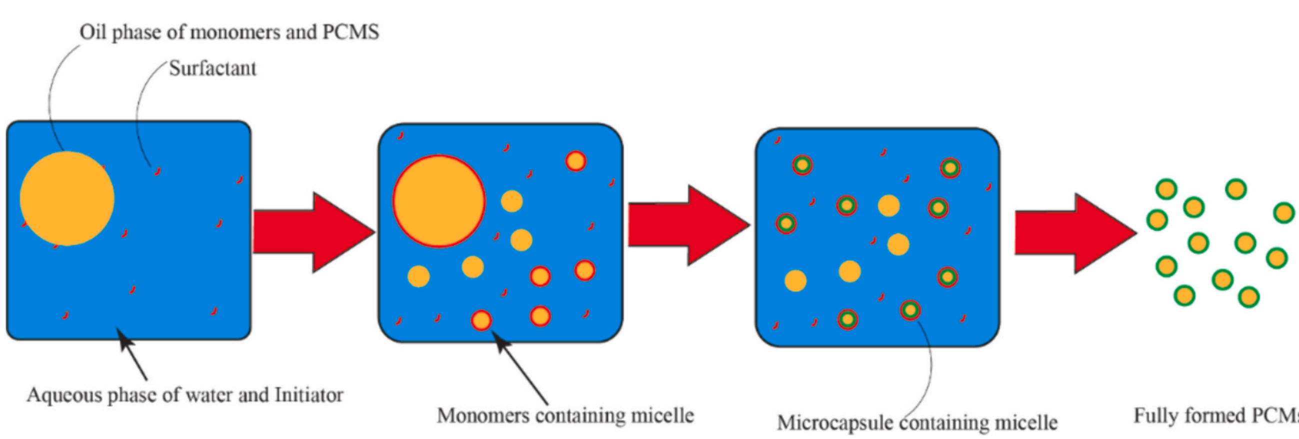

Fig. 11. Schematic of emulsion polymerization [47].

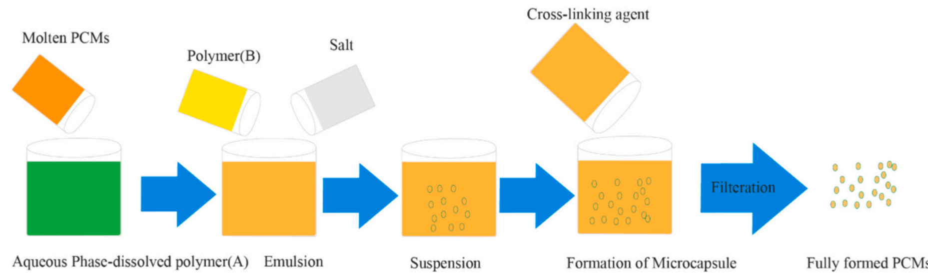

Fig. 12. Coacervation process to produce encapsulation-PCM [47].

encapsulation in the pharmaceutical industry. In this method, polyelectrolytes are used as a crosslinking agent to form hydrogels [72]. The process of ionic gelation is shown in Fig. 13.

2.2.3.3. Solution gelling (sol-gel). This method is commonly used to prepare PCMs having inorganic shell material, whereby this is a relatively cheap and simple process. In this process, at first alkoxides and inorganic precursors are mixed with the solvent and complex agent. As a result, a colloidal solution is formed due to polycondensation, which is later converted into gel. Later, this gel can be used to make 3D structures and then encapsulated PCMs are formed after sintering and drying [73]. One of the first studies on encapsulation using sol-gel method has been reported by Wang et al. [74], using silica as the shell and n-pentadecane as a core material. They investigated the impact of pH and emulsifiers on PCM morphology, showing that surfactants like cetyltrimethylammonium chloride and dodecyltrimethyl-ammonium chloride can be used for the formation of the silica shell. They further investigated charge-controlled and reaction rates-controlled mechanisms for the shell formation and showed that shell formation was due to coulombic interaction and reaction rate mechanisms influencing the cationic emulsifiers. In another study, Fang et al. [75] attempted to encapsulate paraffin in the silica shell using sol-gel method, examining thermal properties through DSC and TGA analyzers. The DSC showed that prepared PCM has a melting point of 58.37 °C and latent heat of 165.68 KJ/Kg when the paraffin was 87.5 % by weight. Moreover, through SEM it was also shown that the prepared capsule had a good structural formation. The process of sol-gel is shown below in Fig. 14.

2.2.4. Conventional preparation of encapsulation PCM

The encapsulated PCM assists to dominate various issues including flammability, sub-cooling, low thermal conductivity, and phase separation. This makes it better for producing encapsulation PCMs using physical, chemical and hybrid encapsulation methods. Some researcher have assisted generation of the encapsulation method using a core (phase change material) and shell (constructed conventionally) [76]. The shell can be produced in various geometries including cylindrical, annular [77] and spherical shapes, and with different materials such as copper, aluminum and other materials depending on their operating temperature. The conventional preparation of encapsulation coupled with solar energy applications can have a significant impact on the improvement of a system's performance.

2.3. Materials for encapsulation

It has been indicated that the thermal conductivity of materials has a significant impact on sealing effectiveness and on the heat transfer between PCM and working fluid. Owing to this, a wide range of materials, including organic, inorganic and hybrid, have been investigated during the encapsulation of PCMs to form a micro/nano capsule. Several combinations of materials have been investigated by many researchers as a core and shall material, whereby a few of these combinations are listed in Table 4.

2.4. Overview of solar energy application by PCM/nano-enhanced PCM

The use of PCM and nano-enhanced PCMs (NPCM) enhance the performance of solar energy systems [108–110]. The high value of thermal energy of solar energy systems can be received by PCM/NPCM when the appeal is less than the needed energy, after which it can be removed from the system as necessary. It could be obtained that the thermal characteristics of nano-enhanced PCM do not reduce even after 300 heat cycles [111,112]. Khalilmoghadam et al. [113] examined the influence of PCM and PHP on the generated freshwater of solar still, where the phase change material was considered to maintain the high temperature of the water and to increase the distillation rate. In this way, a pulsating heat pipe transferred the thermal energy to the phase change material. The findings elucidated that the produced freshwater of the system using PCM was equal to 6.3 L/m^2.day. Kabeel et al. [114] investigated the effect of film glass cooling and PCM on the performance of solar systems. The PV/T was considered as an absorber sheet and the PCM was located below a surface panel to reduce its surface temperature. The results elucidated that the generated water of the system was raised by 36.25 % using fully open valves. Kabeel et al. [115] conducted the efficiency of the tubular solar still by PCM. The copper tubes were utilized to maintain the PCM and were located in the water. The authors noted that productivity was improved by about 115.1 % using PCM. Hafs et al. [116] theoretically developed solar stills using phase change material, using rectangular, triangular and spherical shapes of absorber surfaces. They reported that the freshwater yield of the device with a rectangular shape increased by 109 % and 42 %, respectively, compared

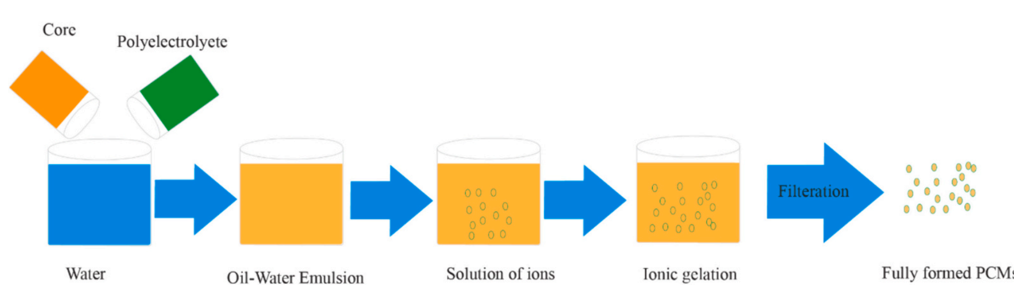

Fig. 13. Ionic gelation process to generate encapsulation PCM [47].

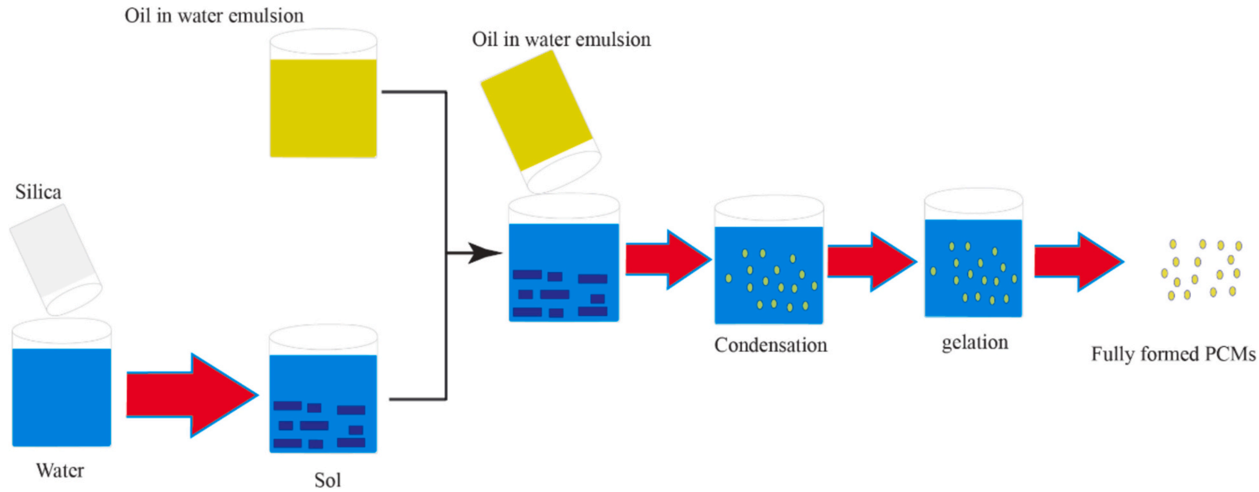

Fig. 14. Sketch of sol-gel process [47].

to conventional and flat shapes with PCM. The assessment of the efficiency of mixing Al_2O_3 nanopowders with PCM in solar desalination was examined by Rajasekhar et al. [117], reporting that the efficiency of the application by NPCM and PCM was apprxoimately 45 % and 40 %, respectively. Yousef and Hassan [118] evaluated the cost analysis of solar desalination with and without PCM, with findings showing that EPBT of the modified system was ineffectual. Ho et al. [119] examined two double-slope solar still using various aspect ratios by Fresnel lens and PCM, reporting the thermal efficiency of the device with Fresnel lens and device with PCM were approximately 37 % and 32 %, respectively.

The phase change material and nano-enhanced PCM have been implemented to decrease the surface temperature of solar panels. *Al-*Waeli et al. [120] increased the electrical efficiency of the photovoltaic/thermal system using cooling techniques. They depicted that the ampere of the solar panel by NPCM and nanofluids was raised from 3.69 A to 4.04 A, in addition to the energy efficiency being varied from 8.07 % to 13.32 %. Jamil et al. [121] performed the influence of cool the solar panel with PCM and NPCM on the power production of the system. The MWCNT, graphene nanoplatelets, and MgO at a volume fraction of 0.25 wt% and 0.5 wt% were implemented to mix in the paraffin wax for generating the NPCM. The findings indicated that the maximum electrical efficiency belonged to graphene/paraffin NPCM at a concentration of 0.5 wt%, which was improved by 33.07 %. In another research study, Al-Waeli et al. [122] combined PV/T with NPCM to increase the electrical performance of a system, where SiC/water nanofluid flowed under the solar panel to decrease PV surface temperature. Their outcomes showed that the maximum energy efficiency of the application by NPCM and nanofluids was 13.7 %. Akshayveer et al. [123] utilized the PCM on increasing the power generation of PV module. Their findings showed that the energy efficiency of a solar panel by PCM and PCM-natural convection were 14.12 % and 19.75 %, respectively. Ahmadi et al. [124] evaluated different types of PV/T modules, reporting that the surface temperature of solar panel with PCM was decreased by 6.8 % and the efficiency of the system improvement by 14 %. Yang et al. [125] improved the energy efficiency of the solar panel with PCM, with results indicating that thermal and electrical efficiencies of solar panel with PCM were 69.84 % and 8.16 %, respectively. Lari and Sahin [126] investigated the impacts of nanofluid and PCM on hot water storage tanks integrated by solar panels, revealing revealed that the thermal and electrical loads of application with PCM can be improved by 27.3 % and 77 %, respectively.

The use of phase change material in solar water can improve the storage of the thermal energy of the sun during the daytime and release it when domestic hot water is needed during the night. Mahfuz et al. [127] investigated the efficiency of solar water heaters with a heat storage media and PCM, findings indicating that the thermal efficiency of the system using flow rates of 0.033 L/min and 0.167 L/min of operating fluid was approximately 63.88 % and 77.41 %, respectively. Tarhan et al. [128] examined the effects of PCM on the performance of the solar water heater, with their outcomes presenting that the thermal characteristic and shape of PCM storage reservoir can favorably control increases and decreases of water temperature during day and night. Kumar and Mylsamy [129] improved the performance of the solar water heater using NPCM, with results showing that the energy efficiency of their applications using NPCM and PCM were approximately 24.6 % and 22 %, respectively. Manirathnam et a. [130] reviewed the impact of NPCM on the efficiency of the solar water heater, whereby the thermal efficiency of application using NPCM and PCM were increased by 13.31 % and 23.37 %, respectively. Algarni et al. [131] examined the influence of the NPCM integrated by ETSC on the performance of solar water heater, with outcomes illustrating the energy efficiency of the application using NPCM to be enhanced by 32 %.

Palanikumar et al. [132] examined the effects of NPCM and mirrors on the performance of the solar box cooker. Their addition of aluminum oxide nanopowders in PCM increased the thermal performance of the system, with results showing the energy efficiency of the conventional system and the system with NPCM were 45.14 % and 53.1 %, respectively. Jawad et al. [133] examined the influence of aluminum chips and NPCM on the efficiency of the solar air heaters, whereby SiC nanopowders were dispersed into the paraffin at a concentration of 3 wt% to boost the thermal characteristic of PCM. They reported that the temperature of the air outlet in the application remained for at least 3 h after sunset. Mehmet et al. [134] designed and experimented with a solar dryer integrated with PV and NPCM, whereby aluminum oxide/paraffin was implemented to increase the thermal performance of the system. Their findings presented that a moisture content of 17.4 g water/g dry matter achieved a final moisture content of 0.051 g water/g dry matter.

2.5. Motivation for performing the present research

The use of phase change materials can have a major impact on the efficiency of the various energy system [135,136]. Accordingly, the phase change material stores the thermal energy of the high-temperature applications and releases it into the system when it is required. The encapsulated PCM can act as a thermal battery to many different solar energy applications, as presented in Fig. 15. These applications include: PV/T [137,138], solar desalination [139–141], solar water heater [142], solar air heater [143], solar power plant, solar cooling systems and others, all of which store thermal energy when a solar source is available and then release it at the time it is needed. In

Table 4
Combination of core and shell materials investigated by various researchers.

Authors	Core material	Shell material
Cho et al. [53]	Octadecane	Polyurea
Lin and Yu [78]	Natural soy wax	Polyurea
Cai et al. [58]	Dodecanol dodecanoate	Polyurea
Liang et al. [79]	Butyl stearate	Polyurea
Zhang et al. [80]	N-octadecane	Inorganic Silica
Siddhan et al. [81]	N-octadecane	Polyurea
Shi et al. [82]	Paraffin	Methyl methacrylate
Nikpourian et al. [83]	Paraffin wax	Polyurethane
Yang et al. [56]	Lauric acid	Silica (SiO_2)
Lu et al. [84]	Butyl stearate	Polyurea
Su et al. [85]	N-octadecane	polyurethane
Salaun et al. [55]	Xylitol	Polyuria-urethane
Hawlader [21]	Paraffin wax	Gelatine and acacia
Wu et al. [86]	Paraffin	Polystyrene
Borreguero et al. [87]	Rubitherm®RT27	LDPE-PEVA
Methaapanon et al. [88]	*N*-octadecanemethyl palmitate	Silica
Es-Haghi [89]	Linseed oil	Silane-treated and untreated Ethyl Cellulose
Fashandi [90]	Palmitic acid (PA)	Polylactic Acid (PLA)
Lin et al. [91]	Myristic acid	Ethyl Cellulose
Khan et al. [92]	Paraffin wax	Poly (MMA-*co*-HEMA)
Wang et al. [93]	N-eicosane	Poly methyl methacrylate
Xing et al. [94]	Eutectic of CA and PA	Polyvinyl Chloride (PVC)
Graham et al. [95]	Mg $(NO_3)_2.6H_2O$	Poly ethyl-2-cyanoacrylate
Qiao & Mao [96]	Paraffin	Urea-formaldehyde (with Graphene Oxide)
Pethurajan and Sivan [97]	Paraffin wax	Urea-formaldehyde
Rakkappan et al. [98]	1-Decanol	Urea-formaldehyde (with GnP and CuO)
Graham et al. [99]	Mg $(NO_3)_2{\cdot}6H_2O$, $Na_2SO_4{\cdot}10H_2O$ and their mixture	Poly ethyl-2- cyanoacrylate (PECA)
Khadiran et al. [100]	N-nonadecane	Styrene (*St*) and methylmethacrylate (MMA)
Huang et al. [101]	N-Octadecane	Melamine–formaldehyde (MF)
Cheng et al. [102]	Capric acid	Poly (methyl methacrylate)
Parvate et al. [103]	Hexadecane	Copper nanoparticles enhanced polydivinylbenzene
Zhao et al. [104]	N-octadecane	Titanium dioxide enhanced PMMA
Maithya et al. [105]	N-eicosane	GO-modified PUA
Zhang et al. [106]	N-octadecane	Poly-pentafluorostyrene
Lashgari et al. [107]	Hexadecane	PMMA and P(BA-co-MMA)

recent years, different review studies have been performed on the performance of solar energy applications with nano-enhanced PCM [144], encapsulation techniques for PCM [47] and the influence of encapsulation of inorganic PCM on thermophysical characteristics [145]. However, to the best of the authors knowledge, there is a gap in review of the performance evaluation of solar energy applications using encapsulated PCM. The present paper aims to perform a review on the production process of encapsulated PCM, analyzing the various material that can used as an encapsulated PCM, and the combination of different solar energy devices with encapsulated PCM materials. In addition, recommendations for future studies to improve the performance of solar energy using thermal battery (encapsulated PCM) have been presented. As such, the review is presented organized under the following subsections:

- Theoretical background

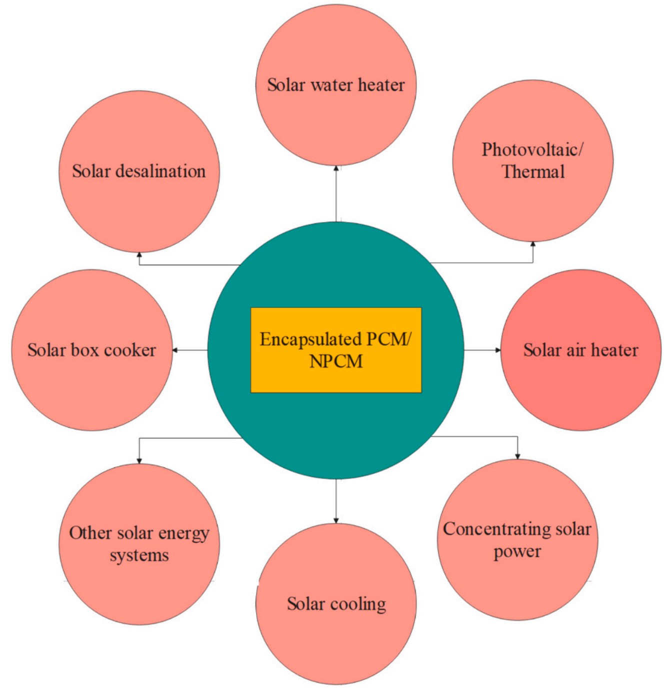

Fig. 15. The classification of solar energy application using encapsulation PCM.

- Solar energy application with encapsulated PCM
- Solar energy application by encapsulation nano-enhanced PCM
- Economic, exergoeconomic and environmental evaluation of the system using encapsulation PCM

3. Theoretical background of energy efficiency

The energy efficiency of solar energy systems is the most important parameter for determining the highest performance techniques coupled to applications. Energy efficiency is generally defined by the energy that enters solar applications, which usually is only solar energy, to the energy produced by the system [146]. The encapsulated phase change material can store a high amount of thermal energy and remove it from the application when required, leading to improved energy efficiency of a system. The calculation of the energy efficiency of varied solar energy applications depends on the types of produced energy including, drinking water [147,148], thermal energy [149], electrical power generation [150,151] and hot water production [152,153]. The energy efficiencies of some energy systems are determined as follows:

3.1. Solar desalination

The energy efficiency of solar desalination is specified as the ratio of distilled water generation of the system to the sum of the energy entered from the sun and other energy sources, including electrical heaters, thermoelectric heater, and others. Thus, the energy efficiency of a solar desalination system can be raised by increasing the water generated by the system. The energy efficiency of the system is calculated by [154,155]:

$$\eta_{\text{Solar desalination}} = \frac{\dot{m}_{ev} h_{fg}}{I_t A_b + \dot{W}} \quad (1)$$

where I_t, $\dot{m}_{ev}$, and h_{fg} depict the solar irradiation, the generated water, and the latent heat of water, respectively. Further, $\dot{W}$ illustrates the thermal or electrical energy sources coupled with a solar still.

3.2. Photovoltaic/thermal system

The energy efficiency of a photovoltaic/thermal application is determined as the ratio of power generation output by solar panels to the solar energy source. The electrical efficiency of PV/T was achieved by [156]:

$$\eta_{PV/T} = \frac{P}{I_t \times A_{panel}} \tag{2}$$

where I_t and A_{panel} depict the solar irradiance and photovoltaic panel area. Additionally, the P shows electricity generation by solar panel. The electrical efficiency of the system is obtained by [134]:

$$P = V_{PV} \times I_{PV} \tag{3}$$

where V_{PV} and I_{PV} are voltage and ampere of the solar panel.

3.3. Solar water heater

The energy efficiency of solar water heaters is related to potential of the water heating by input solar energy to the inlet energy by the solar intensity, as well as other thermal energy sources. The thermal energy of the solar water heater is obtained by [157]:

$$\eta_{Solar\ water\ heater} = \frac{Q_u}{I_t \times A_t} \tag{4}$$

where Q_u presents the heat energy of solar water heater. The useful heat energy of the system is given by:

$$Q_u = \dot{m}_{water} C_{p,water} (T_{outlet} - T_{inlet}) \tag{5}$$

where $\dot{m}_{water}$ show the flow rate of the water, $C_{p,water}$ presents the specific heat of water, T_{inlet} and T_{outlet} show the inlet and outlet water temperature of the solar water heater.

3.4. Solar air heater

The energy efficiency of the solar air heater is calculated by the ratio of the heat transfer rate into ambient air to solar energy. The thermal energy efficiency of the solar air heater is given by [158]:

$$\eta_{Solar\ air\ heater} = \frac{Q_u}{I_t \times A_t} \tag{6}$$

where Q_u presents the thermal energy from solar air heater. The useful collected thermal energy is calculated by the following relationship [159]:

$$Q_u = \dot{m}_{air} C_{p,air} (T_{outlet} - T_{inlet}) \tag{7}$$

where $\dot{m}$ show the flow rate of the air, $C_{p,air}$ indicates the specific heat, T_{inlet} and T_{outlet} present the inlet and outlet air temperature of the solar air heater.

3.5. Solar box cooker

The energy efficiency of the solar box cooker is specified as the ratio of the useful thermal energy to the thermal energy of the solar radiation. The thermal energy efficiency of the solar box cooker is calculated by [160]:

$$\eta_{Solar\ box\ cooker} = \frac{m C_p (T_2 - T_1)}{I_t \times A_t} \tag{8}$$

where m, T_1 and T_2 show the mass of the food, initial and final temperature of the food, respectively.

3.6. Solar pond

The energy efficiency of the solar pond can be shown as follows:

$$\eta_{Solar\ pond} = \frac{q_{ext}}{I} \tag{9}$$

where I indicate the average of solar intensity (in W/m^2) incident on the surface of the application and q_{ext} show the rate of heat extraction in the system.

3.7. Other solar energy applications

Generally, the energy efficiency of solar energy applications is indicated by the ratio of generated energy by the system (thermal energy, electrical energy, hot air, chilling power, hydrogen production, etc) to the energy input to the system. In the majority of cases, the only source of energy input to the system is solar irradiation; however, in some cases other sources of heat, such as electrical heaters, may be used to improve the energy efficiency of the system.

4. Solar energy application with encapsulation PCM

Solar energy applications include: solar desalination system to produce the drinking water from brackish water [161], photovoltaic modules to generate electricity from solar irradiation [162], solar water heaters to supply domestic hot water from the thermal energy of the sun [163] and other applications applied on the basis of the thermal energy of the sun [164–167]. When combining an encapsulated PCM with solar energy applications, solar thermal energy can be stored on the PCM and removed when the system requires thermal energy [168]. Therefore, an encapsulation PCM can have a profound influence on the performance of a solar energy system.

4.1. Solar desalination

The solar desalination system is utilized to produce drinking water from brackish water with a solar energy source [169]. Depending on the input source of energy to water, solar desalination can be separated into two types: active and passive solar desalination. In passive devices, solar energy is the only source of thermal energy to the solar desalination system, which leads to generation of distilled water. Contrastingly, in active devices [170], in addition to the solar energy source, other energy sources such as electrical heaters [171] and heat pipe/pulsating heat pipes [172] can be used to increase the distilled water of the system. The combination of encapsulation phase change material in solar desalination can lead to enhanced evaporation rate of the system when solar irradiation is low during nighttime. Therefore, generated water and efficiency of a system using encapsulated PCM increases. Kannan et al. [173] have assessed the effects of encapsulated PCM and aluminum scraps on produced water of hemispherical solar desalination, whereby paraffin wax in aluminum scrap cans in two configurations of square shape and triangular shape were considered to determine the higher amount of thermal energy. The evaporation surface of solar desalination with an area of 0.1963 m^2 and hemispherical diameters of 0.25 m was tested. The results illustrated that the daily generated freshwater of the system using square shape, triangular shape and conventional system were approximately 5.63 L/m^2, 4.88 L/m^2 and 2.92 L/m^2, respectively. The findings also elucidated that the CPL of the system by square shape, triangular shape and conventional system were approximately 0.0186 $/L, 0.0128 $/L and 0.0111$/L, respectively. Fig. 16 presents the experimental setup using encapsulated PCM.

Arunkumar et al. [76] have designed and tested single-slope and pyramid solar stills using a parabolic concentrator collector and encapsulated phase change material. The evaporation surface of each solar still was 0.25 m^2; the depth of saline water was 0.03 m; and the glass cover with a thickness of 0.004 m was considered to be appropriate

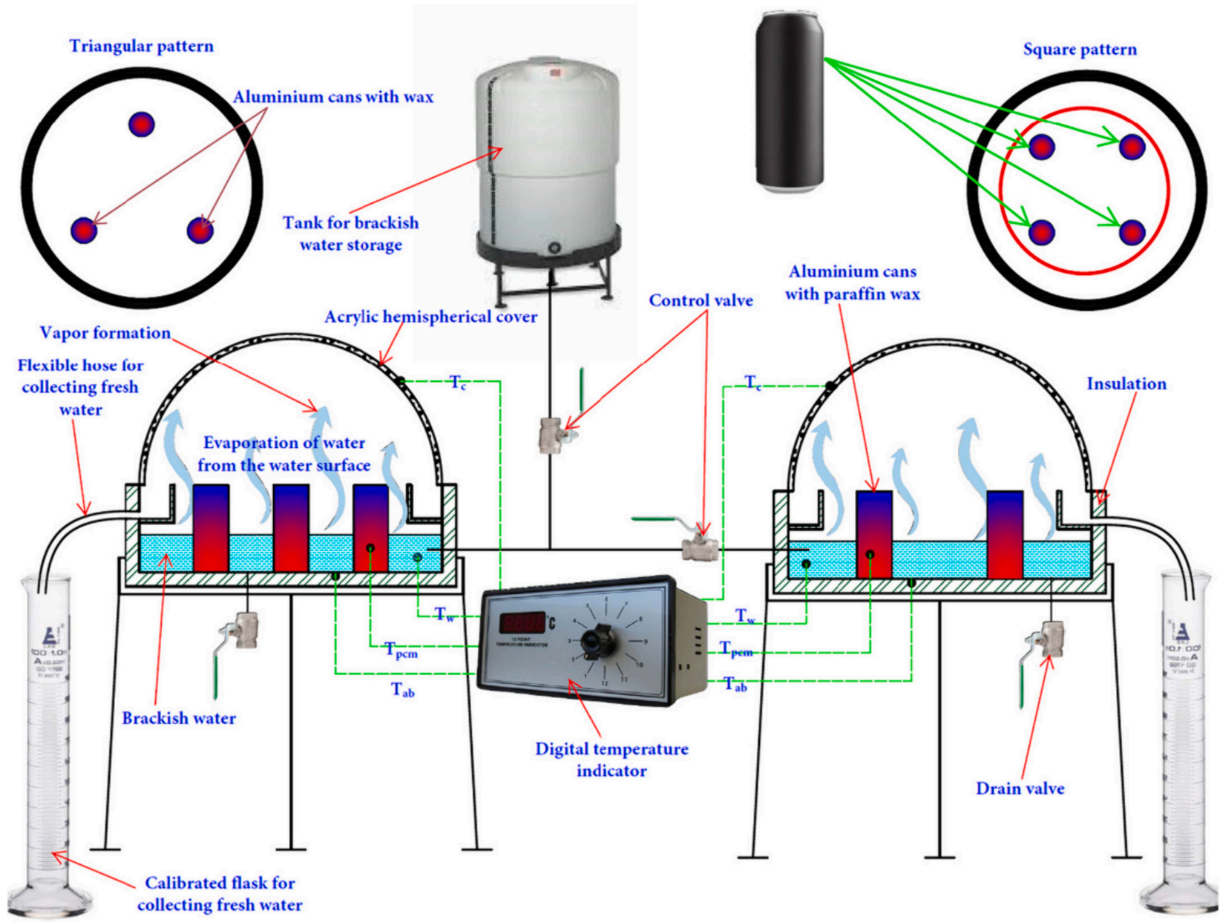

Fig. 16. Hemispherical solar desalination using encapsulated PCM [173].

for transmitting the solar radiation into the absorber surface. The copper balls filled with PCM were considered as a thermal battery, where the findings presented that the produced freshwater of the single slope solar still, pyramid solar still, single slope solar still using encapsulated PCM and pyramid solar still with encapsulated PCM were approximately 2680 mL/m^2.day, 3240 mL/m^2.day, 7160 mL/m^2.day and 7346 mL/m^2.day, respectively. *Al*-harahsheh et al. [174] have further examined the effect of capsules PCM and solar collectors on the efficiency of a solar still, as depicted in Fig. 17. They utilized Sodium Thiosulfate Penta hydrate inorganic salt as their PCM, as this PCM has great latent heat, short variation in volume in melting point and is cost-effective. Receiving the heat energy with the encapsulated PCM during the day,

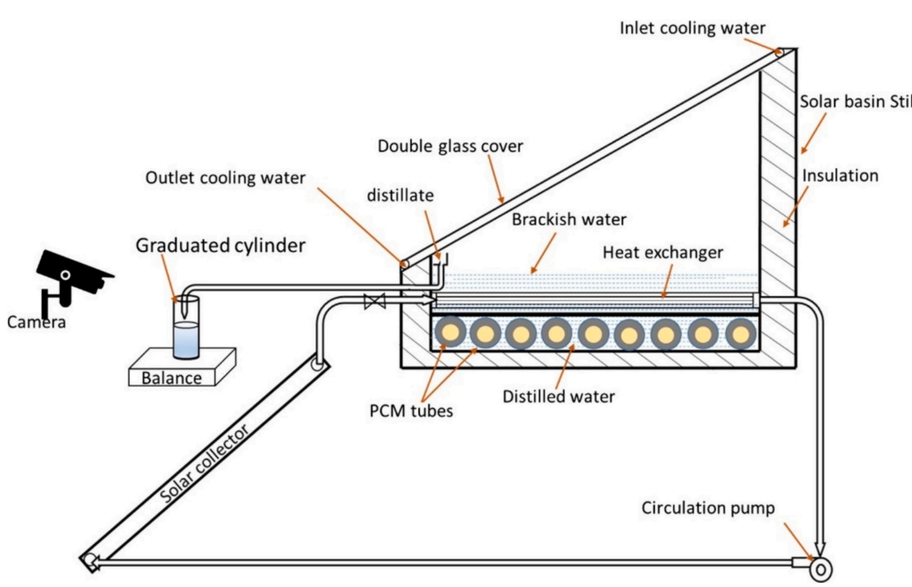

Fig. 17. Single-slope solar still using encapsulated PCM and solar collector [174].

and then utilizing it when it is needed, leads to an increase in the working time of the solar still. In this way, the water is recirculated between the solar still and the solar collector. The authors found that the use of encapsulated PCM in lower depth of the water had greater influence on water generation, where their findings also illustrated that the maximum daily produced water of the device was 4.3 L/m^2.

The influence of single and multi-PCM on water generated by solar desalination systems has also been examined by Vigneswaran et al. [77], reviewing three types of solar stills: 1) conventional solar stills, 2) solar stills using PCM-1 and 3) solar stills using PCM-2. The body of the system was fabricated from a galvanized iron plate with a thickness of 0.0016 m. The PCMs were poured into the annulus pipe and positioned into the water to transfer the heat when required. The produced water of the conventional solar still, the system using PCM-1 and the system using PCM-2 were approximately 3680 mL/m^2.day, 4020 mL/m^2.day and 4400 mL/m^2.day, respectively. Additionally, the exergy efficiency of system numbers 1, 2 and 3 were equal to 3.92 %, 3.23 % and 3.52 %, respectively. Fig. 18 presents a photo of the solar still using encapsulated PCM.

The generated freshwater of the solar still using capsule PCMs, an ultrasonic atomizer and solar collector have been experimentally studied by Abed et al. [175]. In their study, twenty cylindrical-shaped components with a diameter of 25 cm, length of 1 m and filling ratio of 90 % were filled with paraffin as an encapsulated PCM. Their saline water was recycled between the solar collector and solar still to boost the distillation rate of the system. Their outcomes showed that with the use of the encapsulated PCM in solar desalination systems, the produced water was increased by approximately 30.6 %. They also presented that the highest energy efficiency occurred in the solar still using an ultrasonic atomizer, which was 39.3 % for 30 min working time. Fig. 19 illustrates the solar still by a solar collector, ultrasonic atomizer and encapsulated PCM.

4.2. Photovoltaic/thermal (PV/T)

The encapsulated PCM in many applications was utilized to store the thermal energy and release it when required. Due to the enhancement of the electrical efficiency of the PV by reducing the solar panel surface temperature, the encapsulated PCM was considered as a coolant media. In this context, the PCM receives the highest amount of thermal energy from the solar panel surface and assists to increase the electrical power output of the PV. According to a study by Carmona et al. [176], the performance of a hybrid PV and thermal solar collector by encapsulated phase change material was assessed, whereby a flexible layer of self-adhesive polyvinyl acetate foil was placed under the PV panel as an encapsulated PCM to allow heat expansion during the phase change process. Their results indicated that the daily hybrid and electrical efficiencies of the hybrid system using encapsulation PCM were approximately 31.35 % and 13.12 %, respectively. Modjinou et al. [177] have compared three configurations of solar panels including PV/T by microchannel heat pipe, PV/T by encapsulated PCM, and conventional PV/T. In this study, encapsulated PCMs and microchannel heat pipes were placed under the solar panel to receive the thermal energy of the system, as shown in Fig. 20. The experimental test was conducted under weather conditions in China, whereby they presented that the efficiency of the system using encapsulated PCM, the system using heat pipe and conventional system were approximately 36.71 %, 35.53 % and 31.78 % respectively, showing the encapsulated PCM method was better than the microchannel heat pipe method in terms of solar panel cooling.

Hamda et al. [178] have evaluated the innovative design of a double pass photovoltaic thermal system with nano-encapsulated PCM as a coolant. In their study, the multi-functional nano encapsulated PCM dispersion acts at the same time as an optical filter and heat carrier, and stores the material, as illustrated in Fig. 21. Their nano encapsulated PCM was made using silica as a shell and PCM18, PCM26, and PCM32 as a core. The combination of water and encapsulated PCM flowed in the upper and lower the PV panel to cool its surface. Their findings elucidated that by decreasing the surface temperature of PV using modification by 5 °C and 10 °C, the exergy of the system improved by 66 % and 208 %, respectively.

Qui et al. [179] have assessed the influence of micro-encapsulated PCM coupled with solar panels, whereby a PV system with dimensions of 0.8 m × 1.6 m × 0.05 m was tested. The micro-encapsulated paraffin in liquid type was poured into the copper helical pipe and placed under the solar panel surface to decrease its temperature. In their research: the value of working parameters assumed as a micro-encapsulated paraffin mass concentration was 10 %; Reynolds number was approximately 3000; and solar irradiation ranged from 500 W/m^2 to 700 W/m^2. These authors elucidated that the electrical efficiency of the system at working parameters was improved by 10 % to 15 %. Nasef et al. [180] cooled a photovoltaic module using water flow and encapsulated PCM, using a heat exchanger fabricated from Plexiglass 0.442 m × 0.262 m × 0.100 m and with a body thickness of 0.005 m. The encapsulated PCM contained 55 g of RT-44 HC, which was filled by approximately 80 % of pipe

Fig. 18. Single-slope solar still by concentric tube ring encapsulated PCM [77].

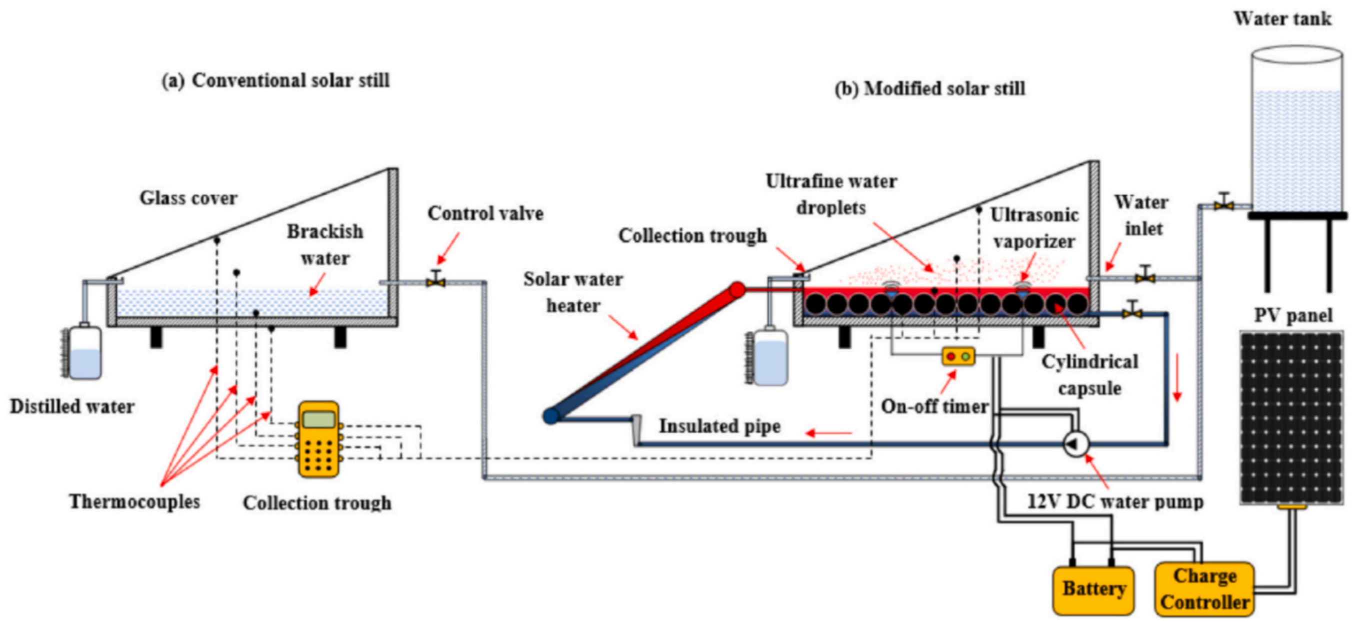

Fig. 19. Schematic view of a) conventional solar still and b) solar still by solar collector, ultrasonic atomizer and encapsulated PCM [175].

volume, as presented in Fig. 22. The experiments were done with three water flow rates of 0.5, 1, and 2 L/min. The obtained outcomes revealed that the mean heat transfer coefficients during the storing of the heat cycle for the parallel alignment were enhanced by 57 %, 104 %, and 130 % in the staggered case at flow rates of 0.5, 1, and 2 L/min, respectively. Fig. 22 depicts the PV/T using different flow rate of cooling water and encapsulated PCM.

Waqas et al. [181] have evaluated the impact of encapsulation phase change materials on electrical efficiency of solar panel systems. In their study, RT24 phase change material was filled in a copper tube and positioned under a photovoltaic panel to reduce its temperature. The results indicated that as the photovoltaic surface by encapsulation PCM cooled by about 6 °C, the electrical efficiency of the system increased by 3 %. Elsabahy et al. [182] deigned, fabricated and tested a concentrator solar panel system using encapsulated phase change material, whereby the shell of encapsulated PCM was made from a rectangular aluminum enclosure and installed under the PV panel. A concentrator, which was made of a mirror, focused the solar irradiation onto the system. Diverse types of phase change materials were applied, using a combination of RT25 and RT35 PCMs including single, double, and triple encapsulation. The results of their work revealed that triple encapsulated PCMs decreased solar panel surface temperature by 16 °C, and also that the electrical efficiency and also improved the energy efficiencies of the modified system by 21.3 % and 5.29 %, respectively. Fig. 23 illustrates the solar panel using RT25 and RT35 encapsulation PCM with reflector.

The effect of solar tracking concentrator, water cooling and encapsulated PCM on performance of photovoltaic/thermal system has been examined by Su et al. [183]. Their encapsulated PCM and water cooling were utilized to cool the surface of a solar panel, in addition to a solar tracking concentrator being used to absorb high solar irradiation into the system. The encapsulated paraffin wax was submerged into the water to receive the heat energy of the water. The results indicated that the electrical and thermal efficiencies of the system using encapsulated PCM were approximately 10 % and 5 %, respectively. Fig. 24 depicts the experimental setup of PV/T using solar tracking and encapsulated PCM.

4.3. Solar water heater

Solar water heaters have major applications with regard to solar energy, whereby they can be used to produce the domestic water heater [184]. In this process, solar irradiation improves the working fluid of solar collector during the day and leads to increased water temperature of the system. Different solar collectors, such as flat plate, evacuated tube heat pipe and parabolic trough solar collectors have been used in solar water heaters [185]. Accordingly, the temperature of water in a storage tank can be enhanced by recycling the working fluid between the storage reservoir and the solar collector. Encapsulation PCMs further help to receive the thermal energy of the sun and transfer it to the water, thereby increasing the performance of the system. Yang et al. [186] have examined the impact of encapsulated PCMs on efficiency in solar water heaters. They used polyethylene glycol as the encapsulated PCM to store a high amount of energy. The results of their study elucidated that the integration of encapsulated polyethylene glycol with solar water heaters can compensate for existing problems, such as low use of solar energy and intermittent solar energy. The influence of encapsulated phase change materials on the performance of solar water heaters has been assessed by Su et al. [187], whereby the core of their encapsulation was made of paraffin wax and the shell of the encapsulation was fabricated from Urea Methacrylate. Their experimental results indicated that 5 wt % of nucleating agent (ammonium chloride) and double emulsions (Brij 35 and Brij 30) led to higher core media content of 68.55 %, and an efficiency of encapsulation of 97.93 %. Yang et al. [188] have used three types of encapsulated phase change materials to enhance the performance of the solar water heater. In their study, the water was heated in a solar collector and flowed into the packed bed of the system via a pump. The melting point of PCM-1 was approximately 60–62 °C. PCM-2 was approximately 50–52 °C and PCM-3 was equal to 42–44 °C. The encapsulated PCM was fabricated from polycarbonate spheres with a diameter of 0.055. Their theoretical findings revealed that modified systems using three types of PCM were more efficient in comparison with conventional systems. Fig. 25 illustrates the solar water heater with combinations of three types of PCM.

Dileep et al. [189] have theoretically investigated the amount of encapsulated phase change material in the storage reservoir of solar water heaters integrated with evacuated tube solar collectors. In their study, paraffin wax was poured into pipes and installed in the storage tank. Three configurations of the system with effective-PCM area were considered for numerical analysis: 1) system by 1 encapsulated PCM, 2) system by 3 encapsulated PCM and increased effective area of 67.4 %, and 3) System by 5 encapsulated PCM and increased effective area of

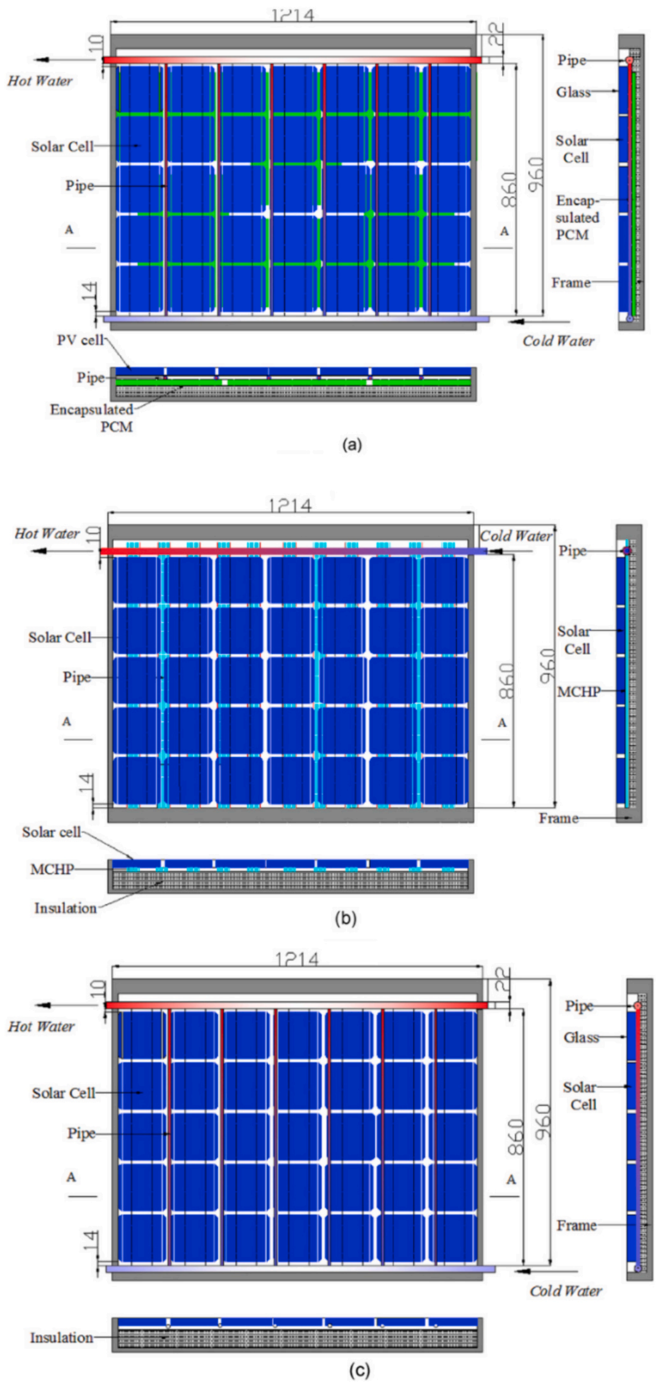

Fig. 20. Photovoltaic/thermal system using a) encapsulated PCM, b) micro-channel heat pipe and c) conventional system [177].

113.9 %. Their findings showed that case number 3 (system with 5 encapsulated PCM) had the best performance during storing and removing of heat. The influence of capsulated phase change material on the performance of solar water heaters has been evaluated by Fazilati and Alemrajabi [190], whereby paraffin wax in spherical capsules were considered as a latent heat storage media to maintain a high water temperature. In their study, approximately 180 capsules with diameters of 0.038 m filled with paraffin wax were located in the storage reservoir, with a volume fraction of 55 %. Their results indicated that the energy storage density and exergy efficiency of the system using encapsulated PCM were approximately 39 % and 16 %, respectively. *Al*-Hinti et al. [191] has further investigated the effect of PCM bottles in storage tanks on the efficiency of solar water heaters. In their study, PCM with a weight of 1 kg were filled into thirty-eight bottles made of aluminum. Then, four flat plate solar collectors with an area of 1.47 m^2 and an angle of 30° were used to transfer the thermal energy of the sun to the working fluid. The obtained outcomes revealed that the water temperature of the storage tank was at least 30 °C more than the ambient temperature over 24 h. Fig. 26 illustrates the solar water heater coupled with a flat plate collector and PCM bottle.

Al-Imam et al. [192] have tested an innovative designed to increase the performance of the solar water heater with encapsulated phase change materials. In their study, a compound parabolic collector (CPC) was installed on both sides of the collector to increase solar irradiance into the collector, as illustrated in Fig. 27. Paraffin wax was used in the storage box and placed under the solar collector to receive the highest thermal energy of the sun during the day. The inlet water to the solar collector flowed into the U-shaped pipe above the encapsulated PCM, with a length of 6.2 m. Their experimental findings revealed that the energy efficiency of the application by PCM was 10–12 % higher than the system without PCM during the times of 4–5 p.m.

Avargani et al. [193] have investigated the influence of encapsulated PCM on the outlet water temperature of a solar water heater. They installed encapsulated paraffin into the storage tank to receive thermal energy during the day and transfer it to the water at night. In their study, the temperature of water increased using a flat plate solar collector, as presented in Fig. 28. The diameters of encapsulated PCM were set to 0.055 m. The CFD analysis indicated that the system could heat 1200 L of water to 60 °C for >8 h.

4.4. Solar air heater

Raju and Kumar [194] enhanced the outlet temperature of an air solar heater using encapsulated phase change materials. In their study, circular and square-shaped capsules poured with paraffin, were installed in the absorber surface of a double-pass solar air heater. The encapsulated paraffin wax was then attached in linear and stepped grids, perpendicular to the air flow direction. The results of the experiment showed that the thermal efficiency of the modified system increased by 15.8 % compared to the system without encapsulated PCM. Singh et al. [195] increased the efficiency of the solar air heater using encapsulated phase change material and circular fins absorber plate in weather conditions of India. Their experiments were performed on three flow rates of 0.01 kg/s, 0.02 kg/s and 0.03 kg/s. The system was made from galvanized iron plate with an area of 5775 cm^2. The paraffin wax was filled into the solar air heater inside the hollow fins. Their results showed that the modification of the system can increase the ambient temperature from 2 °C to 9 °C. They also presented that the thermal efficiency of the system was about 66 % at an optimal condition. Fig. 29 presents the sketch of solar air heater using hollow fins and encapsulated PCM.

Karthikeyan et al. [196] used of packed bed with encapsulated phase change material to increase the efficiency of the solar air heater, applying paraffin in the spherical balls to make an encapsulated PCM. In their study, ambient air was entered from the lower side of the collector and exhausted from the upper side of the solar collector. Their findings presented that the diameters of the encapsulated PCM, inlet temperature and the flow rate, the temperature difference between the heat transfer fluid and PCM, and the coefficient of convective heat transfer between the heat transfer surface and encapsulated PCM all impacted the heat transfer surface in the packed bed. Sudhakar and Cheralathan [197] investigated a solar air heater with and without encapsulation PCM, pouring paraffin into spherical balls installed on the holes of the absorber surface to slightly expand the heat transfer area. Their outcomes illustrated that the average efficiency of the system without encapsulation PCM, system with encapsulation PCM, and system with inclined absorber surface with encapsulation PCM were approximately 31 %, 39 % and 43 %, respectively. Raj et al. [198] have evaluated the effects of macro-encapsulated PCM on the efficiency of the solar air

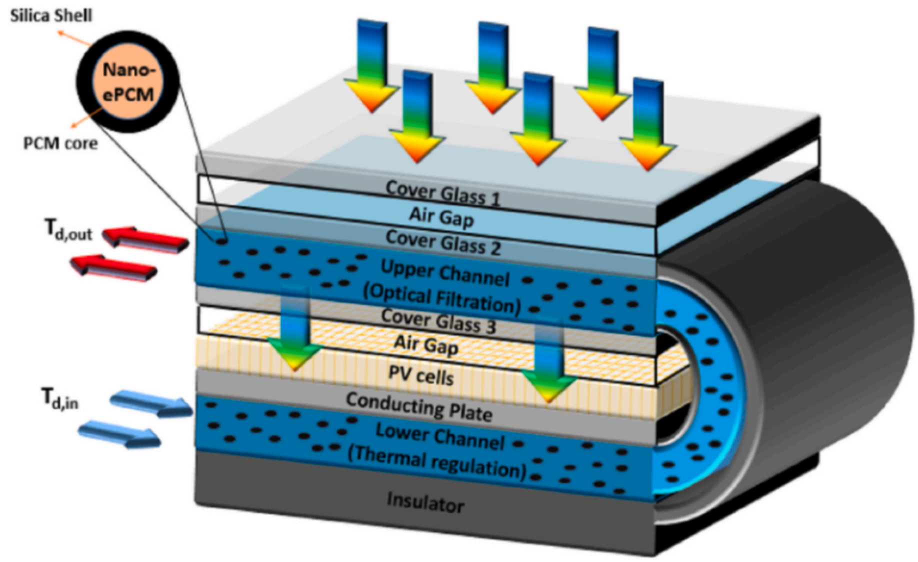

Fig. 21. The PV/T system using combination of water and nano-encapsulated PCM [178].

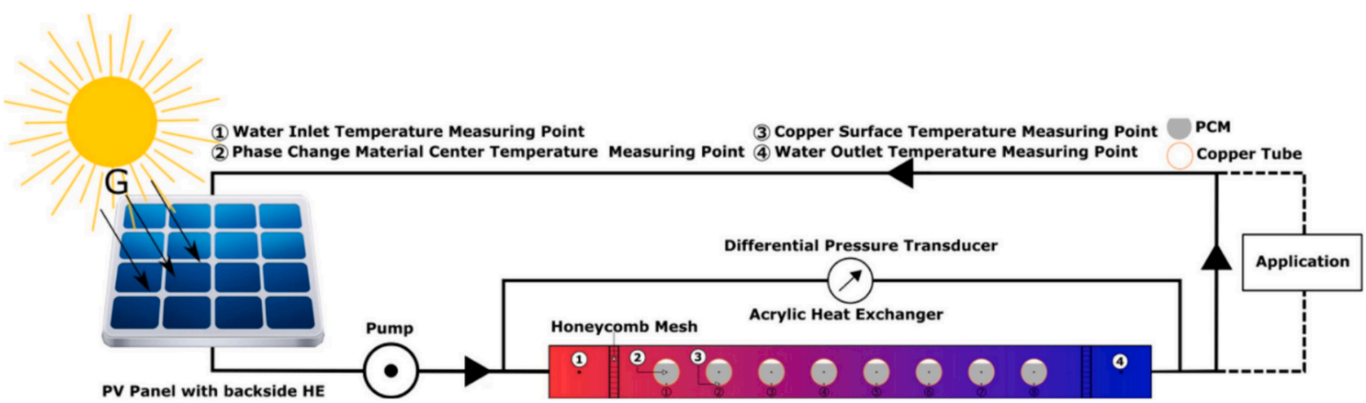

Fig. 22. Schematic of PV/T by encapsulated PCM and various flow rate of cooling water [180].

heater, using. Cylindrical and rectangular-shaped encapsulated PCM located in the system to absorb the thermal energy of the sun and release it during low solar irradiation, as illustrated in Fig. 30. All tests were conducted with a flow rate of 0.02 kg/s via a blower, whereby the encapsulated PCMs were located on the absorber and covered with black dye. The experimental findings illustrated that the average encapsulation PCM efficiency of cylindrical and rectangular shaped designs were approximately 67 % and 47.2 %, respectively.

According to research by Sajawal et al. [199], two types of PCM, RT44HC and RT18HC, were utilized to increase the thermal efficiency of a double-pass solar air heater. They constructed three forms of solar air heater: 1) conventional system; 2) semi-circular encapsulated PCM (RT44HC), located on the top side of the double pass system; and 3) a double stage system with adding the circular encapsulated PCM (RT18HC) in lower side of the system. Their phase change material was filled into the finned aluminum pipes to improve the ambient air temperature of the application, whereby ambient air with a flow rate of 0.02 kg/s flowed to the solar air heater due to force convection heat transfer into the system. To prevent thermal energy loss in the system, 0.025 m of glass wool was covered on the system. The experimental findings showed that the highest thermal performance was obtained by using configuration 3. Further, the energy efficiencies of the system were 53.2 %, 68.4 % and 71.9 %, respectively, in configurations 1, 2 and 3. Fig. 31 depicts the solar air heater with finned aluminum pipe, and RT44HC and RT18HC PCM.

Madhulatha et al. [200] have successfully optimized the location of PCM encapsulation to improve the thermal performance of solar air heaters. In their study, the influence of air speed, different PCM and the location of the encapsulated PCM were evaluated. The air speed with a range of 3.5 m/s to 5.5 m/s (with step of 0.5 m/s) and various types of PCM, including calcium-chloride hexahydrate, *n*-octadecane and paraffin wax, were considered in this research. The thermal absorption of the PCM in tubular configuration of the encapsulated PCM with calcium-chloride hexahydrate, *n*-octadecane and paraffin wax were improved by 1.08 %, 1.55 % and 9.17 %, respectively, in comparison with a staggered arrangement configuration of encapsulation PCM. The effects of two-packed bed encapsulated PCM on the efficiency of the solar air heater have been assessed by Arfaoui et al. [201], whereby the thermal energy of the solar radiation received by the spherical encapsulation AC27 PCM. The solar collector was made of a galvanized plate with a length of 1 m and an air volume of 0.28 m^3. The outcomes revealed that the daily thermal efficiency of the system by encapsulated PCM was approximately 47 %. Bouadila et al. [202] increased the performance of a solar air heater using encapsulated PCM as located within solar collectors. In this study, the spherical-shaped shell was utilized as a capsule, measuring a diameter of 77 mm, made from polyolefin with a thickness of 2 mm. The solar collector had an air volume of 0.28 m^3 and length of 2 m. The glass cover with thickness of 4 mm was installed 0.015 m above the absorber sheet, as presented in Fig. 32. They reported that the daily thermal efficiency of the system with modification was in

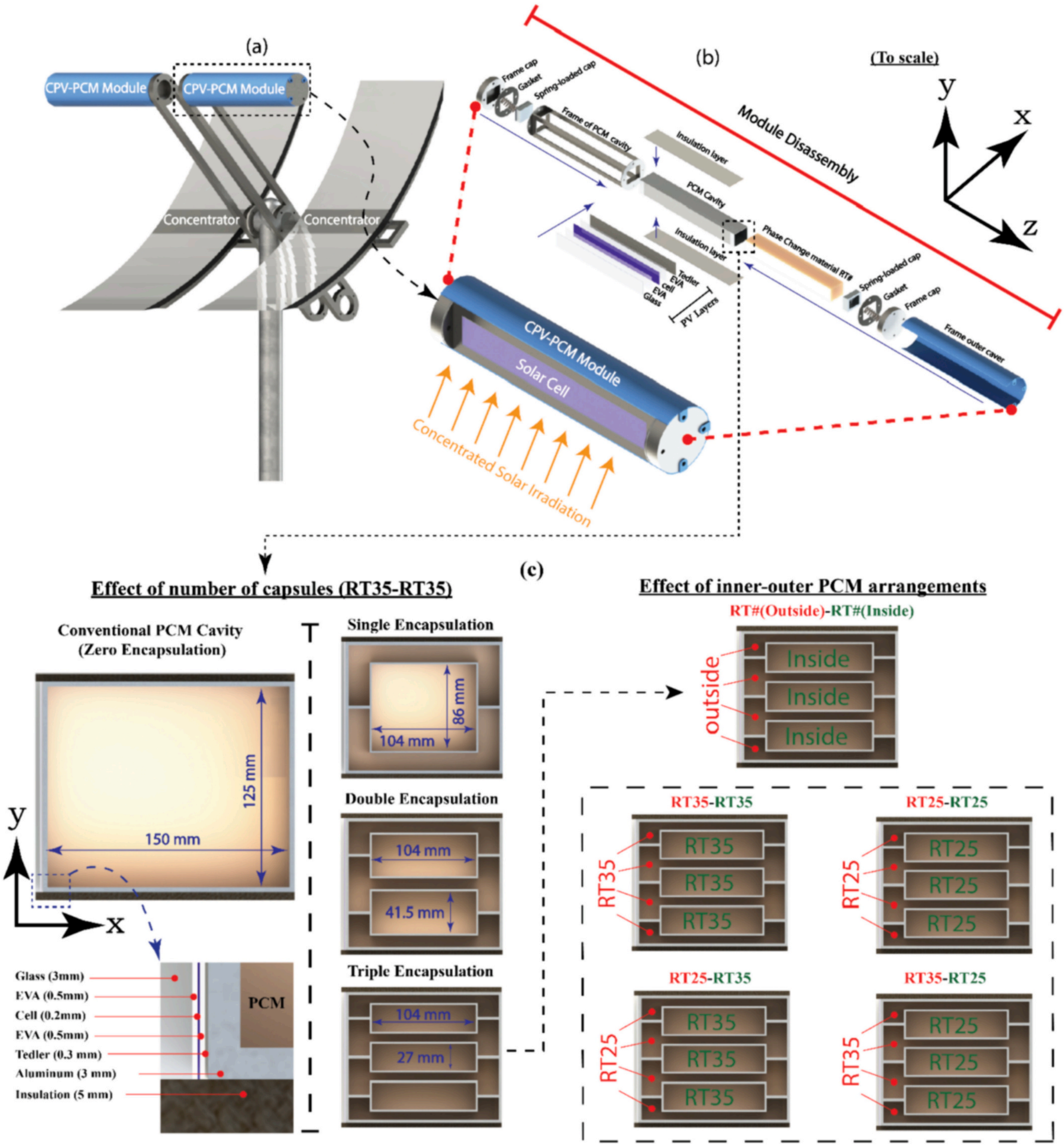

Fig. 23. Solar panel using RT25 and RT35 encapsulation PCM with reflector [182].

the range of 32 % to 45 %. The authors also showed that the exergy efficiency of the modified system varied between 13 % and 25 %.

4.5. Solar box cooker

Shobo and Mawire [203] have considered a spherical encapsulation PCM on the performance of solar box cooker applications, using erythritol as a phase change material and aluminum material in packed bed energy storage material. The wall strength of capsules was theoretically evaluated in capsules with a diameter of 0.05 m, whereby the extracted results illustrated that the thermal conductivity in the charging process time of erythritol increased by enhancing the wall thickness of capsules, and also the average thermal storing rate decreased by raising the wall thickness of capsules. Kumar et al. [204] have utilized energy storage material to augment the potential of cooking with solar energy sources, whereby the evaporation surface of the solar box cooker was filled with capsules-formed filled with paraffin wax to keep high the temperature of the application. The PCM-capsules were placed over the bed in the vertical position to boost the rate of heat transfer into the system to achieve a fast cooking reaction. The findings indicated that the highest

Fig. 24. Photovoltaic/thermal using solar tracking and encapsulated PCM [183].

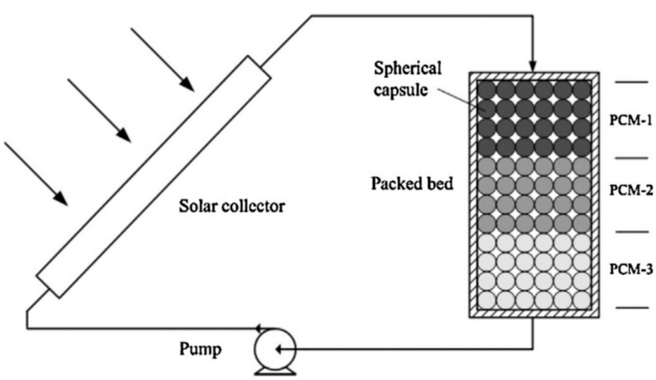

Fig. 25. Solar water heater using three types of PCM [188].

temperature, thermal efficiency, and potential power of cooking of the application were approximately 150 °C, 45.7 % and 54.71 W, respectively. In another study, Kumar et al. [205] drew, constructed and tested a solar box cooker using encapsulated phase change material, whereby 144 encapsulations made of aluminum were filled with organic PCM (RT64HC) to store the thermal energy of the sun. The three configurations of the system included a conventional system, a system using hollow capsules and a system using encapsulated PCM. Their results implied that the thermal efficiency and cooking power of the system using encapsulated PCM were increased by 52.2 % and 53.2 W, respectively. Fig. 33 presents the solar box cooker using encapsulated PCM.

4.6. *Concentrating solar power*

Concentrating solar power (CSP) is one renewable energy plant that generates electricity from solar energy and steam generators. Due to the use of high-scale solar area in this system, high-temperature encapsulated PCMs are required, which are located in a storage tank. Guédez et al. [206] have numerically evaluated the solar power plant using a direct steam generator and high-temperature encapsulated PCM. Spherical KNO_3 was implemented as an encapsulated phase change material due to its high range of melting point. The results of their research showed that the cost of power generation of the power plants with encapsulated PCM was reduced by 8 % and the capacity factor increased by 30 %, in a power block of 80 MW. Zhang et al. [207] enhanced the thermal efficiency of the solar electrical generated plant by using high-temperature encapsulated PCM. The Sb_2O_3 and mixture of Na_2CO_3 and $BaCO_3$ was implemented as a low and high-temperature encapsulated PCM. Outcomes showed that the heat cycle of the selected encapsulation retained its mechanical characteristic for 1250 charge/discharge cycles. Cingarapu et al. [208] have utilized the encapsulated PCM with zinc particles to increase the thermal performance of solar power plants. A combination of alkali chloride salt eutectic and coated Zn microparticles was used to increase the storage of thermal energy in the system. The results elucidated that the thermal storage capacity of encapsulation PCM was increased from 15 % to 34 %, with cycle temperature range of 50 °C to 100 °C. Fig. 34 shows the SEM picture of the material used in this research.

Flueckiger and Garimella et al. [209] have designed and tested a concentrating solar power plant by boosting the latent heat of encapsulated PCM. In this study, different encapsulated PCM with various latent heat and melting points were evaluated to find the highest

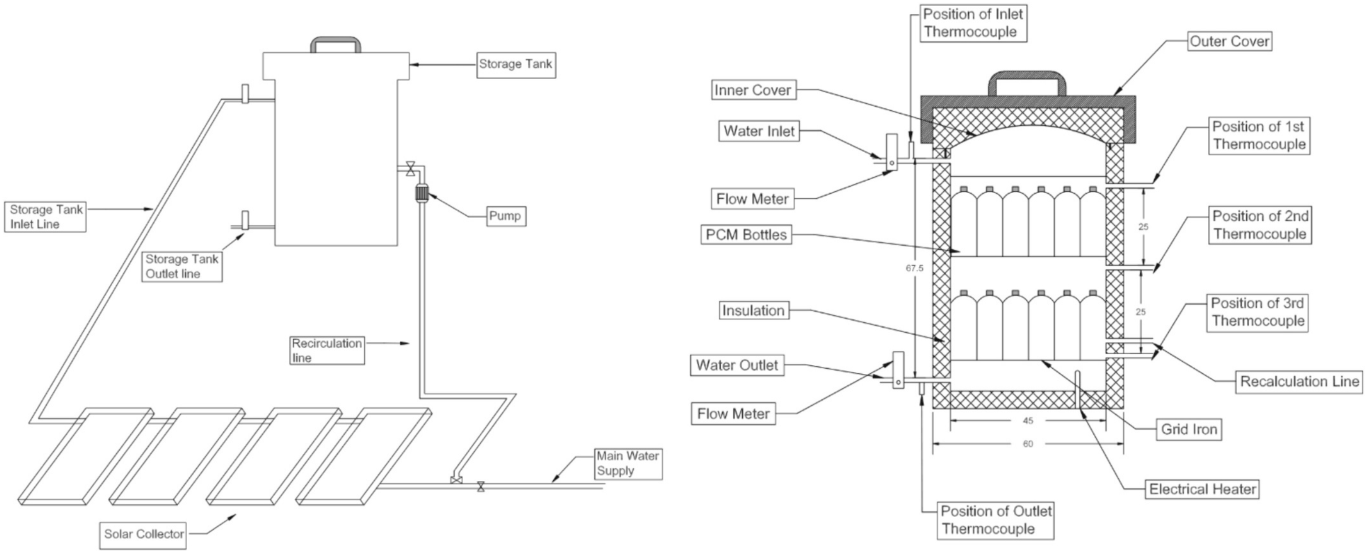

Fig. 26. The solar water heater with four flat plate collector and encapsulate PCM [191].

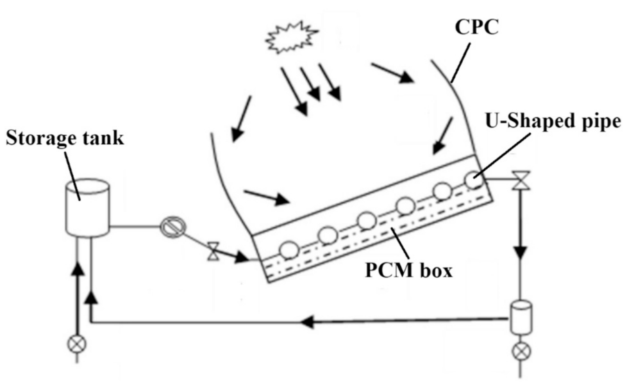

Fig. 27. The solar water heater using encapsulated paraffin wax and CPC [192].

performance of the system. The model used an area of approximately 1,700,000 m^2 for the reflector and a tower height of 194 m, as depicted in Fig. 35. The outcomes illustrated that the use of the porous absorber with a cascaded PCM shape enhanced the use of the latent heat and led to significant increase over the conventional quartzite rock filler. They also indicated that for a PCM with fusion heat of 124.5 kJ/kg (1/Ste. = 0.5), a three-layer cascade shape yields either a 9.7 % improvement in yearly power generation or a 16 % reduction in thermocline reservoir size relative to a quartzite-filled tank.

The economic and performance analysis of solar power plants coupled with encapsulation phase change material was evaluated by Nithyanandam and Pitchumani [210]. Various encapsulated PCM including 35 % Li_2CO_3/65 % Na_2CO_3, 32 % Li_2CO_3/35 % KCO_3/33 % Na_2CO_3 and 51 % KCO_3/33 % Na_2CO_3 was implemented in this research. The results indicate that by reducing the capsule size of the application, the storage capital price decreases, exergy efficiency increases, and provides capacity improvement. Fig. 36 presents the solar power plant using encapsulated PCM.

In another study by Zheng et al. [211], a solar power plant using

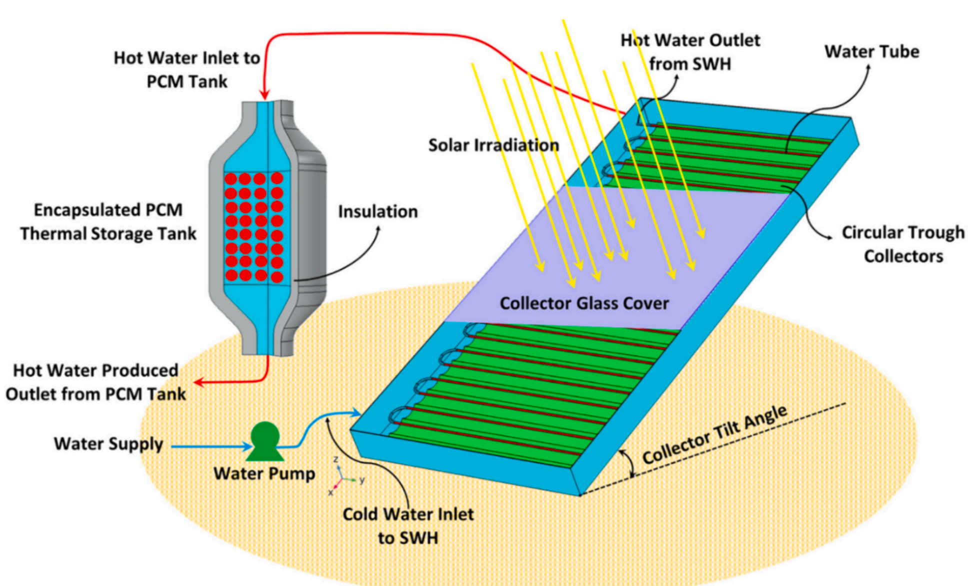

Fig. 28. The solar water heater with encapsulated PCM and flat plate collector [193].

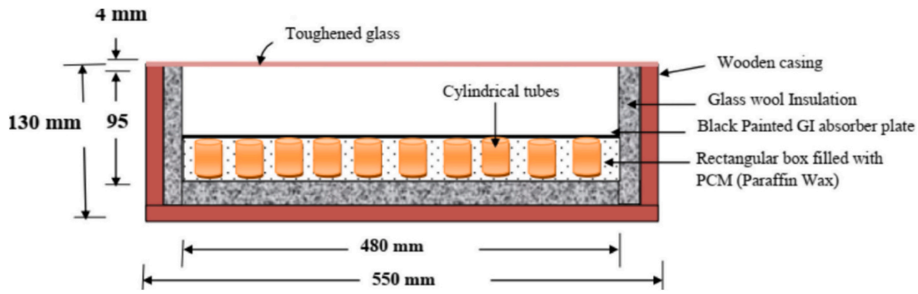

Fig. 29. Sketch of solar air heater using hollow fins and encapsulated PCM [195].

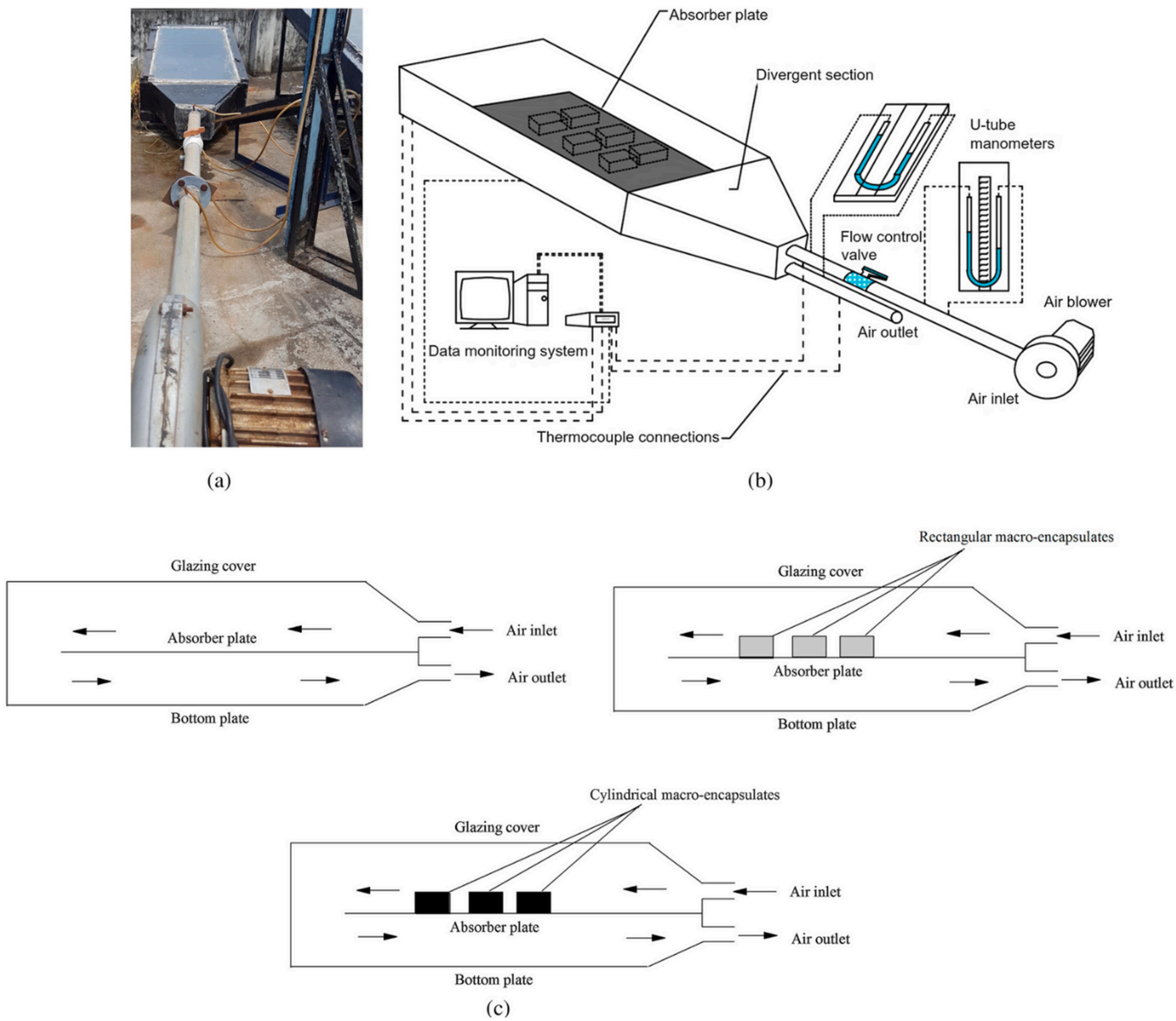

Fig. 30. Photo of a) solar air heater, b) schematic of system and c) system with and without encapsulation PCM [198].

encapsulated phase change materials was numerically and experimentally assessed. In their study, stainless steel shells with $NaNO_3$ PCM with a melting temperature of 440 °C were applied in the concentrating solar tower, whereby compressed air with flow rate of 0.038 kg/s was implemented as a heat transfer fluid. The results indicated that the encapsulated PCM can store thermal energy of approximately 211 kJ/kg in the temperature range of 250 °C to 386 °C. Fig. 37 presents the experimental setup of concentrating solar power with encapsulated PCM.

Prieto and Cabeza et al. [212] enhanced the efficiency of the solar electricity generation plant by using encapsulated PCM. They considered different PCM including $NaNO_3$, NaCl-KCl-LiCl, $MgCl_2$-KCl-NaCl and NaOH-NaCl to increase the thermal efficiency of the system. Their outcomes showed that the studied variants were likely to yield cost removal in cost performance quotient (CPQ) and LCOE as high as 80 % and 10 %, respectively. The evaluation of system-level cyclic heat properties of the molten-salt packed-bed TES by typical shapes on a 1D enthalpy-technique dispersed-concentric (D-C) model was studied by

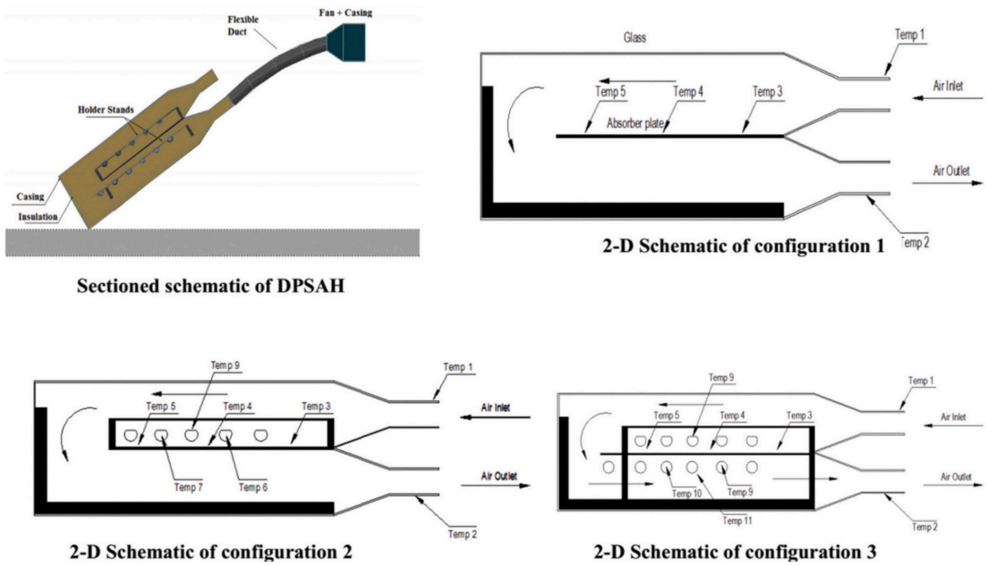

Fig. 31. Three configurations of solar air heater using finned aluminum pipe and PCM [199].

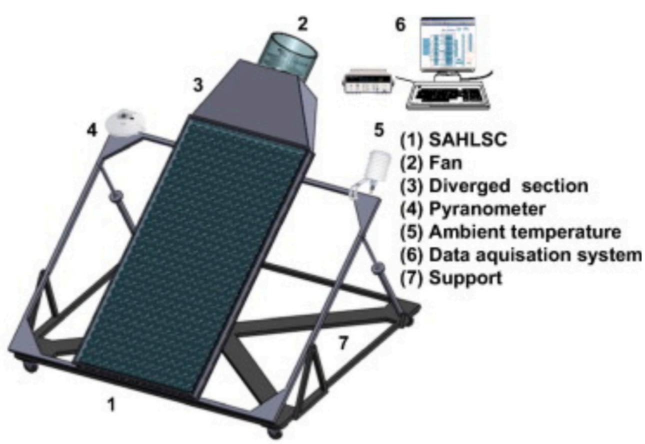

Fig. 32. Sketch of solar air heater using encapsulated PCM [202].

Zhao et al. [213]. In their research, the high-temperature encapsulation PCM of 20%Li_2CO_3/60%Na_2CO_3/20 % K_2CO_3 and the low-temperature encapsulation PCM of $NaNO_3$ were selected, located on the top and bottom of the thermocline storage tank, as shown in Fig. 38. The diameters and thickness of each capsule were equal to 0.03 m and 0.00075 m, respectively. The findings elucidated that the partial charge cycles of the PCMs lead to a better thermocline development into the latent-heat packed-bed surface.

Muñoz-Sánchez et al. [214] have used phase change material to review concentrating solar power systems. Their thermocline system consisted of cost-effective filler material including sand and rocks, whereby two encapsulated PCMs were located at the upper and lower level of the storage tank. A parabolic trough solar system with operating fluid and oil were implemented in this research, with a combination of 60 % $NaNO_3$ and 40 % KNO_3 as encapsulated PCM. The authors reported that a careful selection of the most suitable high-temperature PCMs, their encapsulation materials and encapsulation methods was demonstrated. According to a study by Mehmood et al. [215], the performance of a solar power plant using encapsulated energy storage material was evaluated, as depicted in Fig. 39. Ten capsules of $NaNO_3$- KNO_3 were considered as encapsulated PCM to store the thermal energy of the solar power plant, whereby the PCM tank was constructed of mild steel, in which ten capsules were stacked vertically. Encapsulated PCM was

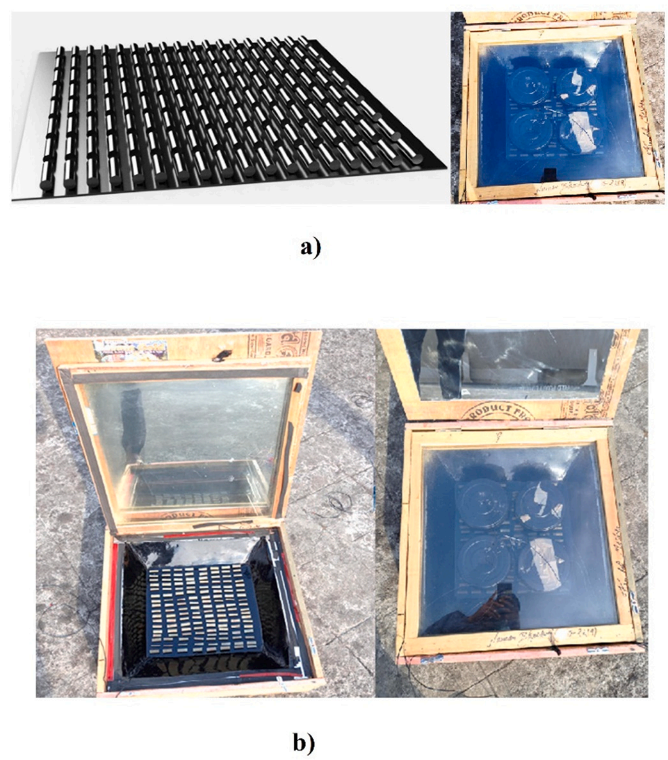

Fig. 33. Solar box cooker using a) encapsulated PCM and b) hollow capsules [205].

cylindrical shaped with a diameter of 0.076 m, length of 0.0256 m and thickness of 0.003175 m and was poured by 1.5 kg of PCM. Their results indicated that the proposed model and experimental analysis showed the model's effectiveness in concentrating solar power application.

Nithyanandam et al. [216] have analyzed the thermocline energy storage system on a solar power plant using encapsulated PCM. The impact of different shapes and working factors on the dynamic storage and delivery efficiency of the application was evaluated in order to identify the highest utilization parameters of the storage system. The PCM was a mixture of 20 % Li_2CO_3/60 % Na_2CO_3/20 % K_2CO_3, and the filler material of the storage tank was granite and quartz rock. The

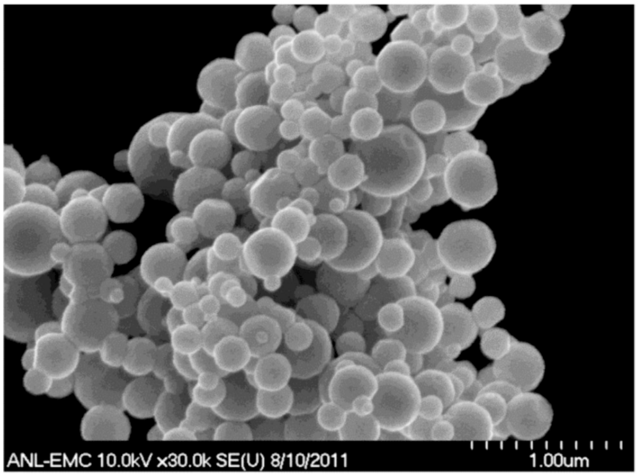

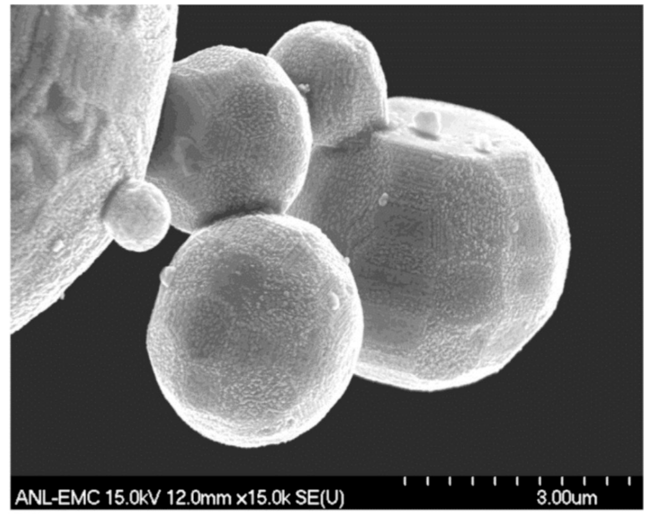

Fig. 34. SEM picture of zinc microparticles used to coating [208].

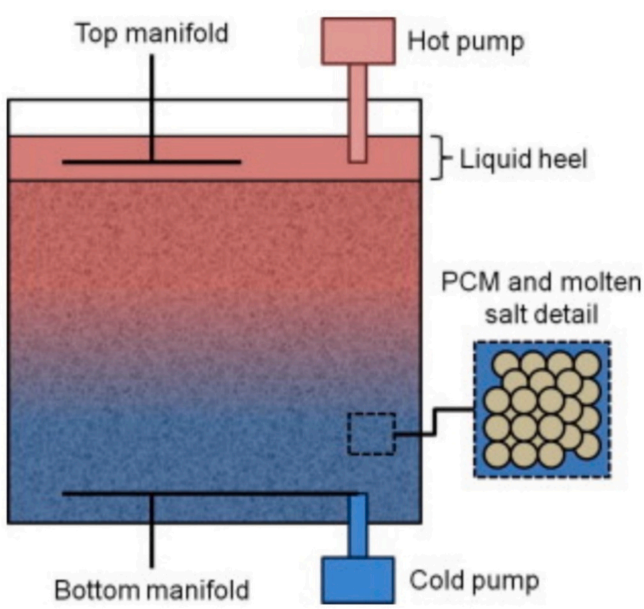

Fig. 35. Sketch of thermocline storage tank with encapsulated PCM [209].

findings showed that by decreasing the encapsulation size, the total and latent implementation was increased. The study also showed that the high Reynolds number and high flow rate causes a reduction in the utilization of the application. Zhao et al. [217] have evaluated the impact of multi-layer encapsulation PCM (MLSPCM) in the storage tank of concentrating solar electrical production plants. The storage tank consists of high temperature (HT-PCM) at the upper level of the tank, solid filler media in the middle of the tank and low temperature (LT-PCM) at the lower level of the storage tank, as presented in Fig. 40. The findings depicted that the MLSPCM thermocline thermal energy storage by optimizing the packed-bed shaped was more cost-effective than other thermocline TES applications.

A comparative investigation of the thermal and economic capacity of varied encapsulated PCMs on the performance of solar power plants has been examined by Tehrani et al. [218]. The experiments were performed for fifteen hours of storing capacity of a 19.9 MWe Gemasolar CSP. The findings revealed that in terms of designing the system with flexible working temperature range, the highest saving in cost was obtained in moving to the alternative TES application. The use of spherical encapsulated PCM to increase the performance of a solar power plant has been numerically studied by Bhagat and Saha [219]. The solar power plant was then integrated with the organic Rankine cycle (ORC) to produce the electrical power, whereby the material of the heat transfer fluid was Hytherm 600, which is an organic grade of commercial oil, so A164 was considered as a phase change material. The thermal storage had a cylindrical shape, whereby dimensions of 0.12 m × 0.25 m were used for heat transfer analysis for a thermal storage capacity of 155 Wh for the charging process. The findings elucidated that the latent heat encapsulated PCM was highly enhanced by improving the flow rate and inlet charging temperature. Fig. 41 depicts the thermal energy storage pack.

4.7. Solar cooling

The influence of micro-encapsulated PCM on improving solar-driven ejector cooling applications in Mediterranean weather condition has been examined by Allouche et al. [220]. The air condition system consisted of thermal cycles, ejector loops and cooling storage-air handling system. A vacuum tube solar collector with an area of 60 m^2 with a storage tank of 3 m^3 was used for the thermal cycle and for supplying the energy for the ejector loop. The cooling water was generated with the ejector loop, which was transferred to 900 L cooling storage reservoir poured with 800 L encapsulated PCM for cooling storage. The Ruitherm RT6 and Linpar 14 were utilized in this research as PCM, with findings presenting that the 5 kW cooling load was produced by this system using encapsulated PCM. Coca-Ortegón et al. [221] have implemented a solar electrical production system using solar panels and paraffin (C5-C20) encapsulated PCM on a 350-l refrigerator system. The solar panel was utilized to supply the direct current compressor to increase the pressure of the refrigerant fluid. The results indicated that the PCM located in the top and middle location of the refrigerator wall reached the temperature required for freezing, whereby it is benefiting from the latent energy storage.

4.8. Perovskite solar cell

Fumani et al. [222] have assessed the influence of encapsulated PCM on prolongation of lifespan of perovskite solar cells (PSC). PCM material was used as a cooling factor and poured into the polymer encapsulation enclosure to decrease moisture loss, increase temperature oscillation, and an unfavorable crystal phase change of the perovskite layer in PSCs under working conditions. The polyethylene-glycol was implemented as a PCM. The findings presented that the modified system acts as a stable

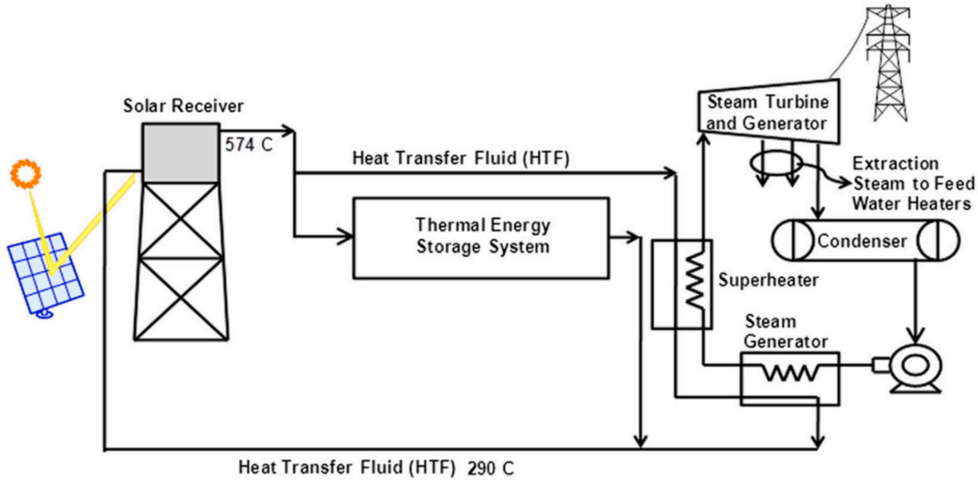

Fig. 36. Solar concentrating electrical generation plant using thermal storage material [210].

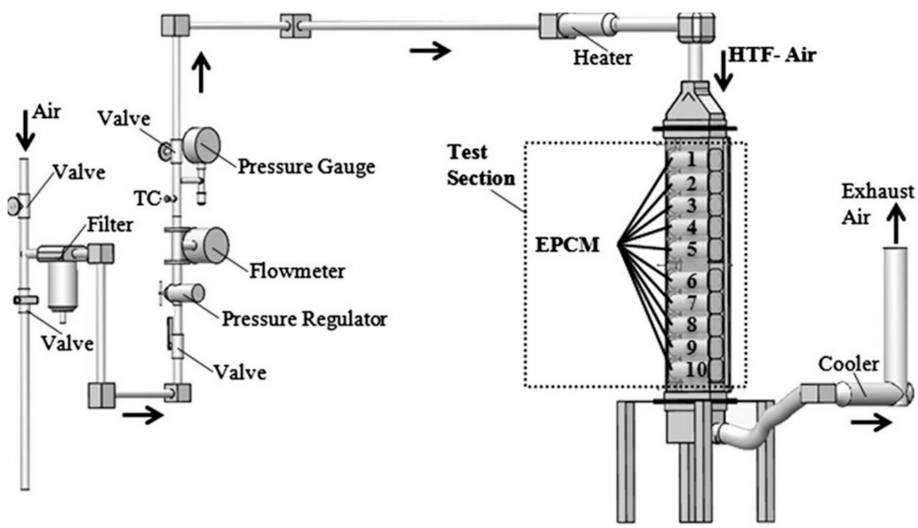

Fig. 37. The experimental setup of concentrating solar power with encapsulated PCM [211].

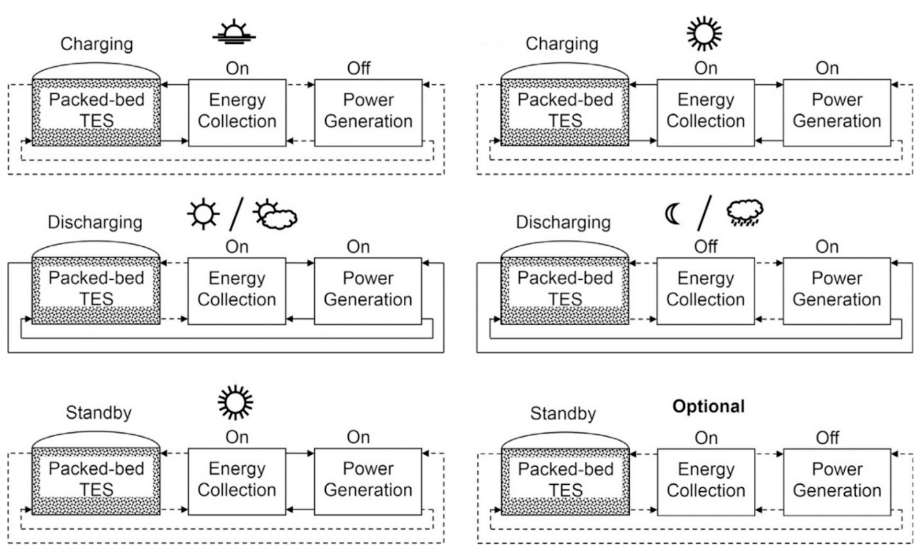

Fig. 38. Typical working case of the solar power plant system [213].

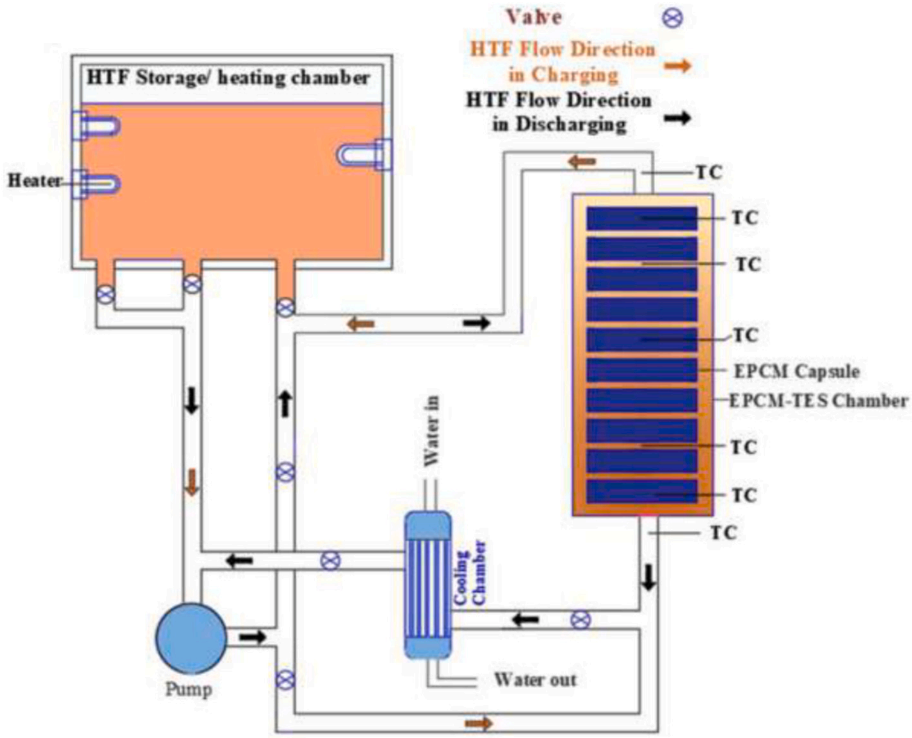

Fig. 39. Sketch of solar power plant using ten encapsulated $NaNO_3$-KNO_3 PCM [215].

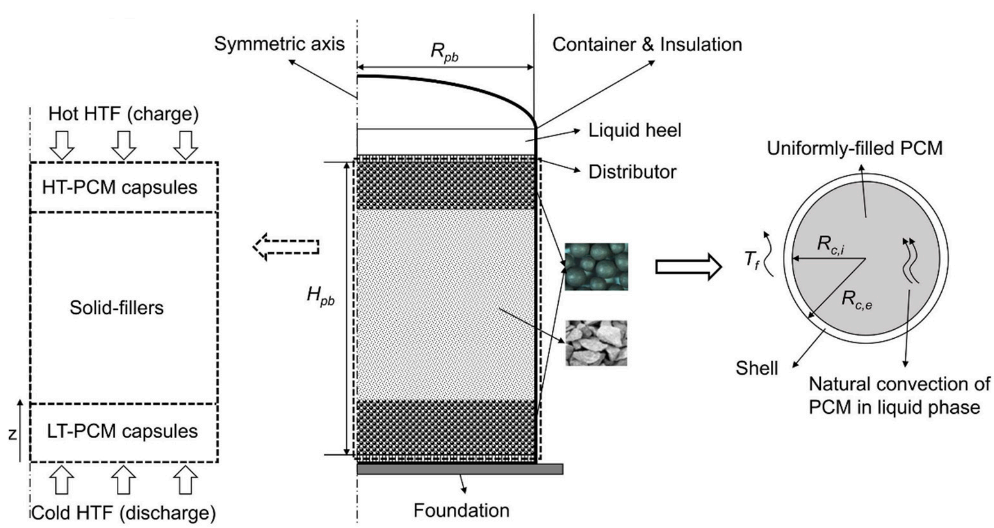

Fig. 40. The storage tank of the CSP with LT-PCM and HT-PCM [217].

application in 2 years, while the efficiency of the conventional system decreased by 50 % after ten days.

4.9. Solar fuels

Peng et al. [223] have constructed an encapsulated phase change material by TiO_2 compound photothermal catalyst as the shell was assembled on encapsulated PCM. The n-eicosane $C_{20}H_{42}$ was implemented with PCM, whereby polyurea and polyurethane were considered as the organic shell media. The ATR@PCM and ATF@PCM were constructed by Au nanopowders added to TNR and TNF. The authors found that when rod and flake-formed Au-TiO_2 photothermal catalysts added on the cover of encapsulated PCM, whereby the amount of light-to-hydrogen efficiency of ATR@PCM and ATF@PCM was about 11.4 % and 5.0 %, respectively, which was about 53.8 % and 56.1 % higher than the pure photothermal catalyst without encapsulated PCM. Fig. 42 presents the SEM picture of ATR@PCM and ATF@PCM, encapsulated PCM and damaged encapsulated PCM.

4.10. Solar pond

The solar pond is a solar energy application that uses salty water to collect and store the highest thermal energy of the sun. A research study by Colarossi and Principi [224] have evaluated the effect of encapsulated PCM on performance of a solar pond. Accordingly, paraffin wax was filled in aluminum cylinders with a diameter of 0.035 m and a

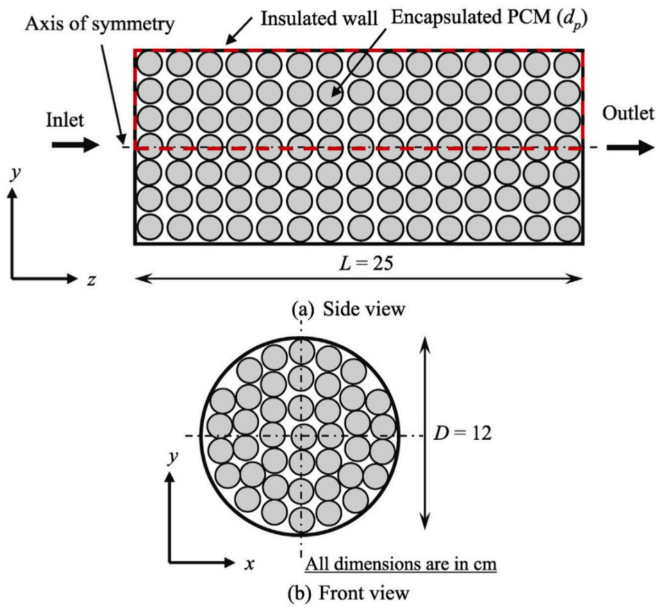

Fig. 41. Dimension and view of thermal storage system using encapsulated PCM [219].

length of 0.075 m to make the encapsulated PCM. Sixteen encapsulated PCM were located on the lower convective zone of the solar pond with a weight ratio of 0.1 to receive high thermal energy from the sun. The findings presented that the temperature of the lower level of the solar pond with PCM was approximately 0.3 °C lower than the solar pond without encapsulated PCM. The effects of encapsulated PCM/steel wire on the exergy efficiency of a solar pond have been examined by Wang et al. [225]. A combination of different concentrations of steel wires with two types of paraffin (RT 50 and RT 60) was poured in capsules to make an encapsulated PCM, as depicted in Fig. 43. The area of the solar pond was 0.48 m^2 and the height of LCZ, NCZ and UCZ were about 40 cm, 40 cm, and 20 cm, respectively. The salinity of the lower and upper convective zones of the system was about 20 % and 2 %, respectively. The highest coefficient of heat transfer of the system using encapsulated PCM was approximately 18.17 W/m^2 °C at concentration of 10 of wire steel and also improvement of 18.84 % in melting temperature. They also elucidated that the temperature difference of the system with and without encapsulated RT50 and RT60 was approximately 2.87 °C and 2.53 °C, respectively.

In another research by Wang [226], the thermal efficiency of a solar pond using thermal energy storage material and an electrical heater was assessed, whereby RT50 and RT60 were considered as PCM. The electrical heater, with a range of 0–500 W, was placed 15 cm above the lower side of the solar pond. The shells were made of stainless steel 304 with a diameter and length of 0.032 m and 0.2 m respectively, with findings showing that the use of encapsulated PCM had a direct impact on maintaining temperature in high range and ensuring stability of the solar pond.

4.11. Solar thermochemical reactor

The solar thermochemical reactor can be utilized to generate cost-effective solar fuel and hydrogen production. One of the major problems of this application is its discontinuation of solar intensity during the day. Thus, this problem can be solved by using a thermal battery, whereby the influence of encapsulated PCM on the efficiency of a solar thermochemical reactor has been evaluated by [227]. The solar collector reactor was filled with encapsulated PCM (Sn@SiO_2), with the inner and outer diameters of the reactor tube at 66 mm and 70 mm, respectively. The melting temperature of the encapsulated PCM was approximately 505 K. The outcomes indicated that the unsteady performance parameter of the solar collector reactor filled with encapsulated PCM was approximately 23.2 % more than system without encapsulated PCM. *Ma* et al. [228] further increased the performance of the solar thermochemical reactor by using encapsulated PCM, whereby their catalytic operation was adjusted by diluting the catalyst with encapsulated PCMs. In their study, Sn and SiO_2 were utilized as PCM and shell, respectively. The obtained outcomes showed that methanol conversion efficiency and generated hydrogen were decreased by 8.4 % and 9.9 % respectively, by reducing the catalytic operation from 0.1 to 0.2. Fig. 44 shows the solar collector reactor using encapsulated PCM.

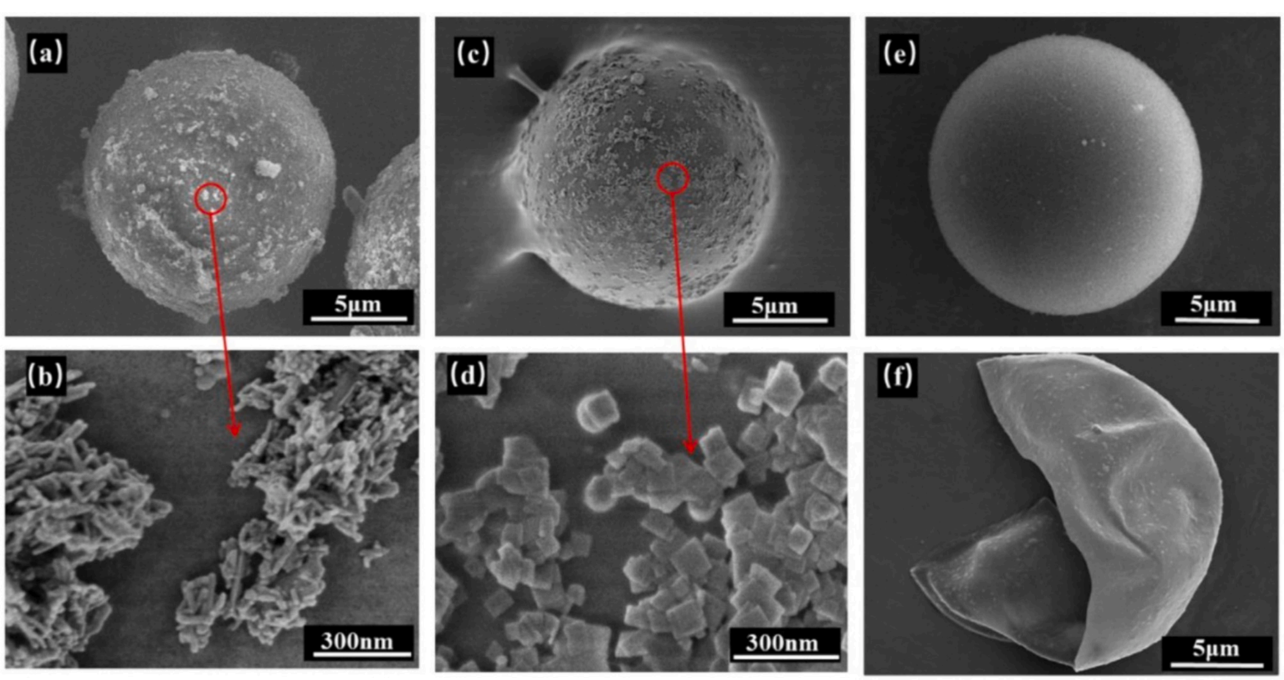

Fig. 42. SEM picture of a and b) ATR@PCM, b and c) ATF@PCM, e) encapsulated PCM and f) damaged encapsulated PCM [223].

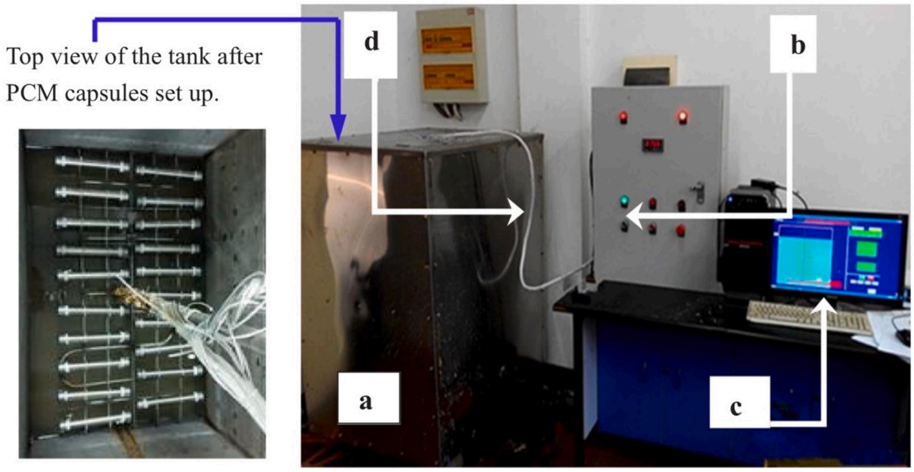

Fig. 43. Picture of solar pond using encapsulated composite PCM (RT 50 and RT 60 with steel wire) [225].

4.12. *Solar greenhouse*

Solar greenhouse is a solar energy sources application that is usually used to assist the growing of plants. Meng and Chu [229] have coupled encapsulated thermal energy storage with a greenhouse in Fuxin City, China, whereby the encapsulated PCM assisted to increase the temperature of the greenhouse when the solar radiation was zero. The greenhouse was divided into four smaller greenhouses, of which the length of left and right greenhouse were approximately 15 m and the length of two other middle greenhouses were 10 m. In their study, 150 UPVC pipes were used as capsules to fill the PCM which was located in the greenhouse, as illustrated in Fig. 45. The PCM was made from 58.04 % H_2O/ 35.96 % $CaCl_2$/3 % $SrCl_2.6H_2O$/3 % CMC. The results showed that the efficiency of phase change thermal receiving and removing were at the highest, and at close to 100 %, in the heat on clear days. Moreover, the highest temperature difference of the contrast greenhouse at clear, cloudy, and snowy weather conditions was approximately 4.1 °C, 2.2 °C and 1.6 °C, respectively.

4.13. *Solar steam generator*

Solar steam generator applications can be implemented to increase the evaporation rate of salty water and desalination processes [230–232]. The improvement of produced freshwater of solar-driven desalination has been evaluated by Liu et al. [233], where twin PCMs made of n-tetracosane and n-eicosane and SiO_2/Fe_3O_4 were considered as a shell with a coating of polypyrrole layer and decorated MXene nanoplates. The results indicated that the distillation rates of the system were approximately 2.04 kg/m^2hr and 4.11 kg/m^2hr respectively, using 1000 W/m^2 and 2000 W/m^2. Chen et al. [234] further improved the desalination performance of combined solar evaporation systems using encapsulated PCM, where the encapsulation was made using SiO_2 as a shell and paraffin wax as a PCM. The mixture of encapsulated PCM with salt water with a concentration of 5 % was considered as an operating fluid of the system. Their findings showed that the freshwater generated by the system using modification was enhanced by 23.1 % at encapsulated PCM weight fraction of 0.18. Zhang et al. [235] have evaluated the influence of encapsulated PCM on the performance of the seawater desalination processes, using n-docosane as a PCM and a combination of SiO_2, sodium alginate and MXene nanoplates considered as a shell and capsules. The simulation was conducted by solar radiation of 1000 W/m^2, whereby the salty water concentration was approximately 3.5 %, as depicted in Fig. 46. The obtained findings showed that the water generation of the system in solar intensity simulation and natural solar radiation was approximately 1.4 L/m^2 and 1.01 L/m^2, respectively.

4.14. *Combined solar energy application*

Tafavogh and Zahedi [236] have performed a numerical comparison study of geothermal heat pump and microalgae pond to generate microalgae biomass with PTC, solar still and PV panel to produce simultaneous water, electrical power and thermal energy needed for encapsulated of n-Octadecane by polymer as a shell with mini-emulsion polymerization and conversion of bio-oil into biodiesel, and wind turbine/PEM to generate energy. MgO/MWCNT-water hybrid nanofluid was utilized to enhance the performance of the solar collector, as

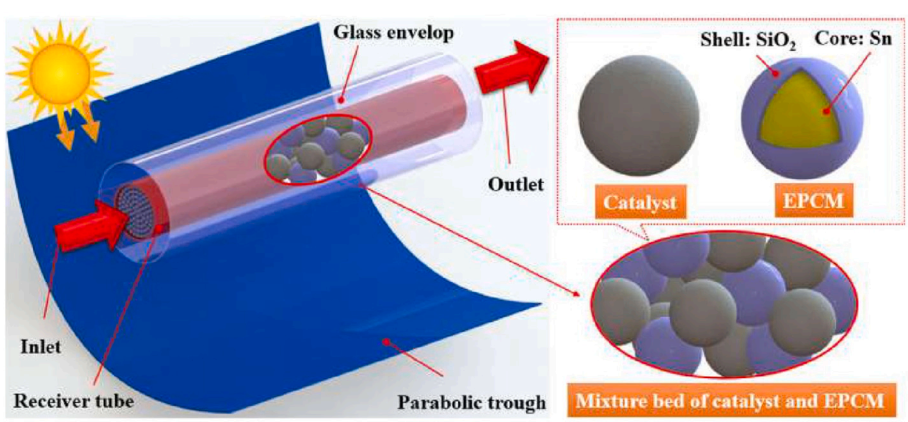

Fig. 44. Solar parabolic trough receiver reactor using encapsulated PCM [228].

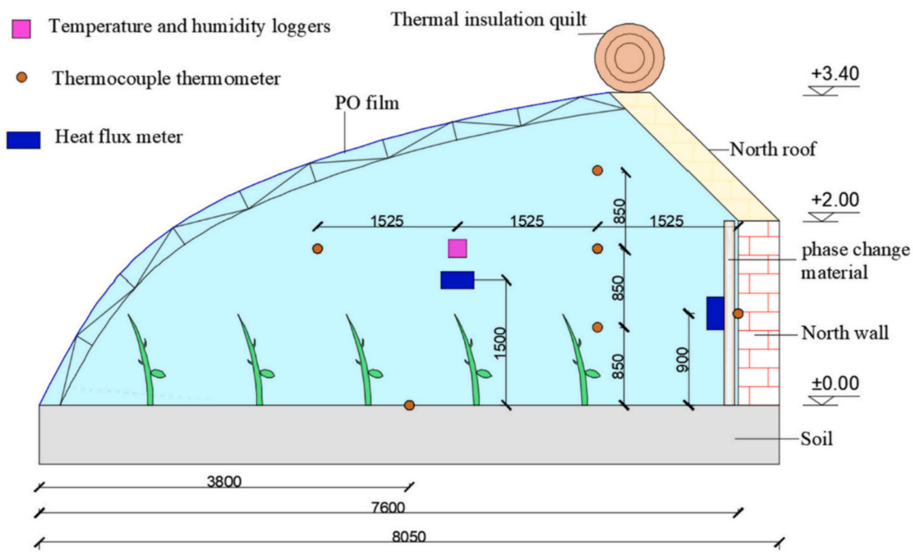

Fig. 45. The greenhouse setup by using encapsulated phase change material [229].

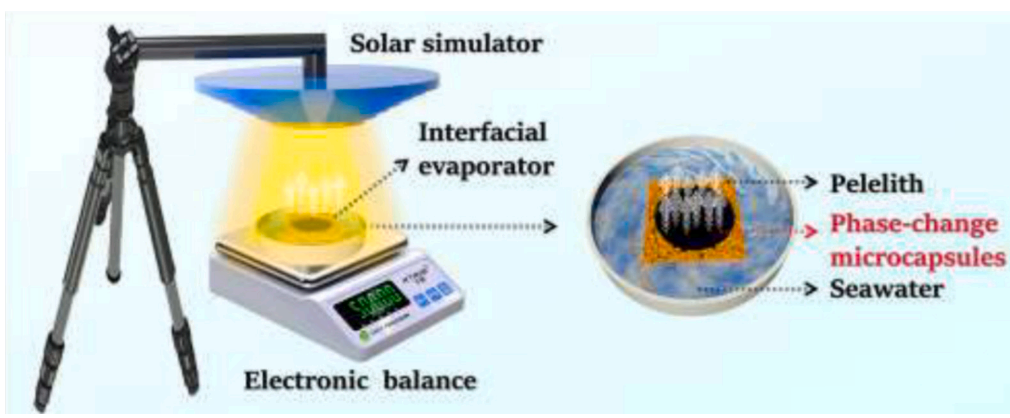

Fig. 46. Solar-driven evaporation process using encapsulation PCM [235].

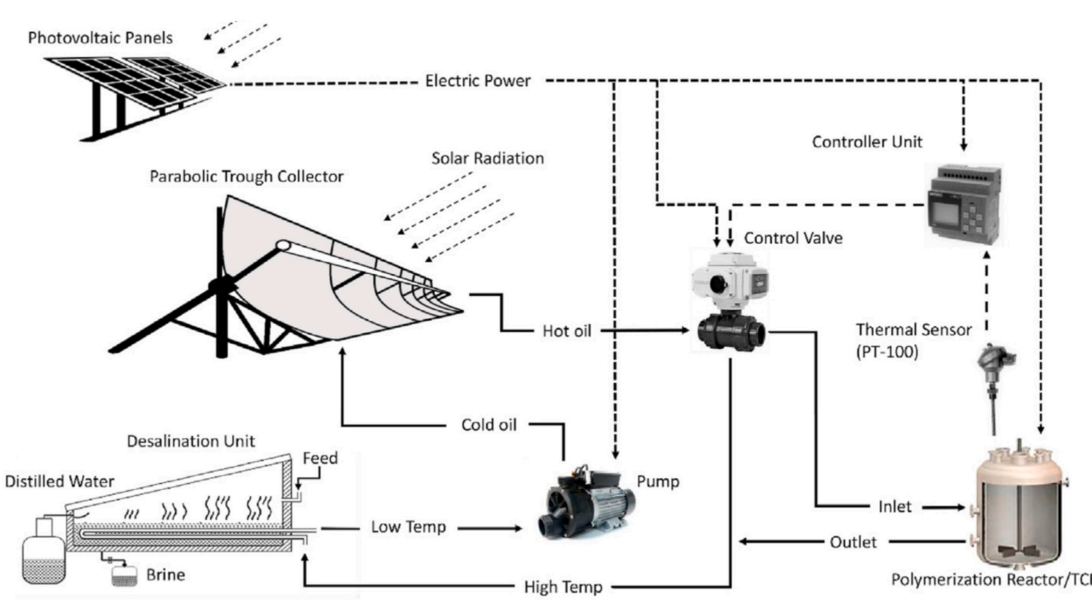

Fig. 47. Hybrid renewable energy system using encapsulated PCM [236].

presented in Fig. 47. The hybrid nanofluid flowed from the solar collector to the copper pipe, which was immersed in the basin water of a solar still with flow rates from 1.5 to 3 L/min. The PEM water was supplied from the saline water of the solar still. Results presented that the use of encapsulation PCM coupled with this hybrid system could improve biodiesel generation by 34.9 %. They also presented that by generating an electrical power of approximately 2.48 kW, the NOx emitted by the system decreased by 12 % compared to pure diesel. Table 5 presents the comparison results of solar energy applications using encapsulation PCM. Their results showed that encapsulated PCM can have a high impact on the improvement of solar energy application performance. The highest water productivity in solar desalination using paraffin wax and copper balls as an encapsulated PCM with integrated CPC and CCC was achieved at an approximate rate of 7346 mL/m^2. Additionally, paraffin wax with different melting points and various shells were used as a coolant for the PV panel. The encapsulated PCM decreased the surface PV panel temperature by about 5 °C, which led to an increase in the exergy efficiency of the system by 66 %. The highest increased energy efficiency of the solar water and air heater coupled with paraffin wax as a PCM were approximately 12 % and 66 %, respectively. Further, it can be seen that the thermal cooking power of solar cookers using paraffin wax/small detachable capsule and RT64HC/aluminum were approximately 54.71 W and 53.21 W, respectively. As observed in their study, the high-temperature salty PCMs/capsules were considered in the concentrating solar power system, whereby the use of alkali chloride salt eutectic as a PCM and zinc capsules increased the thermal efficiency of the concentrating solar power by approximately 45 %. Coupling of Sn/SiO_2 as an encapsulated PCM with solar thermochemical reactor increased the performance of the system by approximately 23.2 % Moreover, water generation from a solar steam generator using paraffin/SiO_2 encapsulated PCM was increased by 23.1 %, while the energy consumption was decreased by approximately 18.3 %.

4.15. Concrete curing based on solar thermal energy storage

In order to prevent concrete from frost damage and rapidly growth of concrete strength in cold climate, curing of concrete has been investigated by various authors using thermal energy storage. Yu et al. [237] used thermal energy storage layer around concrete material having transparent layer outside to fully absorb the solar radiations. The eutectic salt hydrated was applied as a thermal energy storage material and results concluded that this combination gives good curing by taking only 60 h to reach the design strength. The economics aspects also suggested this material as low cost, energy saving and environmentally friendly.

Liu et al. [238] also investigated paraffin/expanded graphite composite PCM in the wall to prevent it from excessive heating and to reduce energy consumption. The PCM material was mixed with cement, foams were added, and mixture was stirred and was put into mold. The results indicated that foamed cement blocks with 30 % PCM contents have the best thermal energy storage performance and can maintain the lowest average indoor temperature. Patel et al. (Location optimization of phase change material for thermal energy storage in concrete block for development of energy efficient buildings) performance study to determine the optimized location of PCM material in concrete wall. Six various combinations having three slots each, embedded with PCM, PU Foam, and air in varying order were set and optimum location of PCM was find out. It was concluded that PCM on outer side, PU Foam on inner side, and air in middle was the best for optimum performance. Ren et al. [239] incorporated encapsulated PCM/carbon nanofibers in concrete wall to improve the properties of wall material. Ternary fatty acid was used as encapsulated PCM as well as with carbon nanofibers incorporated in the concrete wall. The results concluded that 28 days of compressive strength was sustainable by using this combination and they provided excellent thermal conversion. Table 5 illustrates comparison results of encapsulation PCM integrated with solar energy applications.

5. Solar energy application by encapsulation of nano-enhanced PCM

Adding advanced energy materials, including nanoparticles, into the phase change material to generate the nano-enhanced PCM can have a major influence on the performance of thermal batteries [240]. One of the most important parameters when selecting a nano-enhanced PCM is the melting point of the PCM, with consideration of the temperature range of the solar energy application. Accordingly, nanoparticles raise the thermal conductivity of the PCM and also reduce the time speed of storing and removing thermal energy from PCM.

5.1. Solar desalination

Afolabi et al. [241] have examined the impact of encapsulated nano-enhanced PCM on freshwater yield of a double slope solar desalination system, whereby Zn nano powders were dispersed into the paraffin wax and then poured into the rectangular polystyrene mold as an encapsulated nano-enhanced phase change material, as shown in Fig. 48. The resulting measurements were recorded under Malaysian weather conditions, whereby the obtained results indicated that the average produced freshwater of the system, with and without encapsulated nano enhanced PCM, was approximately 4500 mL/m^2 and 2800 mL/m^2, respectively.

The evaluation of solar desalination systems using micro-encapsulated nano-enhanced PCM (MENEPCM) has been performed by Shajahan et al. [242]. In their study, silver nano powders were poured into paraffin wax to increase thermal conductivity, whereby the shell of the encapsulated PCM was constructed using a 0.0015 m thickness aluminum sheet. The results showed that the use of MENEPCM in double solar stills increased freshwater productivity by approximately 62.53 % in comparison with conventional devices. Shoeibi et al. [136] have examined the impact of encapsulated nano-enhanced PCM, nano-coated and porous absorbers on the improvement of solar still water generation. In their study, copper pipes act as shells of encapsulated and paraffin wax/Al_2O_3 and paraffin wax/CuO were considered as a core of the encapsulated PCM. The CuO nano powders were dispersed into black dye and sprayed on the encapsulated copper pipe. Anthracite media was poured into the water to enhance absorption of solar irradiation. The findings elucidated that the produced water of solar desalination using paraffin wax/Al_2O_3 and paraffin wax/CuO encapsulated nano-enhanced PCM were approximately 55.8 % and 49.5 %, respectively. Fig. 49 presents the double slope solar stills using encapsulated nano-enhanced PCM.

In another study by Shoeibi et al. [243], the authors compared various configurations of solar stills using encapsulated PCM, encapsulated nano-enhanced PCM and a porous absorber. Within their study, the evaporation area of the solar still was approximately 0.48 m^2, whereby twelve copper tube was considered as a shell of the encapsulated system and nano enhanced PCM was used as phase change material. Copper oxide/paraffin wax at a concentration of 0.2 % was poured into the copper tube. The results showed that the distilled water of the system using encapsulated nano enhanced PCM improved by 41.94 %. Fig. 50 shows the phase change material and nano enhanced PCM used in the solar still.

5.2. Photovoltaic/thermal

Ramya et al. [244] have boosted the performance of a solar panel using encapsulated nano-enhanced PCM, whereby ZnO nanoparticles dispersed into paraffin with awas used volume fraction of 0.5 % to construct the nano-enhanced PCM. The energy storage material was filled in the aluminum capsules with a thickness of 0.1 m to boost heat

Table 5
The comparison results of encapsulation PCM integrated with solar energy applications.

References	Types of solar energy	Location	PCM material	Capsules material	Other study parameter	Results
[173]	Hemispherical solar desalination	India	Paraffin wax	Aluminum-can		Generated water (Three E-PCM) → 67.12 %↑ Generated water (Four E-PCM) → 92.80 %↑
[76]	Single-slope, tubular and pyramid solar desalination	India	Paraffin wax	Copper balls	Compound parabolic concentrator (CPC) and Compound conical concentrator (CCC)	Generated water (CCC-SSS with E-PCM) → 3240 mL/m^2 Generated water (CPC-CCTSS-PSS with E-PCM) → 7346 mL/m^2
[174]	Single-slope solar desalination		Sodium Thiosulfate Penta hydrate	Stainless steel	Solar collector	Generated water (With E-PCM) → 4300 mL/m^2
[77]	Single-slope solar desalination	India	Two types of paraffin wax	Galvanized iron		Generated water (With E-PCM1) → 4020 mL/m^2 Generated water (With E-PCM2) → 4400 mL/m^2 Generated water (Conventional) → 3680 mL/m^2 Exergy efficiency (With E-PCM1) → 3.23 % Exergy efficiency (With E-PCM2) → 3.52 % Exergy efficiency (Conventional) → 3.92 % Thermal efficiency (With E-PCM1) → 42.29 % Thermal efficiency (With E-PCM2) → 46.29 % Thermal efficiency (Conventional) → 38.72 %
[175]	Single-slope solar desalination	Iraq	Paraffin wax		Ultrasonic vaporizer and solar water heater	Highest generated water→ 415 %↑ Highest energy efficiency→ 39.3 %
[176]	Photovoltaic/thermal	Colombia	Rubitherm, RT-35	Self-adhesive polyvinyl acetate	Cooling fluid	Daily hybrid efficiency (Modified) → 31.35 % Daily electrical efficiency (Conventional) → 13.12 %
[177]	Photovoltaic/thermal	China		Aluminum	Microchannel heat pipe	Daily hybrid efficiency (With E-PCM) → 36.71 % Daily hybrid efficiency (With microchannel heat pipe) → 35.53 % Daily hybrid efficiency (Conventional) → 31.87 %
[178]	Photovoltaic/thermal	Lab condition	PCM18, 26 and 32	Silica	Add PCM to water as a coolant and optical filtration	Solar panel temperature (Cooling channel) → 5 °C↓ Solar panel temperature (Optical filtration) → 10 °C↓ Exergy efficiency (Cooling channel) → 66 %↑ Exergy efficiency (Optical filtration) → 208 %↑
[179]	Photovoltaic/thermal		Paraffin (MPCM 28)	Polymer	Serpentine copper pipe under the PV	Power generation (Modified) → from 10 to 15 %↑
[180]	Photovoltaic/thermal	Lab condition	Rubitherm RT-44 HC	Copper tube	Thermal water bath	Heat transfer coefficient (flow rate of 0.5 L/min) → 57 %↑ Heat transfer coefficient (flow rate of 1 L/min) → 104 %↑ Heat transfer coefficient (flow rate of 2 L/min) → 130 %↑
[181]	Photovoltaic/thermal	China	Paraffin (RT24)	Copper tube		Solar panel temperature →6 °C↓ Electrical efficiency → 3 %↑
[182]	Photovoltaic/thermal		Paraffin (RT25 and RT35)	Aluminum	dual-axis tracked multi-segment mirror concentrator	Total electrical efficiency → 21.3 %↑ Total thermal efficiency → 5.29 %↑
[183]	Photovoltaic/thermal	Macau	Paraffin		Solar tracking	Total electrical efficiency → 10 %↑ Total thermal efficiency → 5 %↑
[186]	Solar water heater		Polyethylene glycol			The couple of encapsulated polyethylene glycol with solar water heater can compensate for existing problems such as low use of solar energy and intermittent solar energy.
[187]	Solar water heater		paraffin wax	Urea methacrylate		The use of dosage of 5 wt% of nucleating agent (ammonium chloride) and double

(continued on next page)

Table 5 (*continued*)

References	Types of solar energy	Location	PCM material	Capsules material	Other study parameter	Results
						emulsions (Brij 35 and Brij 30) led to higher core media content of 68.55 % and efficiency of encapsulation of 97.93 %
[188]	Solar water heater	China	Three types of paraffin wax	Polycarbonate	Flat plate solar collector	The energy and exergy efficiencies of the modified system was more than conventional system.
[189]	Solar water heater		Paraffin wax	Steel cylinders	Evacuated tube solar collector	By increasing the number of encapsulated PCM, time needed for melting complete was decreased
[190]	Solar water heater		Paraffin wax	HDPE	Jacketed shell heat exchanger	Energy storage density → 39 %↑ Exergy efficiency → 16 %↑ Time of hot water supply → 25 %↑
[191]	Solar water heater	Jordan	Paraffin wax	Aluminum bottle	Flat plate solar collector	During experiments (24 h), the stored water temperature remained at least 30 °C more than the ambient temperature.
[192]	Solar water heater	Bangladesh	Paraffin wax	Copper tube	Solar tracker and CPC	Highest water output temperature efficiency → 62 °C Thermal efficiency (between 4 and 5 p. m.) → 10–12 %↑
[193]	Solar water heater	Iran	Paraffin wax		circular trough collectors	The system can supply higher than 1200 l of hot water at temperature of 60 °C in eight hours.
[194]	Solar air heater		Paraffin wax	Aluminum with black paint coated		Energy efficiency (square staggered packed bed) → 15.3 %↑ (other arrangement)
[195]	Solar air heater	India	Paraffin wax	Cylindrical tube	Finned capsulated	Highest energy efficiency → 66 %↑
[196]	Solar air heater		Paraffin wax	Spherical HDPE		Enhancing the difference between the enter temperature of HTF and the phase change temperature of the PCM has high impact on the charging speed in comparison to the influence due to improving the flow rate of the fluid/ reducing the PCM balls size
[197]	Solar air heater	India	Paraffin wax	Stainless steel		Energy efficiency (Flat plate absorber with E-PCM) → 40 % Energy efficiency (Inclined flat plate absorber with E-PCM) → 42.2 %
[198]	Solar air heater	India	Paraffin wax	Metallic capsule	Rectangular and Cylindrical capsules	Energy efficiency (Rectangular macro-capsules) → 47.2 % Energy efficiency (cylindrical macro-capsules) → 67 %
[199]	Solar air heater	Pakistan	Paraffin wax (RT44HC and RT18HC)	Aluminum finned tube		Energy efficiency (conventional) → 53.2 % Energy efficiency (RT44HC located in upper pass of system) → 68.4 % Energy efficiency (RT44HC and RT18HC located in upper and lower pass of system) → 71.9 %
[200]	Solar air heater		Paraffin wax, n-octadecane and calcium-chloride hexahydrate			Heat absorbed (With tube circular arrangement of Paraffin wax) → 9.17 %↑ Heat absorbed (With tube circular arrangement of n-octadecane) → 1.55 %↑ Heat absorbed (With tube circular arrangement of Calcium-chloride hexahydrate) → 1.08 %↑
[201]	Solar air heater	Tunisia	AC27	Rectangular cavity Spherical container		Daily energy efficiency →47 %
[202]	Solar air heater	Tunisia	SN27	Molded from a blend of polyolefin		Daily energy efficiency →from 32 % to 45 % Daily exergy efficiency →from 13 % to 25 %
[203]	Solar box cooker	South Africa	Erythritol	Aluminum alloy		Optimal thermal performance was obtained in capsules with 50 mm radius and wall thickness of 1 mm
[204]	Solar box cooker	India	Paraffin wax	Small detachable capsule		Thermal energy efficiency →45.7 % Cooking power →54.71 W
[205]	Solar box cooker	India	RT64HC	Aluminum		Thermal energy efficiency →52.2 % Cooking power →53.21 W
[206]	Concentrating solar power		KNO3	Stainless steel	Numerical study	For a power block of 80 MWe a mitigation in levelized electricity prices of 8 % was calculated together with an improve in capacity factor by 30 %.
[207]	Concentrating solar power		Sb_2O_3, $BaCO_3$ and Na_2CO_3	Stainless steel	Numerical study	The heat cycling of the E-PCM shows that the core and shell material retains its

(*continued on next page*)

Table 5 (*continued*)

References	Types of solar energy	Location	PCM material	Capsules material	Other study parameter	Results
						mechanical characteristic for 1250 charge/discharge cycles.
[208]	Concentrating solar power		Alkali chloride salt eutectic	Encapsulated zinc particles		System energy efficiency → 45 %↑
[209]	Concentrating solar power		60 wt% $NaNO_3$, 40 wt % KNO_3		Numerical study	By E-PCM heat of fusion of 124.5 kJ/kg, a three-layer cascade structure yields either a 9.7 % improve in annual power generation and 16 % reduce in thermocline tank diameter relative to a quartzite-filled tank.
[210]	Concentrating solar power		Li_2CO_3(35 %)-Na_2CO_3 (65 %)/ Li_2CO_3(32 %)-K_2CO_3(35 %)-Na_2CO_3(33 %)/K_2CO_3(51 %)-Na_2CO_3(49 %)		HTF of $NaNO_3$-KNO_3 And KCl-$MgCl_2$	By reducing the capsules size, the storage capital price decreases, exergy efficiency increases, and provides capacity improves.
[211]	Concentrating solar power		$NaNO_3$	Copper	Numerical study	The EPCM storage density is expected to be even higher for plant size TES systems with higher size capsules.
[212]	Concentrating solar power	Phoenix, AZ	$NaNO_3$ /NaCl (33 %)-KCl (24 %)-LiCl (43 %) /NaOH (80 %)-NaCl (20 %) /$MgCl_2$ (60 %)-KCl (20.4 %)-NaCl (19.6 %)	Stainless steel	Numerical study	The cost decreases in cost performance quotient (CPQ) as high at 80 % and in LCOE as high as 10 %.
[213]	Concentrating solar power		Li_2CO_3–60% Na_2CO_3–20 % K_2CO_3 (HT)/ $NaNO_3$ (LT)		Numerical study	The partial charge cycles of the PCMs lead to a better thermocline development into the latent-heat packed-bed surface.
[214]	Concentrating solar power		$NaNO_3$/ KOH, Zn/Al/Mg, Zn/Al, (Li,Na,K)$_2CO_3$, Al/Si/Mg, Al/Cu/Mg	C. steel, S. steel, Ni 200/201, Haynes 188 and 556, Haynes 188 and 556, 316 S. steel, Ti and its alloys Ceramics, Ti and its alloys Ceramics	Numerical study	Careful selection of the most suitable high-temperature PCMs, their encapsulation materials and encapsulation methods were demonstrated.
[215]	Concentrating solar power		$NaNO_3$-KNO_3	Stainless steel 316	Numerical study	The proposed model and experimental analysis presented that the model was best fits in concentrating solar power application.
[216]	Concentrating solar power		Li_2CO_3(20 %)–Na_2CO_3 (60 % (–K_2CO_3(20 %)		Numerical study	By decreasing the encapsulation size, the total and latent implementation was increased
[217]	Concentrating solar power		$NaNO_3$/ Li_2CO_3–60% Na_2CO_3–20 % K_2CO_3		Numerical study	MLSPCM thermocline thermal energy storage by an optimizing the packed-bed shaped was high cost-effective than the other thermocline TES application.
[218]	Concentrating solar power		H325, H425, H525		Numerical study	The optimal performance of DMT or ST can be obtained with an effective area per unit volume of about 150 $m^2\ m^{-3}$. Beyond this amount, enhancing the surface area will only add extra unnecessary price.
[219]	Concentrating solar power		A164		Numerical study	The ability of the latent heat TES to receive and remove heat is high enhanced by improving flow rate and inlet charging temperature.
[220]	Solar cooling	Tunisia	Ruitherm RT6 and Linpar 14		TRNSYS model	The EPCM shows in order to determine the appropriate solution for thermal storage
[221]	Solar cooling	Kenya	Paraffin C5-C20	Aluminum		The EPCM located in the top and middle location of the refrigerator wall was reached the temperature required for freezing and is benefiting from the latent energy storage.
[222]	Perovskite solar cell		Ethylene glycol	Polymer resin		The charge transport resistance has no high change during 450 days of storage, which confirms no enhance in the defect density.
[223]	Solar fuels	China	n-Eicosane $C_{20}H_{42}$	Polyurea and polyurethane		The rod and flake-formed Au-TiO_2 photothermal catalysts added on the cover of encapsulated PCM, the amount of light-to-hydrogen efficiency of ATR@PCM and ATF@PCM was about 11.4 % and 5.0 %, respectively, which was about 53.8 % and

(*continued on next page*)

Table 5 (*continued*)

References	Types of solar energy	Location	PCM material	Capsules material	Other study parameter	Results
						56.1 % more than the pure photothermal catalyst without encapsulated PCM
[224]	Solar pond	Italy	Paraffin (RT 35HC)	Plexiglass		The heat convection in the reference case is higher and damage the interface until break.
[225]	Solar pond	China	Paraffin (RT 50 and RT 60)	Stainless steel		The installing EPCM to solar pond enhancers the quality of the heat energy of system.
[226]	Solar pond	China	Paraffin (RT 50 and RT 60)	Stainless steel	Numerical study	The, add of EPCM to the system has a direct impact on maintaining the stable temperature and stability of system.
[227]	Solar thermochemical reactor		Sn	SiO_2	Numerical study	EPCM enhances the performance indicator of reactor about 23.2 %.
[228]	Solar thermochemical reactor		Sn	SiO_2	Numerical study	Optimal catalytic distribution has a high enhance steady and unsteady performance.
[229]	Solar greenhouse	China	Calcium chloride hexahydrate	U-PVC		Confirmed the feasibility of external hung EPCM in severe cold regions of Northeast China
[233]	Solar steam generator	China	*n*-tetracosane and *n*-eicosane as twin PCM	SiO_2/Fe_3O_4 composite		The water vapor enhances in evaporation mass under intermittent solar illumination.
[234]	Solar steam generator		Paraffin	SiO_2		Water production →23.1 % ↑ Energy consumption→ 18.3 %↓
[235]	Solar steam generator	China	*n*-docosane	SiO_2		The evaporator has a high yield of distilled freshwater under intermittent solar illumination.
[236]	Combined solar energy application	Iran	n-Octadecane	Polymer		Decreasing the pollutant was obtained by designing a biodiesel/diesel/hydrogen for power generation.

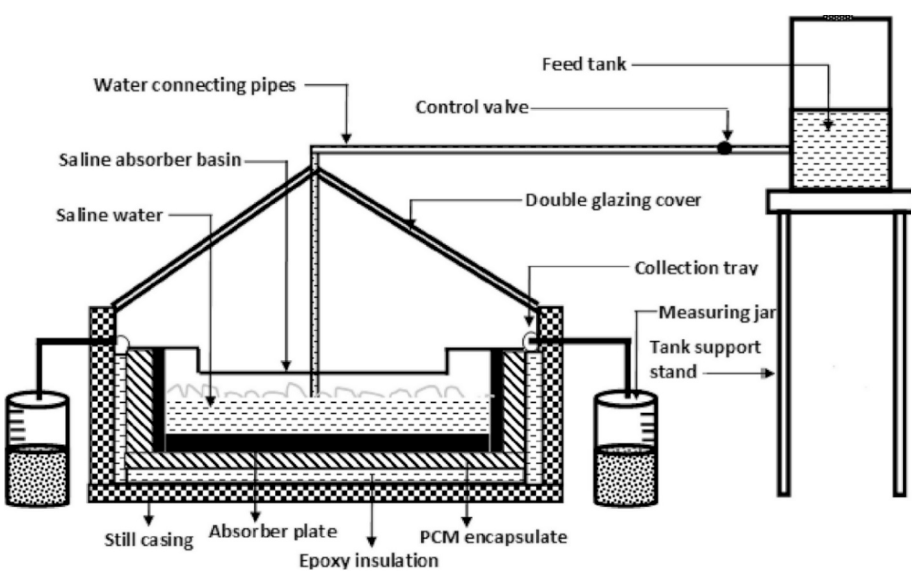

Fig. 48. Double-slope solar still by encapsulated nano-enhanced PCM [241].

transfer. Capsules were applied in cube formed to perfectly attached under the solar panel. The outcomes presented that the surface temperature of the PC panel using modification decreased by 28.9 %, where also the power efficiency of the system was enhanced by 14.88 %. The influence of nanofluid recirculation by micro-fin pipe and encapsulation of mixing nano-PCM on the electrical efficiency of the photovoltaic thermal system was assessed by Bassam et al. [245]. The operating fluid, which was made from SiC nanopowders mixed with water at a concentration of 0.6 %, was recycled between the water tank and attached copper pipes under the PV panel to cool the panel surface, as presented in Fig. 51. The SiC nanopowders were applied into the paraffin wax with volume fraction of 1 %, and then poured into capsules and installed under the solar panel. The results indicated that the maximum energy efficiency of the system was approximately 77.5 %, which was obtained in the system using nanofluid and encapsulated nano-PCM.

5.3. Solar water heater

Rinawa et al. [246] have assessed the effect of encapsulated hybrid nano-enhanced PCM on the performance of a solar water heater using a vacuum tube solar collector. Accordingly, CuO and SiO_2 nano powders of the same weight were mixed with 14 kg of paraffin wax at concentrations of 1 %. An aluminum cylinder with a diameter of 0.2 m and length of 0.25 m was filled with hybrid nano enhanced PCM and

Fig. 49. Double slope solar still using encapsulated nano-enhanced PCM, nano-coated and absorber media [136].

Fig. 50. The photo of a) PCM and b) nano-enhanced PCM used in solar still [243].

installed at the top of the water reservoir. The vacuum tube collector slope was selected to be at 26°. The experimental outcomes revealed that the water temperature of the solar water heater in the system using encapsulated PCM and the system using encapsulated hybrid nano enhanced PCM improved by 8.8 °C and 11.7 °C, respectively. Fig. 52 illustrates the experimental setup.

Kumar and Mylsamy [247] have introduced encapsulation of nano-enhanced PCMs to increase the efficiency of solar water heaters. In their study, CeO_2 nano powders were added to paraffin in mass fractions of 0.5 %, 1 % and 2 %. Five configurations of the system were used including: a conventional system, a system using PCM, a system using encapsulated nano-enhanced PCM at 0.5 % mass fraction, a system using encapsulated nano-enhanced PCM at 1 % mass fraction and a system using encapsulated nano-enhanced PCM at 2 % mass fraction. The highest energy and exergy efficiency of the system belonged to the system using encapsulated nano enhanced PCM at 1 % mass fraction, measuring at 79.2 % and 5.1 %, respectively. According to a study by Dhaou et al. [248], the efficiency of a solar water heater using nano-enhanced PCM capsules was increased. Two types of solar water heater, including jacketed shell and spiral heat exchanger with paraffin-copper at concentrations of 3.3 % as an encapsulated nano/PCM were compared, as presented in Fig. 53. Twenty cylindrical capsules with diameters of 0.006, a height of 0.12 m and thickness of 0.001 were considered to encapsulate the nano enhanced PCM and were installed in a circular array into the reservoir. Results presented that the speed of storing and removing the thermal energy of the encapsulated nano enhanced PCM was decreased by 12.5 % and 23.51 %, respectively.

5.4. Solar air heater

The impact of encapsulated nano-enhanced PCM on thermal efficiency of a solar air dryer has been evaluated by Subramaniam et al. [249]. In their study, aluminum oxide was dispersed in a stearic acid phase change material at a volume fraction of 0.3 %, and then filled in rectangular capsules with dimensions of 0.4 m × 0.4 m × 0.004 m. Parabolic solar concentrators were used to increase the temperature of the working fluid of the storage tank. The encapsulation nano/PCM was located in the storage tank, whereby water and engine oil with flow rates of 0.035 L/s, 0.045 L/s and 0.065 L/s were considered as a working fluid for recirculation between the solar air dryer and storage tank. Results indicated that the produced energy of the system using engine oil at a flow rate of 0.035 L/s was approximately 12.4, 14 and 15.1 less than the produced output of groundnut, ginger, and turmeric, respectively.

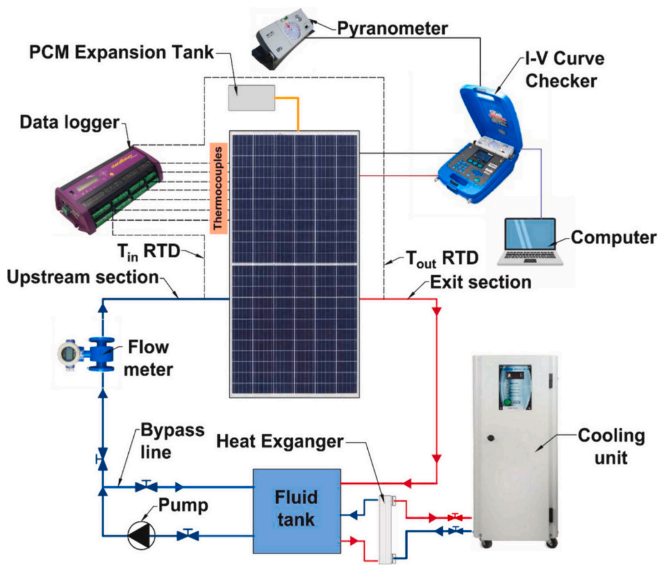

Fig. 51. The PV/T system by nanofluid and nano-encapsulation PCM cooling method [245].

5.5. Solar cooling

The influence of encapsulated nano-enhanced PCM and fins on performance of solar absorption cooling applications have been examined by Singh et al. [250]. In this study, graphene was added into 50 % $LiNO_3$/50 % KCl and filled into a conical-shaped shell both with and without fins to make encapsulated nano-enhanced PCMs. The obtained outcomes of their research showed that the melting speed of the NPCM decreased by 57 % by the proposed thermal design compared to the conventional system. The authors also showed that the CuO, SiO_2 and TiO_2 were not suitable nanopowders to design rapid charging solar chilling storage applications. Fig. 54 depicts the conical storage tank nano-enhanced PCM and fins.

5.6. Solar pond

Sarathkumar et al. [251] have enhanced the performance of a solar pond by using the nano-enhanced PCMs. They applied Al_2O_3 mixed with liquid paraffin filled in a copper rod to enhance the water temperature of their system. The solar pond body was constructed with a galvanized plate with dimensions of 0.6 m × 0.5 m × 0.6 m. The encapsulated PCM was located on the LCZ (lower convective zone), with findings showing that the highest value of the useful thermal energy of the system was approximately 167 W. Table 6 indicates the results of various nano-enhanced encapsulated PCM used in solar energy applications, whereby the extracted results show that the highest improvement in water productivity of solar desalination using nano-enhanced encapsulation PCM was achieved in the system by adding silver nanoparticles in paraffin and covering them in an aluminum sheet, where results were increased by 62.53 %. The electrical efficiency and thermal efficiency of the PV panel with added SiC nanopowders and paraffin as a nano-enhanced PCM and copper as a shell were approximately 9.6 % and 77.5 %, respectively. Thus, it can be seen that the nano-enhanced encapsulated PCM has a high impact on thermal performance of solar water and air heaters. In addition, the melting time of 50 % $LiNO_3$/50 % KCl as a PCM was decreased by adding nanoparticles to the solar cooling application. Table 6 depicts the comparison of nano-enhanced encapsulated PCM coupled with solar energy applications.

6. Operating temperature of encapsulation PCM

One important parameter for selecting encapsulated PCM/PCM materials is their melting point, where the amount of heat flux and temperature of the solar energy application can have a direct relationship with melting point of the energy storage material, which in turn leads to increased thermal performance of a solar energy application. In

Fig. 52. The photograph solar water heater using encapsulated hybrid nano-enhanced PCM [246].

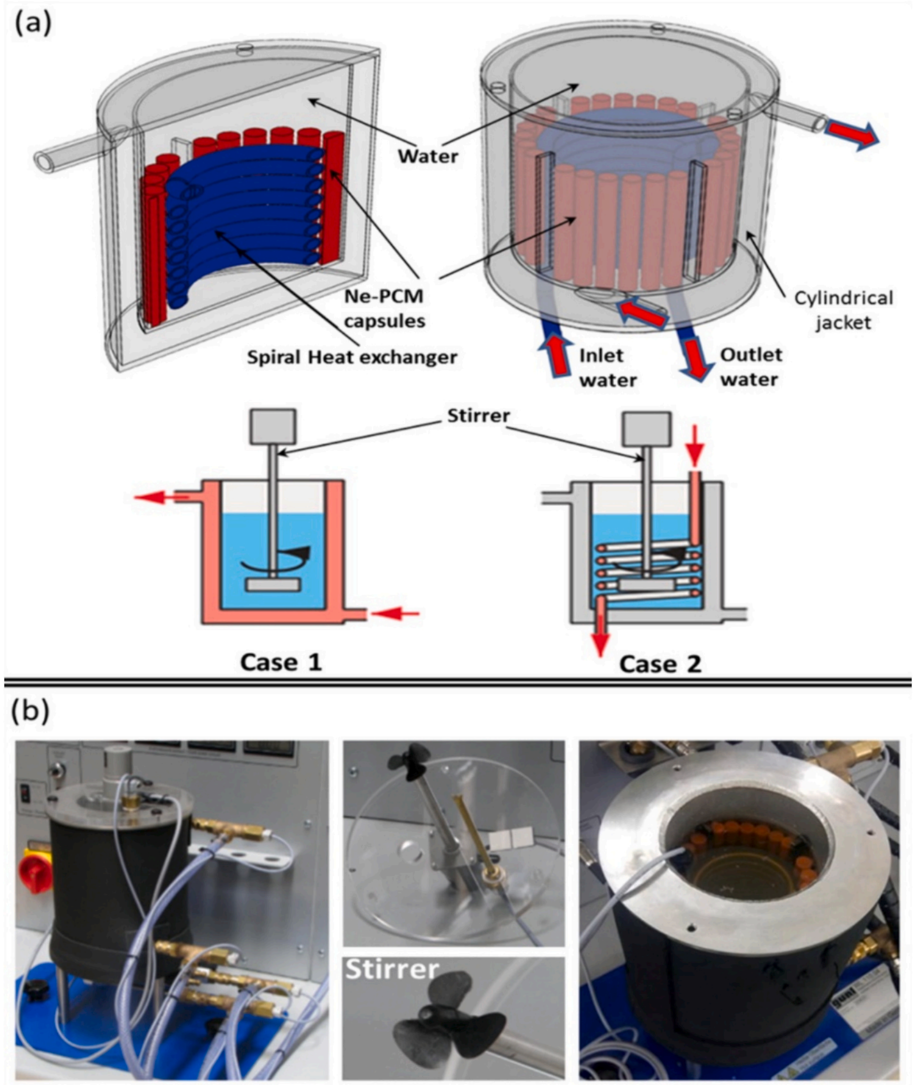

Fig. 53. Experimental setup with encapsulated nano-enhanced PCM [248].

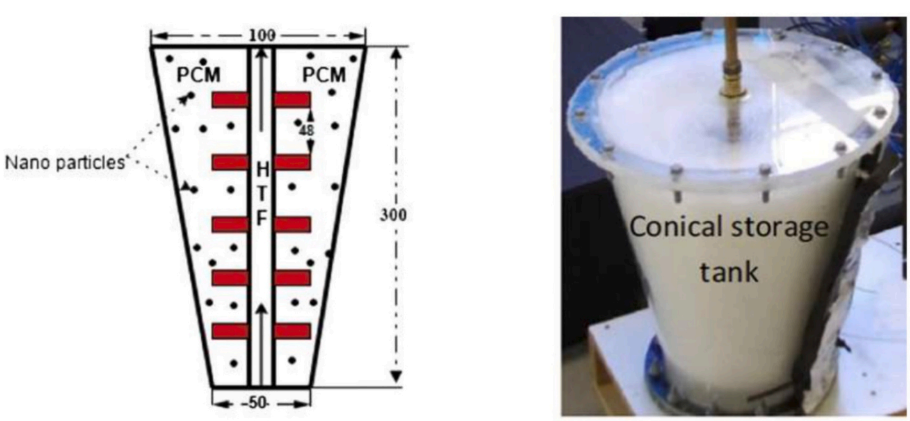

Fig. 54. Conical storage tank using nano-enhanced PCM and fins [250].

this study, encapsulated PCMs are divided into the categories: low temperature encapsulated PCMs with a melting range under the 30 °C; middle-temperature encapsulated PCMs with a melting range of 30 °C-100 °C; and high-temperature encapsulated PCMs with a melting range of over 100 °C. Table 7 presents the melting point of encapsulated PCM in various solar energy applications. As can be noted in the table, the low-temperature encapsulated PCMss including paraffin C5-C20/aluminum and calcium chloride hexahydrate/UPVC were considered in solar cooling and solar greenhouse. The middle temperature of encapsulation PCM was selected in solar desalination, PV/T, solar air

Table 6
The comparison table of nano-enhanced encapsulated PCM coupled with solar energy applications.

References	Types of solar energy	Location	PCM material	Capsules material	Nanomaterials	Results
[241]	Solar desalination	Malaysia	Paraffin wax	Epoxy resin composite	Zn	Water production→7.5 L
[242]	Solar desalination	India	Paraffin wax	Aluminum sheet	Silver	Water production→62.53 %↑
[136]	Solar desalination	Iran	Paraffin wax	Copper	Al_2O_3 and CuO	Water production (Paraffin/Al_2O_3) → 55.8 %↑ Water production (Paraffin/CuO) → 49.5 %↑
[243]	Solar desalination	Iran	Paraffin wax	Copper	CuO	Water production (Paraffin/CuO) → 41.94 %↑
[244]	PV/T		Paraffin wax	Aluminum	ZnO	Electrical efficiency →14.88 %↑
[245]	PV/T	Malaysia	Paraffin wax	Copper	SiC	Electrical efficiency →9.6 % Thermal efficiency →77.5 %
[246]	Solar water heater	India	Paraffin wax	Aluminum	Hybrid CuO and SiO_2	Water temperature (Paraffin wax) → 8.8 °C↑ Water temperature (Paraffin wax/Hybrid nanoparticles) → 11.7 °C↑
[247]	Solar water heater	India	Paraffin wax	Aluminum	CeO_2	Highest energy efficiency →79.2 % Highest exergy efficiency →5.1 %
[248]	Solar water heater		Paraffin wax		Cu	Completion time for charging and discharging is decreased by 12.5 % and 23.51 %
[249]	Solar air heater		Stearic acid		Al_2O_3	The produced energy of the system using engine oil at flow rate of 0.035 L/s was about 12.4, 14 and 15.1 less than produced output of groundnut, ginger, and turmeric.
[250]	Solar cooling		50 % $LiNO_3$/ 50 % KCl		Graphene, Al_2O_3, CuO, SiO_2, and TiO_2	Melting time →57 %↓
[251]	Solar pond		Paraffin wax	Copper	Al_2O_3	Highest useful heat→167 W

and water heaters, solar fuels, solar ponds, solar steam generator and perovskite solar cells, due to the operating temperature of these systems. In addition, the concentrating solar power and solar thermochemical reactor were in the high-temperature encapsulation PCM. The outcomes show that the highest and lowest melting point of encapsulated PCM was obtained in cubic $BaCO_3$ and paraffin C5-C20, which were approximately equal to 982 °C and 5 °C, respectively. Table 7 shows melting point of various encapsulation PCM/Nano-enhanced PCM used in solar energy applications.

7. Economic and environmental evaluation

7.1. Trade-offs and synergies in solar schemes

The use of encapsulation PCMs have many advantages and disadvantages. The use of this method can store thermal energy as a thermal battery in different solar energy systems with a wide temperature range. Choosing the correct shell and core is very important in solar energy systems, whereby failure to choose the right material can damage the shell at high operating temperatures. One of the most important problems with encapsulated PCMs/Nano-PCMs is the failure of the shell structure at high temperatures or when they are hit, which in solar energy systems including solar still desalination, solar steam generator and solar cookers, all of which increase the possibility of water or food intoxication. High resistance to impact and temperature can be a suitable solution for this problem. The main source of thermal energy in solar energy systems is the sun, which in the most optimistic case transfers energy to the earth for approximately 10 h during daytime. Therefore, only thermal energy storage in encapsulated PCMs can increase the performance of a solar energy system, but it is not yet possible to use these systems throughout the night when there is no sun. As can be seen in Section 5, there is yet to be a study on concentrating solar power systems using encapsulation nano-enhanced PCM to improve the power of a system. The mixing of nanoparticles in PCMs increases the thermal properties of the PCMs themselves and leads to an enhancement of the performance of a system.

Application of phase change materials is not a novel approach, where in the spacecraft environment this has been extensively and practically explained as early as in 1971. Accordingly, in recent years PCMs at different temperature ranges of 5–15 °C, 25–45 °C, 55–75 °C, 100–175 °C and >300 °C have been utilized in different applications, such as building temperature regulation, preheat of domestic hot water, absorption cycle and concentrated solar power plant, respectively [217]. However, PCM utilization in solar energy schemes experience several problematic issues regarding the type of application; hence, the encapsulation process is an appropriate approach that has been proposed to fill existing gaps. At the forefront of synergies of encapsulation processes, which are common in most solar energy applications, is prevention of direct contact of PCMs with structure, materials and/or liquid/solid mediums (i.e., water, absorbers etc.). This, in turn, results in a PCM not being subjected to any changes in initial chemical structure, and to maintaining its original characteristics. Furthermore, encapsulated PCMs are easier to install in solar-driven systems as compared to pure PCMs, since leakage phenomenon to the system during phase transition is plausible. Impressively, encapsulation at different sizes makes this mode a flexible option for a wide range of applications in solar energy. For instance, in solar stills macro-encapsulated PCMs can be adjusted to the size of solar stills [136], while for solar steam generators, which generally are a smaller size, micro-encapsulated PCMs are used [235]. Meanwhile, the response time for storing and releasing energy can vary for different types of solar energy systems, where subsequently the type of encapsulation plays a vital role. It is important to note here that whilst PCM response time is a function of melting temperature and specific heat capacity, storing and releasing nano-encapsulated PCMs in similar conditions (i.e., similar core/shell materials) compared to macro-encapsulated PCM occurs at a faster pace. Lastly, the encapsulated PCMs can increase the heat load capacity of solar energy systems to harness the maximum energy entered into the systems, subsequently leading to improved performance.

Although encapsulated PCMs at all sizes have been considered as a modification method to improve the performance of systems, this strategy also has several obstacles, which should be managed carefully. Perhaps, one of the most well-known trade-offs of encapsulated PCMs are the negative effects that reduce the effectiveness of PCMs related to the shell material. Even with superior thermal conductivity, these can negatively impact available energy storage and release to solar energy systems because a certain amount of entered solar energy would be exploited for increasing the temperature of encapsulation shells. Furthermore, another issue regarding encapsulated PCMs is the fracture of shells as a result of being hit by hard surfaces and/or edges, making PCMs inefficient. In addition to this, leaking of PCMs through shell cracks can make the system at risk of spilling PCM materials into the

Table 7
The melting point of various encapsulation PCM/Nano-enhanced PCM used in solar energy applications.

References	Type of solar application	PCM material	Capsules material	Melting point (°C)
Low temperature encapsulation PCM				
[221]	Solar cooling	Paraffin C5-C20	Aluminum	5–6 °C
[229]	Solar greenhouse	Calcium chloride hexahydrate	U-PVC	26.5 °C
Middle temperature encapsulation PCM				
[173]	Hemispherical solar desalination	Paraffin wax	Aluminum-can	58–60 °C
[183]	Photovoltaic/thermal	Paraffin wax		50 °C
[187]	Solar water heater	PARAFFIN wax	Urea Methacrylate	48 °C
[190]	Solar water heater	Paraffin wax	HDPE	55 °C
[193]	Solar water heater	Paraffin wax		60 °C
[195]	Solar air heater	Paraffin wax	Cylindrical tube	54 °C
[198]	Solar air heater	Paraffin wax	Metallic capsule	58–60 °C
[205]	Solar box cooker	RT64HC	Aluminum	64 °C
[222]	Perovskite solar cell	Ethylene glycol	Polymer resin	43–60 °C
[223]	Solar fuels	n-Eicosane $C_{20}H_{42}$	polyurea and polyurethane	39.5–40 °C
[224]	Solar pond	Paraffin wax (RT 35HC)	Plexiglass	34–36 °C
[225]	Solar pond	Paraffin (RT 50 and RT 60)	Stainless steel	RT 50 → 47 °C to 56 °
[226]	Solar pond	Paraffin (RT 50 and RT 60)	Stainless steel	RT 50 → 48 °C to 50° RT 50 → 58 °C to 60 °
[233]	Solar steam generator	*n*-Tetracosane and *n*-eicosane as twin PCM	SiO_2/Fe_3O_4 composite	In the range of 48–50 °C and 50–45 °C
[234]	Solar steam generator	Paraffin	SiO_2	45.9–62.3 °C
[236]	Combined solar energy application	n-Octadecane	Polymer	34.1 °C
[241]	Solar desalination	Paraffin wax/Zn-nanoparticles	Epoxy resin composite	Paraffin wax → 38 to 45 °C Paraffin wax/Zn → 36 to 42 °C
[136]	Solar desalination	Paraffin wax/Al_2O_3 and CuO	Copper	Paraffin wax → 52 °C
[243]	Solar desalination	Paraffin wax/CuO	Copper	Paraffin wax → 52
[244]	PV/T	Paraffin wax/ZnO	Aluminum	40–45 °C
[247]	Solar water heater	Paraffin wax /CeO_2	Aluminum	Paraffin wax → 63.74 °C Paraffin wax /CeO_2 (0.5 wt%) → 63.44 °C Paraffin wax /CeO_2 (1 wt%) → 62.66 °C Paraffin wax /CeO_2 (2 wt%) → 63.01 °C
[248]	Solar water heater	Paraffin wax/Cu		Paraffin wax → 52 °C
High temperature encapsulation PCM				
[207]	Concentrating solar power	Sb_2O_3, $BaCO_3$ and Na_2CO_3	Stainless steel	Sb_2O_3 (656 °C) Hexagonal $BaCO_3$ (811 °C) Cubic $BaCO_3$ (982 °C) Na_2CO_3 (858 °C)
[208]	Concentrating solar power	Alkali chloride salt eutectic	Encapsulated zinc particles	400 °C
[209]	Concentrating solar power	60 wt% $NaNO_3$, 40 wt% KNO_3		300–600 °C
[210]	Concentrating solar power	Li_2CO_3(35 %)- Na_2CO_3 (65 %)/ Li_2CO_3(32 %)- K_2CO_3(35 %)-Na_2CO_3(33 %)/ K_2CO_3(51 %)-Na_2CO_3(49 %)		Li_2CO_3(35 %)- Na_2CO_3 (65 %) (505 °C) /Li_2CO_3(32 %)- K_2CO_3(35 %)-Na_2CO_3(33 %) (397 °C) /K_2CO_3(51 %)-Na_2CO_3(49 %) (710 °C)
[211]	Concentrating solar power	$NaNO_3$	Copper	308 °C
[212]	Concentrating solar power	$NaNO_3$ /NaCl (33 %)-KCl (24 %)-LiCl (43 %) /NaOH (80 %)-NaCl (20 %) /$MgCl_2$ (60 %)-KCl (20.4 %)-NaCl (19.6 %)	Stainless steel	$NaNO_3$ (310 °C) /NaCl (33 %)- KCl (24 %)- LiCl (43 %) (346 °C) /NaOH (80 %)-NaCl (20 %) (370 °C) /$MgCl_2$ (60 %)- KCl (20.4 %)-NaCl (19.6 %) (380 °C)
[213]	Concentrating solar power	Li_2CO_3-60%Na_2CO_3-20 % K_2CO_3 (HT)/ $NaNO_3$ (LT)		High temperature EPCM→ 550 °C Low temperature EPCM→ 308 °C
[214]	Concentrating solar power	$NaNO_3$/ KOH, Zn/Al/Mg, Zn/Al, $(Li,Na,K)_2CO_3$, Al/Si/Mg, Al/Cu/Mg	C. steel, S. steel, Ni 200/201, Haynes 188 and 556, Haynes 188 and 556, 316 S. steel, Ti and its alloys Ceramics, Ti and its alloys Ceramics	296–315 °C, 370–390 °C. 540–560 °C
[215]	Concentrating solar power	$NaNO_3$-KNO_3	Stainless steel 316	220 °C

(continued on next page)

Table 7 (*continued*)

References	Type of solar application	PCM material	Capsules material	Melting point (°C)
[216]	Concentrating solar power	Li_2CO_3(20 %)–Na_2CO_3 (60 %(–K_2CO_3(20 %)		550 °C
[217]	Concentrating solar power	$NaNO_3$/ Li_2CO_3–60%Na_2CO_3–20 % K_2CO_3	Stainless steel	
[218]	Concentrating solar power	H325, H425, H525		H325 → 323 °C H425 → 423 °C H525 → 523 °C
[219]	Concentrating solar power	A164		171 °C
[227]	Solar thermochemical reactor	Sn	SiO_2	505 °C
[228]	Solar thermochemical reactor	Sn	SiO_2	505 °C

structure and/or medium, while from another viewpoint this can also lead to environmental contamination through organic/inorganic chemical compounds. Moreover, in nano-encapsulation processes, the matter of the high-cost of manufacturing is of great importance, where this has not been thoroughly addressed in the literature. In contrast, fault diagnosis of nano-capsules in systems is another trade-off that has yet to be recognized. Interestingly, in relation to fault detection, taking advantage of internet of the thing (IoT) could be an efficient strategy. Further, in encapsulated PCMs, increasing the number of cycles of thermophysical properties and stability of the materials could reduce the performance of system as a result of deteriorating PCM properties. Some modifications could also be considered as having a 'double-edged sword' effect, like utilizing nanomaterial in PCMs. Generally, nanomaterials are used in PCMs in order to increase thermal conductivity, thus, they may address the reduction of PCM's effectiveness as the result of encapsulation. However, determining the type of used nanomaterial should be considered carefully, since highly efficient nanoparticles like graphene oxide could have a negative effect on the performance of a solar energy system [252]. Moreover, nanomaterials in PCMs tend to agglomerate, either via inappropriate well-dispersion during preparation processes or at the time of phase transition of PCMs; hence, particle aggregation can lead to a loss of positive impact on nano-enhanced encapsulated PCMs, and even prompt a negative effect on system performance. In contrast, immethodical increasing of thermal conductivity via adding nanomaterials could impact convective heat transfer of liquid-solid PCMs; hence, a rational procedure to improve thermal conductivity while maintaining good convection heat transfer characteristics is required.

7.2. Cost per productivity

In general, improving the productivity of solar energy applications and reducing the cost of their productivity are significant parameters for designing solar energy systems. The use of encapsulated PCM as a thermal battery in solar energy systems can have a high influence towards enhancing energy output and decreasing costs of productivity. By using high-cost methods, the productivity of solar energy systems is enhanced, whereby economical designs can decrease the primary cost of the systems. The balance between economical design and different methods in primary design contributes to better performance and leads to more cost-effective solar energy systems. The optimized design of solar energy systems can lead to an increase in distilled water from solar desalination systems, improving the electrical generation of photovoltaic panels, increasing the hot water generation of solar water heaters, enhancing the ambient air temperature of solar air heaters, improving the temperature of food in solar box cookers and reducing costs of productivity in these systems at the same time. Many methods have been utilized to analyse the economic parameters of solar energy applications. One of the most popular economic methods used to determine the production cost of the solar energy application is given by the following formula [253,254]:

$$\mathrm{CRF} = \mathrm{i}(1+\mathrm{i})^{\mathrm{n}} \Big/ \left[(1+\mathrm{i})^{\mathrm{n}-1}\right] \tag{10}$$

$$\mathrm{SFF} = \mathrm{i} \Big/ \left[(1+\mathrm{i})^{\mathrm{n}-1}\right] \tag{11}$$

$$\mathrm{ASC} = (\mathrm{SFF})\ \mathrm{S} \tag{12}$$

where

$$\mathrm{S} = 0.2\mathrm{P} \tag{13}$$

$$\mathrm{AC} = \mathrm{FAC} + \mathrm{AMC} - \mathrm{ASV} \tag{14}$$

$$\mathrm{FAC} = \mathrm{P}(\mathrm{CRF}) \tag{15}$$

$$\mathrm{AMC} = 0.15\ \mathrm{FAC} \tag{16}$$

where P, i and n present the present capital factor, interest rate and lifetime of solar energy application, respectively. The cost of distilled water in solar still application calculated by [255–257]:

$$\mathrm{CPL} = \mathrm{AC}/\mathrm{M} \tag{17}$$

where AC and M show the annual cost and produced water by solar still application. Further, for power generation of a photovoltaic thermal system, cost per power generation can be calculated by [138,258]:

$$\mathrm{CPP} = \mathrm{AC}/\mathrm{G} \tag{18}$$

where G presents the power production in one year by a solar panel.

7.3. Economic benefits of using encapsulated PCMs

Various authors investigated economic aspects of encapsulated PCMs in various solar systems and compared with conventional ones. Ahmed et al. [259] carried out economic analysis using finned-encapsulated PCM in pyramid solar still and compared with conventional solar still. The basin area of pyramid solar still was 1 m^2 and an overall efficiency of 49.9 % was observed using 40 mm encapsulated PCM fins in comparison to conventional one having 34.6 %. The cost of 1 L water produced from conventional, and 40 mm finned absorber with PCM pyramid solar stills were 0.047 and 0.043 \$/L respectively. Tyagi et al. [260] carried out economic analysis of encapsulated PCM in buildings to energy peak energy demand. The considered system was tested with air conditioning system having three heating loads of 1, 2, 3 KW. The per unit cost of power by coal, diesel and solar energy ere INR 5.5, INR 10 and INR 15, respectively however the payback period with solar energy was 0.94-year, 1.27 year and 1.26 year, respectively, for 1 kW, 2 kW and 3 kW. While it was 1.4-year, 1.9-year, 1.9 year, and 2.57-year, 3.46-year, 3.43 year for diesel and Coal in case of 1 kW, 2 kW and 3 kW respectively.

Faraj et al. [261] conducted energetic and economic analyses using macro-encapsulated PCM's with active underfloor hydronic heating system. It was concluded that 32 USD annual saving was found by this as compared to conventional one. By combining active and passive systems, annual savings of 227 USD could be achieved. Raj and Jayaraj [198] used macro-encapsulates in double pass solar air heaters for its cost analysis. The geometry of encapsulated PCM was varied and its effects were measured on the performance. The results concluded that having small margin in constructional cost, the operational time of the system was enhanced and heating cost for 1 kg of hot air was 0.0074$. Jacob et al. [262] carried out economic analysis using encapsulated PCM. From the results, it was found that PCM cost should be below $0.8/kg and cost of encapsulation depends mainly on shell material which should be optimized. The marginal savings were also found when carbon steel tank was used instead of stainless-steel tank. Table 8 indicates the economic assessment of systems using encapsulated PCMs.

7.4. Economic considerations for selecting encapsulation materials and compositions

The various economic aspects for selecting encapsulation materials should be considered in terms of respective application usage. The factors affecting during preparation of encapsulation PCM should be considered to optimize its cost. The core shell encapsulated PCM is expensive while shape stabilized is cost effective production process [266]. The materials cost in the preparation of encapsulation PCM is the core cost as an economic aspect for its selection. The initial cost and payback period should be calculated based on the prepared encapsulated PCM as it directly affects the overall calculations. The economic feasibility in the selection of encapsulated PCM is a key parameter as it determines the initial investment cost, return on investment and lifetime costs. Due to high production cost, the commercialization of encapsulated PCM is still challenging [267]. The lifetime of encapsulated PCM is also critical which directly links with economic aspect of it. The major economic considerations for selecting encapsulation materials and compositions are summarized in Fig. 55.

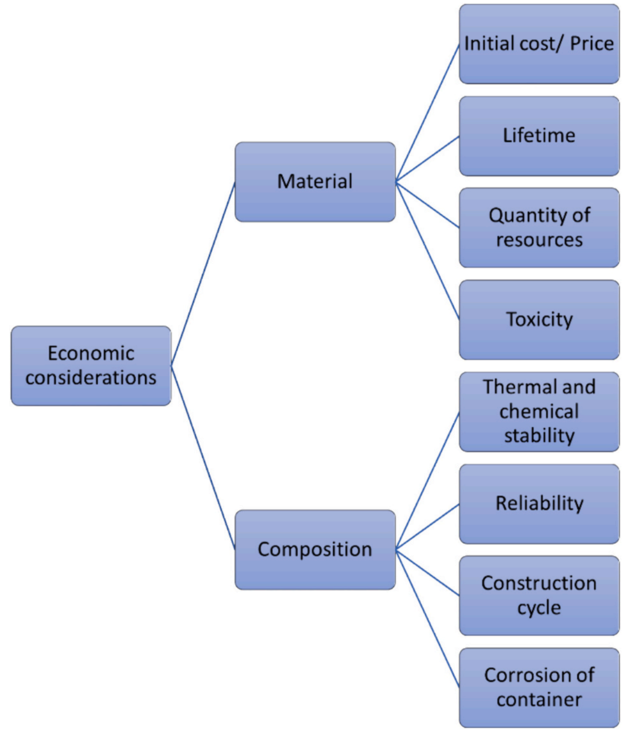

Fig. 55. Economic aspects for selecting encapsulation materials.

7.5. Exergoeconomic evaluation

The exergoeconomic parameter is an important parameter in solar energy systems due to its application in different fields. The exergoeconomic parameter has been utilized as an engineering and design technique, conducting thermodynamic balance by coupling exergy and cost-effective evaluation [268]. This parameter assists to collect information that cannot be extracted from energy, exergy, and economic assessment, where it can play a major role in designing and utilizing economical applications [139]. The exergoeconomic parameter is determined by produced energy and exergy to the AC of a solar energy application, and is calculated by [269]:

$$R_{Ex} = \frac{(E_{en})_{out}}{AC} \tag{19}$$

$$R_{En} = \frac{(E_{ex})_{out}}{AC} \tag{20}$$

where R_{En} and R_{Ex} present the exergoeconomic parameter with considering the energy and exergy, respectively. Further, $(E_{ex})_{out}$ and $(E_{en})_{out}$ depict the yearly generated exergy and energy of solar energy [270,271].

7.6. Greenhouse gases emission/mitigation

Besides economic and exergoeconomic parameters, environmental evaluation is a significant factor in designing solar energy systems, aiming to decrease environmental pollution by considering carbon dioxide removal. Environmental parameter sare one of the important analysis factors for solar energy application, which determine carbon dioxide emission mitigation by systems [272]. CO_2 emission reduction can be improved by increasing energy production from solar energy applications. Annual energy production can be obtained from annual CO_2 emission reduction in a solar energy application, which is approximately $(E_{en})_{out} \times 2$. Therefore, CO_2 emission reduction during the lifetime (n) of the application can be determined by $(E_{en})_{out} \times 2 \times n$ [273]. The net value of CO_2 emission reduction during a device's lifetime is the energy production by the solar energy application except for the embodied energy. The environmental factor of the solar energy application can be defined by [274,275]:

$$G_{co_2} = \frac{2\left((E_{en})_{out} \times n - E_{in}\right)}{1000} \tag{21}$$

where E_{in} and $(E_{en})_{out}$ presents the embodied energy (the energy

Table 8
Initial investment costs, operational expenses, lifecycle costs, and return on investment (ROI) for different solar technologies.

Module	Efficiency (%)	Performance ratio	Lifetime (years)	Payback period	ROI	References
Monocrystalline silicon panel	14.2	0.75	28.9	–	–	[263]
Polycrystalline silicon panel	13.2	0.77	29.8	–	–	[263]
Polycrystalline PV system	15.39	–	25	6.7 years	1.61	[264]
Pyramid solar still	34.6	–	10	10 years		[259]
Root zone heating	24.6	–	–	792 days/year	–	[265]
Underfloor hydronic heating system	227 USD annual saving	–	–	3.94 years		[261]
Solar air heater	47.2	–	10	–	0.17	[198]

required for the generation of the goods) and energy production by solar energy application.

7.7. Levelized cost of energy (LCOE)

The levelized cost of energy (LCOE) can be used as an economic parameter to determine cost evaluations of various systems, and is calculated by [276–278]:

$$LCOE = \frac{Xo + \sum_{i=1}^{N} \frac{OPE\ Xi}{(1+t)^{i}}}{\sum_{i=1}^{N} \frac{production\ ni}{(1+t)^{i}}} \tag{22}$$

where Xo, OPE Xi, production, t and N present the cumulative investment prices of the system, operation and maintenance cost of the system, annual electrical power production by the system, the discount rate of the project and lifespan of the system, respectively. Table 9 presents the economic and environmental parameters of different solar energy applications. The table's results showed that the encapsulation PCM/Nano-PCM decreases the cost per liter and enhances carbon dioxide reduction of solar water desalination systems. The lowest CPL and highest CO_2 reduction of solar desalination was achieved in the hemispherical solar still using paraffin/aluminum, which were 0.0111 $/L and 15.4 tons, respectively. Moreover, the cost per power generation of the PV panel using RT24/Copper encapsulation PCM reached to 0.6 $/W. In addition, the levelized cost of energy of concentrating power plant using KNO_3/stainless steel was reduced by 1.5 %. Table 9 represents the economic, exergoeconomic and environmental parameters of solar energy application using EPCM/Nano-enhanced PCM.

8. A new horizon towards realizing sustainable development goals (SDGs)-SDG7

When evaluating the development of renewable energy systems in the context of engineering, one pivotal area that has featured prominently relates to technical aspects and ways to further improve the performance of systems. However, there is another related consideration that has not received enough attention to date. The United Nations (UN) in 2015 announced Sustainable Development Goals (SDGs), consisting of 17 goals and 169 targets [279], calling on all governments to address their goals and targets by making practical efforts towards realizing them. Accordingly, these goals have interrelation with each other, whereby modifying one SDGs may benefit or impact other SDGs.

Table 9
The economic, exergoeconomic and environmental parameters of solar energy application using EPCM/Nano-enhanced PCM.

References	Types of solar energy	PCM material	Capsules material	Results
[173]	Hemispherical solar desalination	Paraffin wax	Aluminum	CPL (Three E-PCM) → 0.0128 $/L CPL (Four E-PCM) → 0.0111 $/L CPL (Conventional) → 0.0186 $/L CO_2 removal (Three E-PCM) → 13.44 tons CO_2 removal (Four E-PCM) → 15.4 tons CO_2 removal (Three E-PCM) → 8.19 tons
[174]	Single-slope desalination	Sodium thiosulfate penta hydrate	Stainless steel	Revenue in drinking water→78 $ Payback period→2.5 years
[175]	Single-slope solar desalination	Paraffin wax		CPL (Conventional) → 0.037 $/L CPL (E-PCM) → 0.056 $/L CPL (E-PCM and solar water heater) → 0.04 $/L CPL (E-PCM, solar water heater and ultrasonic vaporizer) → 0.028 $/L
[181]	Photovoltaic/thermal	RT24	Copper tube	Total cost of the system →0.028 $/m^2 Cost per power generation →0.6 $/W
[198]	Solar air heater	Paraffin wax	Metallic capsules	Hot air production cost→0.0074 $/kg
[204]	Solar box cooker	Paraffin wax	Small detachable capsule	The cost of solar box cooker → 48.19$
[205]	Solar box cooker	RT64HC	Aluminum	The cost of solar box cooker → 55.01$
[206]	Concentrating solar power	KNO3	Stainless steel	LCOE → 1.5 %↓
[210]	Concentrating solar power	Li_2CO_3(35 %)-Na_2CO_3 (65 %)/Li_2CO_3(32 %)-K_2CO_3(35 %)-Na_2CO_3(33 %)/K_2CO_3(51 %)-Na_2CO_3(49 %)		Storage cost <15$/kWh LCOE <0.6 $/kWh
[212]	Concentrating solar power	$NaNO_3$ /NaCl (33 %)-KCl (24 %)-LiCl (43 %) /NaOH (80 %)-NaCl (20 %) /$MgCl_2$ (60 %)-KCl (20.4 %)-NaCl (19.6 %)	Stainless steel	The cost reductions in LCOE as high as 10 %.
[217]	Concentrating solar power	$NaNO_3$/ Li_2CO_3–60%Na_2CO_3–20 % K_2CO_3		The system with optimum configuration reduces capital cost by 39.2 % for operating time durations of 12 h.
[242]	Solar desalination	Paraffin wax/Silver	Aluminum sheet	CPL → 0.046 $/L (3.8 INN/L) Payback Time→2 years
[243]	Solar desalination	Paraffin wax/CuO	Copper	CPL (Conventional) → 0.121 $/L CPL (Porous surface) → 0.107 $/L CPL (Encapsulated PCM) → 0.106 $/L CPL (Encapsulated nano/PCM) → 0.098 $/L Exergoeconomic (Conventional) → 0.51 kWh/$ Exergoeconomic (Porous surface) → 0.59 kWh/$ Exergoeconomic (Encapsulated PCM) → 0.64 kWh/$ Exergoeconomic (Encapsulated nano/PCM → 0.72 kWh/$ CO_2 mitigation (Conventional) → 10.52 tons CO_2 mitigation (Porous surface) → 12.31 tons CO_2 mitigation (Encapsulated PCM) → 13.32 tons CO_2 mitigation (Encapsulated nano/PCM) → 14.91 tons

Numerous instances have been documented by researchers to show the interdependency of SDGs. For example, SDG1 and SDG2 have synergies with most SDGs (and in some cases vice versa [280]), whereas reducing poverty (SDG1) has positive impact on SDG2 and SDG6 [281]. In a target-level meta-analysis on interactions of four SDGs it has been elucidated that for SDG2, SDG3, SDG7 and SDG14 approximately 50, 81, 46 and 61 positive interactions were associated, respectively. Among all of these goals, it has become realized that SDG7 "Clean and Affordable Energy", has an extraordinary impact on all SDGs [282]. In a target-level study, Fuso-Nerini et al. have shown that SDG7 has a vital role in 113 targets and found links between 143 targets and SDG7 [283].

In this regard, developing modern renewable-energy-driven systems (including solar/wind/tidal/biomass energy) can assist the UN 2030 agenda in concurrently reaching some of its most important goals, including SDGs7 and SDG13, [284]. Although the main purpose of Goal 7 is "Clean and Affordable Energy" for all, the international renewable energy agency, in their 2020 report, have stated that by 2030 > 600 million people still will not have access to electricity as one of the most crucial forms of secondary energy. Solar energy as one of the most well-established renewable energy sources plays a vital role in tackling this, whereby boosting solar-driven energy systems with advanced materials (in this context encapsulated PCMs/nano-enhanced PCMs) is even more important, as low efficiency and/or reliability of systems remains a concern. Among the varied solar energy schemes utilized by encapsulation PCMs/nano-enhanced PCM, some have great importance, as they directly produce electricity, which is the cornerstone of development [285]. Hence, small and large-scale solar-driven power generator systems and their positive impact on assisting to meet other SDGs and targets of SDG7, such as Targets 7.1 and 7.2 can be realized, with greater impact for large-scale power plants, such as CSPs, rather than small-scale power generator schemes like PVTs. Furthermore, other solar energy systems utilized by encapsulation PCMsm such as solar air/water heaters, solar dryers and solar cookers, can directly support reaching Target 7.2, which seeks that "By 2030, a substantial share of global energy mix should be obtained by renewable energies". With a broader view of this context, all 15 applications of solar energy utilized by encapsulation PCMs support endeavours for meeting Target 7.2.

Moreover, among the aforementioned solar-driven systems, solar stills and solar interfacial evaporations are aimed at providing safe drinking water, as related to SDG6 "Clean Water and Sanitation" and directly supporting Target 6.1 that states "By 2030, global and equal access to safe and affordable drinking water for all" should be achieved. Although the interrelation of these systems with Target 6.1 is apparent, they also lead to some steps regarding Target 7.2 of SDG7 concurrently. Importantly, clean water as the cornerstone of human health is both directly and indirectly related to other SDGs. A good example of this direct relationship is the role of solar desalination systems and their impact on SDG3. In this regard, providing safe drinking water by solar desalination systems results in a reduction of water-related disease, which is part of Target 3.3 of SDG3 that focuses on "Good Health and Well-being". Moreover, the interdependency of clean water and SDG11 is a good instance of indirect relations. As SDG11 focused on "Make cities inclusive, safe, resilient and sustainable", numerous parameters can contribute to realize this goal in terms of financial, technical and cultural aspects. From a technical viewpoint, Target 11.1 states to "ensure access for all to adequate, safe and affordable housing and basic services and upgrade slums". The term "basic services" designates all services that are essential for a healthy life, where accordingly, access to safe drinking water would be one the first parameters in this context. Furthermore, upgrading slum communities is a broad term which would be included in many items. Although the target has not explicitly noted the importance of drinking water to upgrade slums, one of the main critical issues that repeatedly reported by global organizations and researchers is the problem of safe drinking water in poor communities [286–288], where unsafe water sources are responsible for >1.2 million annual deaths, mainly in the developing world [289].

Importantly, a vital point in utilizing encapsulation PCMs in solar energy systems and their interrelation by realizing SDGs is evident in Target 7.3 of SDG7 which states that "By 2030, improving the worldwide rate of energy efficiency should be doubled". This target explicitly highlights the importance of augmenting efficiency of energy systems (at the forefront of them renewable energy schemes), which means any modification towards meeting this target. Accordingly, encapsulated PCMs from low-to-high temperatures, as discussed above, can considerably improve the performance of systems, not only from an efficiency viewpoint but also in terms of lowering the risks of systems failure and increasing safety. Hence, utilizing encapsulated PCMs can directly contribute to meeting Target 7.3. Similarly, the same is true for the application of nanomaterials in encapsulation PCM structures, as they have a substantial impact on the efficiency of solar energy systems. Indeed, nanomaterials can boost the performance of encapsulated PCMs that are utilized in solar energy systems.

Lastly, it is worth noting that our aim in this section by presenting this discussion is not to thoroughly examine the exact effect of each solar energy system for meeting SDGs or elucidating the interactions of systems by other SDGs, as this is not the subject of this review, but rather to show how wide the application of solar energy utilized by encapsulated PCMs is from another point of view, beyond engineering prospects, and to identify the potential for future works to explicitly realize links and interactions related to UN SDGs.

9. Challenges and future works

Encapsulated PCMs have a wide range of applications, not only in solar energy systems (with >15 applications), also in other areas ranging from building application to the food industry.

- Although encapsulations have numerous advantages, developing this technology into a practical strategy is challenging from technical and economical point of views. At the centre of these technical challenges, utilizing highly efficient core-shell materials can play a key role, whereby selecting the most appropriate options, considering the type of application, is of great importance.
- Furthermore, utilizing nanomaterials can be considered as good strategy for improving the thermal performance of PCMs inside of capsules; however, the aggregation of nanoparticles either by several solidification-liquid process or due to inhomogeneous dispersion of particles has not been fully studied. By comprehending the above-mentioned research gaps, researchers can give new ways to minimalize the problems of aggregation. In contrast, examining the thermal conductivity of nanomaterial-enhanced PCM is not an explicit method and procedure, which is a very important factor to address, because designing the thermal load and performance of solar energy systems assisted by nano-enhanced encapsulated PCMs can be accurately simulated, whereby this can be translated to real world application.
- It is important to note here that increasing the thermal conductivity by nanoparticles might also have a negative impact on convective heat transfer in the medium, if it is not implemented rationally, thus when utilizing nanomaterials inside PCMs, a meticulous understanding on heat transfer inside the system should examined to reduce trade-offs.
- Moreover, maintaining the effectiveness of encapsulated-PCM after several cycles in a system is a remaining challenge, one which has not been fully realized thus long-term stability of PCMs during operation is another crucial factor that requires further attention.
- The size and shape of encapsulation at all states –macro, micro and nano- is another matter of research which requires further consideration.
- Thus far, most studies have focused on applications of macro and micro-encapsulation PCMs in solar energy systems. However, examining the optimal size of macro/micro-encapsulation has not

been outshined thoroughly, whereby one important research gap is to find the optimal size of capsules taking the application of solar energy system into account.
- Similarly, comparing the effectiveness of different shapes of capsules to examine the highly efficient geometries for each application would be another wide avenue for further research in this field. For nano-encapsulation PCMs this research gaps are more intensive since the number of studies on its application in solar energy is rare, and mostly remained in theoretical stages rather than the experimental stage. This may be justified because of the fact that progress in nano-encapsulation depends on material scientists rendering the manufacturing process of this technology as efficient from the cost viewpoint in order to be applicable in solar energy systems. For instance, novel highly efficient encapsulated methods, such as microfluidic preparation -in spite of their limitation- would open new opportunities for high-performance encapsulated PCMs in different solar energy applications, while the practicality and endurance for real world application are also consider as important parameters. Moreover, the appropriate location for encapsulated PCMs is an important criterion; however, finding the optimum location of encapsulated PCMs in all the aforementioned solar energy systems in order to maximize their performance has not yet been recognized. In this regard, one interesting research gap for future studies would be to find the optimal location of encapsulated PCMs considering their size and taking into account the type of solar energy system.
- Further research should be conducted with regard to these applications such as solar fuels, solar ponds, and solar value-added chemicals as limited studies have been conducted.
- Importantly, application of artificial intelligent-based methods for designing highly efficient encapsulated PCMs considering the type of solar energy system is a crucial research gap, one which has been overlooked in this context, in which, most research have mainly focused on experimental studies or theoretical modelling with simple assumptions. Accordingly, applying advanced machine learning and deep learning methods based on previous experiments and more complex assumptions (based on actual conditions) might make great progress towards realizing encapsulation PCMs for real world applications.
- Lastly, encapsulation PCMs utilized in order to store a part of entered energy to the system, however, climate condition - particularly solar intensity- parameter can also play a key role in this context. Accordingly, in regions with low solar flux, utilizing encapsulation PCMs should performed cautiously since the entering energy should be spend for the system rather than the storing in encapsulated PCMs, otherwise utilizing them can become a negative effect on efficiency of systems which could be more deleterious in low-temperature systems such as solar desalination.
- Moreover, for cold seasons when the rate of solar energy is lower than other seasons, whereby the practicality and positive impact of the encapsulated PCMs should be carefully examined. Therefore, as a useful research direction it is recommended to evaluate the positive/negative effects of the encapsulated PCMs in solar energy–specifically in low-temperature- systems in cold seasons.

10. Conclusions

The major concluded remarks of this review are:

- Section 1 summarized solar energy systems for drinking water, hot water, and electricity purposes in arid, semi-arid, and remote communities.
- Section 2 highlighted the major production processes of encapsulation materials that have their advantages and disadvantages discussed in this section.
- Section 3 summarized the theoretical background of energy efficiency of various solar energy systems.
- Sections 4 and 5 discussed in detail about solar energy application with encapsulation PCM and solar energy application with nano-enhanced encapsulation PCM.
- Notwithstanding the aforementioned applications of encapsulated PCMs in various solar energy systems that include solar stills, solar steam generators and photovoltaic/thermal systems have extensively applied encapsulated PCMs.
- Section 6 summarized the operating temperature of encapsulated PCM while Section 7 discussed economic and environmental evaluation of encapsulated PCM.
- Section 8 related to the SGs goal of encapsulated PCM while Sections 9 and 10 represented various challenges and future directions.

CRediT authorship contribution statement

Shahin Shoeibi: Writing – original draft. **Furqan Jamil:** Writing – review & editing, Writing – original draft, Investigation, Data curation, Conceptualization. **Seyed Masoud Parsa:** Writing – review & editing. **Sadaf Mehdi:** Writing – review & editing. **Hadi Kargarsharifabad:** Writing – review & editing. **Seyed Ali Agha Mirjalily:** Writing – review & editing. **Wenshan Guo:** Writing – review & editing, Methodology. **Huu Hao Ngo:** Writing – review & editing, Data curation. **Bing-Jie Ni:** Writing – review & editing, Investigation. **Mehdi Khiadani:** Writing – review & editing, Investigation, Formal analysis, Conceptualization.

Declaration of competing interest

The authors confirm that there are no known conflicts of interest associated with this publication and there has been no significant financial support for this work that could have influenced its outcome.

Data availability

Data will be made available on request.

References

[1] E. Oró, A. De Gracia, A. Castell, M.M. Farid, L.F. Cabeza, Review on phase change materials (PCMs) for cold thermal energy storage applications, Appl. Energy 99 (2012) 513–533.

[2] S.D. Zwanzig, Y. Lian, E.G. Brehob, Numerical simulation of phase change material composite wallboard in a multi-layered building envelope, Energy Convers. Manag. 69 (2013) 27–40.

[3] F. A. Essa *et al.*, "Wall-suspended trays inside stepped distiller with Al2O3/paraffin wax mixture and vapor suction: experimental implementation," J. Energy Storage, vol. 32, p. 102008, 2020/12/01/ 2020, doi:https://doi.org/10.1016/j.est.2020.102008.

[4] M. Chaabane, H. Mhiri, and P. Bournot, "Thermal performance of an integrated collector storage solar water heater (ICSSWH) with phase change materials (PCM)," Energy Convers. Manag., vol. 78, pp. 897–903, 2014/02/01/ 2014, doi: https://doi.org/10.1016/j.enconman.2013.07.089.

[5] A.H.A. Al-Waeli, M.T. Chaichan, K. Sopian, H.A. Kazem, H.B. Mahood, A. A. Khadom, Modeling and experimental validation of a PVT system using nanofluid coolant and nano-PCM, Sol. Energy 177 (2019) 178–191, https://doi.org/10.1016/j.solener.2018.11.016.

[6] S.H. Sonawane, B.A. Bhanvase, M. Sivakumar, S.B. Potdar, Current overview of encapsulation, in: Encapsulation of Active Molecules and Their Delivery System, 2020, pp. 1–8.

[7] A. Mostafaeipour, S. M. Mohammadi, F. Najafi, and A. Issakhov, "Investigation of implementing solar energy for groundwater desalination in arid and dry regions: a case study," Desalination, vol. 512, p. 115039, 2021/09/15/ 2021, doi:https://doi.org/10.1016/j.desal.2021.115039.

[8] D. P. S. Cunha and K. V. Pontes, "Desalination plant integrated with solar thermal energy: a case study for the Brazilian semi-arid," J. Clean. Prod., vol. 331, p. 129943, 2022/01/10/ 2022, doi:https://doi.org/10.1016/j.jclepro.2021.129943.

[9] F. Esmaeilion, A. Ahmadi, S. Hoseinzadeh, M. Aliehyaei, S. A. Makkeh, and D. Astiaso Garcia, "Renewable energy desalination; a sustainable approach for water scarcity in arid lands," Int. J. Sustain. Eng., vol. 14, no. 6, pp. 1916–1942, 2021/11/02 2021, doi: https://doi.org/10.1080/19397038.2021.1948143.

[10] M. Suwaed, S. Alturki, A. Ghareeb, A. Al-Rubaye, and O. Awad, "Techno-economic feasibility of various types of solar collectors for solar water heating

systems in hot and semi-arid climates: a case study," Results Eng., vol. 20, p. 101445, 09/30 2023, doi: https://doi.org/10.1016/j.rineng.2023.101445.

[11] W. Hou *et al.*, "Comprehensive regionalization and potential water crisis for solar power development in arid and semi-arid regions of northwest China," Resour. Conserv. Recycl., vol. 193, p. 106939, 2023/06/01/ 2023, doi:https://doi.org/10.1016/j.resconrec.2023.106939.

[12] S. M. Parsa *et al.*, "Advanced nanostructured materials in solar interfacial steam generation and desalination against pathogens: combatting microbial-contaminants in water – a critical review," J. Mater. Chem. A, https://doi.org/10.1039/D3TA03343K vol. 11, no. 34, pp. 18046–18080, 2023, doi: https://doi.org/10.1039/D3TA03343K.

[13] S. M. Parsa *et al.*, "A comprehensive study to find the optimal fraction of nanoparticle coated at the interface of solar desalination absorbers: 5E and GHGs analysis in different seasons," Sol. Energy Mater. Sol. Cells, vol. 256, p. 112308, 2023/07/01/ 2023, doi:https://doi.org/10.1016/j.solmat.2023.112308.

[14] A. El Mansouri, M. Hasnaoui, A. Amahmid, and S. Hasnaoui, "Feasibility analysis of reverse osmosis desalination driven by a solar pond in Mediterranean and semi-arid climates," Energy Convers. Manag., vol. 221, p. 113190, 2020/10/01/ 2020, doi:https://doi.org/10.1016/j.enconman.2020.113190.

[15] H. Liu, X. Wang, D. Wu, Innovative design of microencapsulated phase change materials for thermal energy storage and versatile applications: a review, Sustain. Energy Fuels 3 (5) (2019) 1091–1149.

[16] T. Kawaguchi, H. Sakai, R. Ishida, Y. Shimizu, A. Kurniawan, T. Nomura, Development of core-shell type microencapsulated phase change material with Zn-30 mass% Al alloy and its shell formation mechanism, J. Energy Storage 55 (2022) 105577.

[17] A. F. Regin, S. C. Solanki, and J. S. Saini, "Heat transfer characteristics of thermal energy storage system using PCM capsules: a review," Renew. Sust. Energ. Rev., vol. 12, no. 9, pp. 2438–2458, 2008/12/01/ 2008, doi:https://doi.org/10.1016/j.rser.2007.06.009.

[18] P. K. S. Rathore and S. K. Shukla, "Potential of macroencapsulated PCM for thermal energy storage in buildings: a comprehensive review," Constr. Build. Mater., vol. 225, pp. 723–744, 2019/11/20/ 2019, doi:https://doi.org/10.1016/j.conbuildmat.2019.07.221.

[19] B. K. Green and S. Lowell, "Oil-containing microscopic capsules and method of making them," ed: Google Patents, 1957.

[20] B. K. Green, "Oil-containing microscopic capsules and method of making them," ed: Google Patents, 1957.

[21] M. Hawlader, M. Uddin, M.M. Khin, Microencapsulated PCM thermal-energy storage system, Appl. Energy 74 (1–2) (2003) 195–202.

[22] T. Kawaguchi, H. Sakai, N. Sheng, A. Kurniawan, T. Nomura, Microencapsulation of Zn-Al alloy as a new phase change material for middle-high-temperature thermal energy storage applications, Appl. Energy 276 (2020) 115487.

[23] Y. Shimizu, T. Kawaguchi, H. Sakai, K. Dong, A. Kurniawan, T. Nomura, Al–Ni alloy-based core-shell type microencapsulated phase change material for high temperature thermal energy utilization, Sol. Energy Mater. Sol. Cells 246 (2022) 111874.

[24] H. Sakai, N. Sheng, A. Kurniawan, T. Akiyama, T. Nomura, Fabrication of heat storage pellets composed of microencapsulated phase change material for high-temperature applications, Appl. Energy 265 (2020) 114673.

[25] F. He, S. Chao, X. He, M. Li, Inorganic microencapsulated core/shell structure of Al–Si alloy micro-particles with silane coupling agent, Ceram. Int. 40 (5) (2014) 6865–6874.

[26] K. Li, Z. Gu, X. Zhu, Y. Wei, H. Wang, Facile synthesis of Al@Al2O3 microcapsule for high-temperature thermal energy storage, ACS Sustain. Chem. Eng. 6 (10) (2018) 13226–13236.

[27] J. Sun, R. Zhang, Z. Liu, G. Lu, Thermal reliability test of Al–34% Mg–6% Zn alloy as latent heat storage material and corrosion of metal with respect to thermal cycling, Energy Convers. Manag. 48 (2) (2007) 619–624.

[28] A. Sarı, C. Alkan, A. Karaipekli, O. Uzun, Microencapsulated n-octacosane as phase change material for thermal energy storage, Sol. Energy 83 (10) (2009) 1757–1763.

[29] R. Yang, H. Xu, Y. Zhang, Preparation, physical property and thermal physical property of phase change microcapsule slurry and phase change emulsion, Sol. Energy Mater. Sol. Cells 80 (4) (2003) 405–416.

[30] K. Peippo, P. Kauranen, P. Lund, A multicomponent PCM wall optimized for passive solar heating, Energy Build. 17 (4) (1991) 259–270.

[31] M. Koschenz, B. Lehmann, Development of a thermally activated ceiling panel with PCM for application in lightweight and retrofitted buildings, Energy Build. 36 (6) (2004) 567–578.

[32] D. Feldman, D. Banu, DSC analysis for the evaluation of an energy storing wallboard, Thermochim. Acta 272 (1996) 243–251.

[33] Z. Ma, W. Lin, M.I. Sohel, Nano-enhanced phase change materials for improved building performance, Renew. Sust. Energ. Rev. 58 (2016) 1256–1268.

[34] G. Fang, H. Li, F. Yang, X. Liu, S. Wu, Preparation and characterization of nano-encapsulated n-tetradecane as phase change material for thermal energy storage, Chem. Eng. J. 153 (1–3) (2009) 217–221.

[35] X. Qiu, W. Li, G. Song, X. Chu, G. Tang, Fabrication and characterization of microencapsulated n-octadecane with different crosslinked methylmethacrylate-based polymer shells, Sol. Energy Mater. Sol. Cells 98 (2012) 283–293.

[36] X. Hu, Z. Huang, Y. Zhang, Preparation of CMC-modified melamine resin spherical nano-phase change energy storage materials, Carbohydr. Polym. 101 (2014) 83–88.

[37] S. Park, et al., Magnetic nanoparticle-embedded PCM nanocapsules based on paraffin core and polyurea shell, Colloids Surf. A Physicochem. Eng. Asp. 450 (2014) 46–51.

[38] Y. Fang, H. Yu, W. Wan, X. Gao, Z. Zhang, Preparation and thermal performance of polystyrene/n-tetradecane composite nanoencapsulated cold energy storage phase change materials, Energy Convers. Manag. 76 (2013) 430–436.

[39] S.T. Latibari, M. Mehrali, M. Mehrali, T.M.I. Mahlia, H.S.C. Metselaar, Synthesis, characterization and thermal properties of nanoencapsulated phase change materials via sol–gel method, Energy 61 (2013) 664–672.

[40] Z.-H. Chen, F. Yu, X.-R. Zeng, Z.-G. Zhang, Preparation, characterization and thermal properties of nanocapsules containing phase change material n-dodecanol by miniemulsion polymerization with polymerizable emulsifier, Appl. Energy 91 (1) (2012) 7–12.

[41] C. Chen, Z. Chen, X. Zeng, X. Fang, Z. Zhang, Fabrication and characterization of nanocapsules containing n-dodecanol by miniemulsion polymerization using interfacial redox initiation, Colloid Polym. Sci. 290 (4) (2012) 307–314.

[42] A. Sarı, C. Alkan, D.K. Döğüşcü, A. Biçer, Micro/nano-encapsulated n-heptadecane with polystyrene shell for latent heat thermal energy storage, Sol. Energy Mater. Sol. Cells 126 (2014) 42–50.

[43] K. Tumirah, M. Hussein, Z. Zulkarnain, R. Rafeadah, Nano-encapsulated organic phase change material based on copolymer nanocomposites for thermal energy storage, Energy 66 (2014) 881–890.

[44] G.H. Zhang, S.A. Bon, C.-Y. Zhao, Synthesis, characterization and thermal properties of novel nanoencapsulated phase change materials for thermal energy storage, Sol. Energy 86 (5) (2012) 1149–1154.

[45] G.-H. Nan, J.-P. Wang, Y. Wang, H. Wang, W. Li, X.-X. Zhang, Preparation and properties of nanoencapsulated phase change materials containing polyaniline, Acta Phys. -Chim. Sin. 30 (2) (2014) 338–344.

[46] Y. Fang, X. Liu, X. Liang, H. Liu, X. Gao, Z. Zhang, Ultrasonic synthesis and characterization of polystyrene/n-dotriacontane composite nanoencapsulated phase change material for thermal energy storage, Appl. Energy 132 (2014) 551–556.

[47] Y. Huang, A. Stonehouse, C. Abeykoon, Encapsulation methods for phase change materials–a critical review, Int. J. Heat Mass Transf. 200 (2023) 123458.

[48] J.E. Vandegaer, Microencapsulation: Processes and Applications, Springer Science & Business Media, 2012.

[49] S.S. Jyothi, A. Seethadevi, K.S. Prabha, P. Muthuprasanna, P. Pavitra, Microencapsulation: a review, Int. J. Pharm. Biol. Sci. 3 (2012) 509–531.

[50] A. Jamekhorshid, S. Sadrameli, M. Farid, A review of microencapsulation methods of phase change materials (PCMs) as a thermal energy storage (TES) medium, Renew. Sust. Energ. Rev. 31 (2014) 531–542.

[51] J.E. Cadotte, R. Petersen, R. Larson, E. Erickson, A new thin-film composite seawater reverse osmosis membrane, Desalination 32 (1980) 25–31.

[52] J. Cadotte, R. Forester, M. Kim, R. Petersen, T. Stocker, Nanofiltration membranes broaden the use of membrane separation technology, Desalination 70 (1–3) (1988) 77–88.

[53] J.-S. Cho, A. Kwon, C.-G. Cho, Microencapsulation of octadecane as a phase-change material by interfacial polymerization in an emulsion system, Colloid Polym. Sci. 280 (3) (2002) 260–266.

[54] X.Z. Lan, Z.C. Tan, G.L. Zou, L.X. Sun, T. Zhang, Microencapsulation of n-eicosane as energy storage material, Chin. J. Chem. 22 (5) (2004) 411–414.

[55] F. Salaün, G. Bedek, E. Devaux, D. Dupont, L. Gengembre, Microencapsulation of a cooling agent by interfacial polymerization: influence of the parameters of encapsulation on poly (urethane–urea) microparticles characteristics, J. Membr. Sci. 370 (1–2) (2011) 23–33.

[56] X. Yang, et al., Synthesis of high latent heat lauric acid/silica microcapsules by interfacial polymerization method for thermal energy storage, J. Energy Storage 33 (2021) 102059.

[57] X. Wang, C. Li, M. Wang, T. Zhao, W. Li, Bifunctional microcapsules with n-octadecane/thyme oil core and polyurea shell for high-efficiency thermal energy storage and antibiosis, Polymers 12 (10) (2020) 2226.

[58] C. Cai, et al., Co-solvent free interfacial polycondensation and properties of polyurea PCM microcapsules with dodecanol dodecanoate as core material, Sol. Energy 199 (2020) 721–730.

[59] X. Wang, C. Li, T. Zhao, Fabrication and characterization of poly (melamine-formaldehyde)/silicon carbide hybrid microencapsulated phase change materials with enhanced thermal conductivity and light-heat performance, Sol. Energy Mater. Sol. Cells 183 (2018) 82–91.

[60] Y. Fan, X. Zhang, X. Wang, J. Li, Q. Zhu, Super-cooling prevention of microencapsulated phase change material, Thermochim. Acta 413 (1–2) (2004) 1–6.

[61] L. Sánchez, E. Lacasa, M. Carmona, J.F. Rodriguez, P. Sánchez, Applying an experimental design to improve the characteristics of microcapsules containing phase change materials for fabric uses, Ind. Eng. Chem. Res. 47 (23) (2008) 9783–9790.

[62] J.M. Koehler, N. Visaveliya, A. Knauer, Controlling formation and assembling of nanoparticles by control of electrical charging, polarization, and electrochemical potential, Nanotechnol. Rev. 3 (6) (2014) 553–568.

[63] C. Liu, Z. Rao, J. Zhao, Y. Huo, Y. Li, Review on nanoencapsulated phase change materials: preparation, characterization and heat transfer enhancement, Nano Energy 13 (2015) 814–826.

[64] W. Cho, J.-W. Kook, S.M. Lee, W.-g. Koh, J.H. Kim, Modification of heat storage ability and adhesive properties of core/shell structured phase change material nanocapsules, Macromol. Res. 24 (6) (2016) 556–561.

[65] A. Sarı, C. Alkan, A. Karaipekli, Preparation, characterization and thermal properties of PMMA/n-heptadecane microcapsules as novel solid–liquid microPCM for thermal energy storage, Appl. Energy 87 (5) (2010) 1529–1534.

[66] W. Fortuniak, S. Slomkowski, J. Chojnowski, J. Kurjata, A. Tracz, U. Mizerska, Synthesis of a paraffin phase change material microencapsulated in a siloxane polymer, Colloid Polym. Sci. 291 (3) (2013) 725–733.
[67] N.V.N. Jyothi, P.M. Prasanna, S.N. Sakarkar, K.S. Prabha, P.S. Ramaiah, G. Srawan, Microencapsulation techniques, factors influencing encapsulation efficiency, J. Microencapsul. 27 (3) (2010) 187–197.
[68] X. Yin, H.D. Stöver, Hydrogel microspheres formed by complex coacervation of partially MPEG-grafted poly (styrene-alt-maleic anhydride) with PDADMAC and cross-linking with polyamines, Macromolecules 36 (23) (2003) 8773–8779.
[69] Y.-I. Huang, Y.-H. Cheng, C.-C. Yu, T.-R. Tsai, T.-M. Cham, Microencapsulation of extract containing shikonin using gelatin–acacia coacervation method: a formaldehyde-free approach, Colloids Surf. B: Biointerfaces 58 (2) (2007) 290–297.
[70] M. Uddin, H. Zhu, M. Hawlader, Effects of cyclic operation on the characteristics of a microencapsulated PCM storage material, Int. J. Solar Energy 22 (3–4) (2002) 105–114.
[71] Y. Özonur, M. Mazman, H. Paksoy, H. Evliya, Microencapsulation of coco fatty acid mixture for thermal energy storage with phase change material, Int. J. Energy Res. 30 (10) (2006) 741–749.
[72] Y. Yeo, N. Baek, K. Park, Microencapsulation methods for delivery of protein drugs, Biotechnol. Bioprocess Eng. 6 (4) (2001) 213–230.
[73] A. Arshad, M. Jabbal, Y. Yan, J. Darkwa, The micro-/nano-PCMs for thermal energy storage systems: a state of art review, Int. J. Energy Res. 43 (11) (2019) 5572–5620.
[74] L.-Y. Wang, P.-S. Tsai, Y.-M. Yang, Preparation of silica microspheres encapsulating phase-change material by sol-gel method in O/W emulsion, J. Microencapsul. 23 (1) (2006) 3–14.
[75] G. Fang, Z. Chen, H. Li, Synthesis and properties of microencapsulated paraffin composites with SiO2 shell as thermal energy storage materials, Chem. Eng. J. 163 (1–2) (2010) 154–159.
[76] T. Arunkumar, et al., Effects of concentrator type and encapsulated phase change material on the performance of different solar stills: an experimental approach, Desalin. Water Treat. 87 (2017) 1–13, https://doi.org/10.5004/dwt.2017.21268.
[77] V. S. Vigneswaran, G. Kumaresan, B. V. Dinakar, K. K. Kamal, and R. Velraj, "Augmenting the productivity of solar still using multiple PCMs as heat energy storage," J. Energy Storage, vol. 26, p. 101019, 2019/12/01/ 2019, doi:https://doi.org/10.1016/j.est.2019.101019.
[78] C.-H. Liu, X. Yu, Microencapsulation of biobased phase change material by interfacial polycondensation for thermal energy storage applications, J. Biobaased Mater. Bioenergy 7 (3) (2013) 331–335.
[79] C. Liang, X. Lingling, S. Hongbo, Z. Zhibin, Microencapsulation of butyl stearate as a phase change material by interfacial polycondensation in a polyurea system, Energy Convers. Manag. 50 (3) (2009) 723–729.
[80] H. Zhang, S. Sun, X. Wang, D. Wu, Fabrication of microencapsulated phase change materials based on n-octadecane core and silica shell through interfacial polycondensation, Colloids Surf. A Physicochem. Eng. Asp. 389 (1–3) (2011) 104–117.
[81] P. Siddhan, M. Jassal, A.K. Agrawal, Core content and stability of n-octadecane-containing polyurea microencapsules produced by interfacial polymerization, J. Appl. Polym. Sci. 106 (2) (2007) 786–792.
[82] J. Shi, X. Wu, R. Sun, B. Ban, J. Li, J. Chen, Nano-encapsulated phase change materials prepared by one-step interfacial polymerization for thermal energy storage, Mater. Chem. Phys. 231 (2019) 244–251.
[83] H. Nikpourian, A.R. Bahramian, M. Abdollahi, On the thermal performance of a novel PCM nanocapsule: the effect of core/shell, Renew. Energy 151 (2020) 322–331.
[84] S. Lu, J. Xing, Z. Zhang, G. Jia, Preparation and characterization of polyurea/polyurethane double-shell microcapsules containing butyl stearate through interfacial polymerization, J. Appl. Polym. Sci. 121 (6) (2011) 3377–3383.
[85] J.F. Su, L.X. Wang, L. Ren, Z. Huang, X.W. Meng, Preparation and characterization of polyurethane microcapsules containing n-octadecane with styrene-maleic anhydride as a surfactant by interfacial polycondensation, J. Appl. Polym. Sci. 102 (5) (2006) 4996–5006.
[86] W. Wu, et al., Jet impingement and spray cooling using slurry of nanoencapsulated phase change materials, Int. J. Heat Mass Transf. 54 (13–14) (2011) 2715–2723.
[87] A. Borreguero, J. Valverde, J. Rodríguez, A. Barber, J. Cubillo, M. Carmona, Synthesis and characterization of microcapsules containing Rubitherm® RT27 obtained by spray drying, Chem. Eng. J. 166 (1) (2011) 384–390.
[88] R. Methaapanon, S. Kornbongkotmas, C. Ataboonwongse, A. Soottitantawat, Microencapsulation of n-octadecane and methyl palmitate phase change materials in silica by spray drying process, Powder Technol. 361 (2020) 910–916.
[89] H. Es-Haghi, S. Mirabedini, M. Imani, R. Farnood, Preparation and characterization of pre-silane modified ethyl cellulose-based microcapsules containing linseed oil, Colloids Surf. A Physicochem. Eng. Asp. 447 (2014) 71–80.
[90] M. Fashandi, S.N. Leung, Preparation and characterization of 100% bio-based polylactic acid/palmitic acid microcapsules for thermal energy storage, Mater. Renew. Sustain. Energy 6 (3) (2017) 1–10.
[91] Y. Lin, C. Zhu, G. Alva, G. Fang, Microencapsulation and thermal properties of myristic acid with ethyl cellulose shell for thermal energy storage, Appl. Energy 231 (2018) 494–501.
[92] A. Khan, P. Saikia, R. Saxena, D. Rakshit, S. Saha, Microencapsulation of phase change material in water dispersible polymeric particles for thermoregulating rubber composites—a holistic approach, Int. J. Energy Res. 44 (3) (2020) 1567–1579.
[93] F. Wang, et al., Cellulose nanocrystals-composited poly (methyl methacrylate) encapsulated n-eicosane via a Pickering emulsion-templating approach for energy storage, Carbohydr. Polym. 234 (2020) 115934.
[94] J. Xing, et al., Microencapsulation of fatty acid eutectic with polyvinyl chloride shell used for thermal energy storage, J. Energy Storage 34 (2021) 101998.
[95] M. Graham, E. Shchukina, P.F. De Castro, D. Shchukin, Nanocapsules containing salt hydrate phase change materials for thermal energy storage, J. Mater. Chem. A 4 (43) (2016) 16906–16912.
[96] Z. Qiao, J. Mao, Enhanced thermal properties with graphene oxide in the urea-formaldehyde microcapsules containing paraffin PCMs, J. Microencapsul. 34 (1) (2017) 1–9.
[97] V. Pethurajan, S. Sivan, Fabrication, characterisation and heat transfer study on microencapsulation of nano-enhanced phase change material, Chem. Eng. Process. Process Intensif. 133 (2018) 12–23.
[98] S.R. Rakkappan, S. Sivan, V. Pethurajan, A. Aditya, H. Mittal, Preparation and thermal properties of encapsulated 1-Decanol for low-temperature heat transfer fluid application, Colloids Surf. A Physicochem. Eng. Asp. 614 (2021) 126167.
[99] M. Graham, J.A. Coca-Clemente, E. Shchukina, D. Shchukin, Nanoencapsulated crystallohydrate mixtures for advanced thermal energy storage, J. Mater. Chem. A 5 (26) (2017) 13683–13691.
[100] T. Khadiran, M.Z. Hussein, Z. Zainal, R. Rusli, Nano-encapsulated n-nonadecane using vinyl copolymer shell for thermal energy storage medium, Macromol. Res. 23 (7) (2015) 658–669.
[101] C. Huang, et al., A novel bifunctional microencapsulated phase change material loaded with ZnO for thermal energy storage and light–thermal energy conversion, Sustain. Energy Fuels 4 (10) (2020) 5203–5214.
[102] J. Cheng, et al., The thermal behavior and flame retardant performance of phase change material microcapsules with modified carbon nanotubes, Energy 240 (2022) 122821.
[103] S. Parvate, J. Singh, J.R. Vennapusa, P. Dixit, S. Chattopadhyay, Copper nanoparticles interlocked phase-change microcapsules for thermal buffering in packaging application, J. Ind. Eng. Chem. 102 (2021) 69–85.
[104] J. Zhao, et al., Microencapsulated phase change materials with TiO2-doped PMMA shell for thermal energy storage and UV-shielding, Sol. Energy Mater. Sol. Cells 168 (2017) 62–68.
[105] O.M. Maithya, X. Li, X. Feng, X. Sui, B. Wang, Microencapsulated phase change material via Pickering emulsion stabilized by graphene oxide for photothermal conversion, J. Mater. Sci. 55 (18) (2020) 7731–7742.
[106] K. Zhang, J. Wang, L. Xu, H. Xie, Z. Guo, Preparation and thermal characterization of n-octadecane/pentafluorostyrene nanocapsules for phase-change energy storage, J. Energy Storage 35 (2021) 102327.
[107] S. Lashgari, H. Arabi, A.R. Mahdavian, V. Ambrogi, Thermal and morphological studies on novel PCM microcapsules containing n-hexadecane as the core in a flexible shell, Appl. Energy 190 (2017) 612–622.
[108] S. K. Pathak, V. V. Tyagi, K. Chopra, R. Rejikumar, and A. K. Pandey, "Integration of emerging PCMs and nano-enhanced PCMs with different solar water heating systems for sustainable energy future: a systematic review," Sol. Energy Mater. Sol. Cells, vol. 254, p. 112237, 2023/06/01/ 2023, doi:https://doi.org/10.1016/j.solmat.2023.112237.
[109] Z. A. Nawsud, A. Altouni, H. S. Akhijahani, and H. Kargarsharifabad, "A comprehensive review on the use of nano-fluids and nano-PCM in parabolic trough solar collectors (PTC)," Sustain. Energy Technol. Assess., vol. 51, p. 101889, 2022/06/01/ 2022, doi:https://doi.org/10.1016/j.seta.2021.101889.
[110] V. R. Pawar and S. Sobhansarbandi, "Heat transfer enhancement of a PCM-porous metal based heat pipe evacuated tube solar collector: an experimental study," Sol. Energy, vol. 251, pp. 106–118, 2023/02/01/ 2023, doi:https://doi.org/10.1016/j.solener.2022.10.054.
[111] I.-H. Kim, H.-W. Sim, H.-H. Hong, D.-W. Kim, W. Lee, D.-K. Lee, Effect of filler size on thermal properties of paraffin/silver nanoparticle composites, Korean J. Chem. Eng. 36 (6) (2019) 1004–1012.
[112] M. K. Rathod, "Phase change materials and their applications," Phase Change Materials and Their Applications, vol. 37, 2018.
[113] P. Khalilmoghadam, A. Rajabi-Ghahnavieh, M.B. Shafii, A novel energy storage system for latent heat recovery in solar still using phase change material and pulsating heat pipe, Renew. Energy 163 (2021) 2115–2127, https://doi.org/10.1016/j.renene.2020.10.073.
[114] A. E. Kabeel, R. Sathyamurthy, S. A. El-Agouz, A. Muthu manokar, and E. M. S. El-Said, "Experimental studies on inclined PV panel solar still with cover cooling and PCM," J. Therm. Anal. Calorim., vol. 138, no. 6, pp. 3987–3995, 2019/12/01 2019, doi: https://doi.org/10.1007/s10973-019-08561-6.
[115] A. E. Kabeel, M. Abdelgaied, K. Harby, and A. Eisa, "Augmentation of diurnal and nocturnal distillate of modified tubular solar still having copper tubes filled with PCM in the basin," J. Energy Storage, vol. 32, p. 101992, 2020/12/01/ 2020, doi: https://doi.org/10.1016/j.est.2020.101992.
[116] H. Hafs *et al.*, "Numerical simulation of the performance of passive and active solar still with corrugated absorber surface as heat storage medium for sustainable solar desalination technology," Groundw. Sustain. Dev., vol. 14, p. 100610, 2021/08/01/ 2021, doi:https://doi.org/10.1016/j.gsd.2021.100610.
[117] G. Rajasekhar, M. Eswaramoorthy, Performance evaluation on solar still integrated with nano-composite phase change materials, Appl. Solar Energy 51 (1) (2015) 15–21, https://doi.org/10.3103/s0003701x15010119.
[118] M.S. Yousef, H. Hassan, Energy payback time, exergoeconomic and enviroeconomic analyses of using thermal energy storage system with a solar desalination system: an experimental study, J. Clean. Prod. 270 (2020) 122082, https://doi.org/10.1016/j.jclepro.2020.122082.

[119] Z. Y. Ho, R. Bahar, and C. H. Koo, "Passive solar stills coupled with Fresnel lens and phase change material for sustainable solar desalination in the tropics," J. Clean. Prod., vol. 334, p. 130279, 2022/02/01/ 2022, doi:https://doi.org/10.1016/j.jclepro.2021.130279.
[120] A.H.A. Al-Waeli, et al., Comparison of prediction methods of PV/T nanofluid and nano-PCM system using a measured dataset and artificial neural network, Sol. Energy 162 (2018) 378–396, https://doi.org/10.1016/j.solener.2018.01.026.
[121] F. Jamil, et al., Evaluation of photovoltaic panels using different nano phase change material and a concise comparison: an experimental study, Renew. Energy 169 (2021) 1265–1279, https://doi.org/10.1016/j.renene.2021.01.089.
[122] A.H.A. Al-Waeli, K. Sopian, H.A. Kazem, M.T. Chaichan, Evaluation of the electrical performance of a photovoltaic thermal system using nano-enhanced paraffin and nanofluids, Case Stud. Therm. Eng. 21 (2020) 100678, https://doi.org/10.1016/j.csite.2020.100678.
[123] Akshayveer, A. P. Singh, A. Kumar, and O. P. Singh, "Effect of natural convection and thermal storage system on the electrical and thermal performance of a hybrid PV-T/PCM systems," Mater. Today: Proc., vol. 39, pp. 1899–1904, 2021/01/01/ 2021, doi:https://doi.org/10.1016/j.matpr.2020.08.010.
[124] R. Ahmadi, F. Monadinia, and M. Maleki, "Passive/active photovoltaic-thermal (PVT) system implementing infiltrated phase change material (PCM) in PS-CNT foam," Sol. Energy Mater. Sol. Cells, vol. 222, p. 110942, 2021/04/01/ 2021, doi: https://doi.org/10.1016/j.solmat.2020.110942.
[125] X. Yang, L. Sun, Y. Yuan, X. Zhao, and X. Cao, "Experimental investigation on performance comparison of PV/T-PCM system and PV/T system," Renew. Energy, vol. 119, pp. 152–159, 2018/04/01/ 2018, doi:https://doi.org/10.1016/j.renene.2017.11.094.
[126] M. O. Lari and A. Z. Sahin, "Effect of retrofitting a silver/water nanofluid-based photovoltaic/thermal (PV/T) system with a PCM-thermal battery for residential applications," Renew. Energy, vol. 122, pp. 98–107, 2018/07/01/ 2018, doi:https://doi.org/10.1016/j.renene.2018.01.034.
[127] M. H. Mahfuz, M. R. Anisur, M. A. Kibria, R. Saidur, and I. H. S. C. Metselaar, "Performance investigation of thermal energy storage system with phase change material (PCM) for solar water heating application," Int. Commun. Heat Mass Transf., vol. 57, pp. 132–139, 2014/10/01/ 2014, doi:https://doi.org/10.1016/j.icheatmasstransfer.2014.07.022.
[128] S. Tarhan, A. Sari, and M. H. Yardim, "Temperature distributions in trapezoidal built in storage solar water heaters with/without phase change materials," Energy Convers. Manag., vol. 47, no. 15, pp. 2143–2154, 2006/09/01/ 2006, doi: https://doi.org/10.1016/j.enconman.2005.12.002.
[129] P. Manoj Kumar, K. Mylsamy, Experimental investigation of solar water heater integrated with a nanocomposite phase change material, J. Therm. Anal. Calorim. 136 (1) (2018) 121–132, https://doi.org/10.1007/s10973-018-7937-9.
[130] A.S. Manirathnam, M.K. Dhanush Manikandan, R. Hari Prakash, B. Kamesh Kumar, M. Deepan Amarnath, Experimental analysis on solar water heater integrated with nano composite phase change material (SCi and CuO), Mater. Today: Proc. 37 (2021) 232–240, https://doi.org/10.1016/j.matpr.2020.05.093.
[131] S. Algarni, S. Mellouli, T. Alqahtani, K. Almutairi, A. Khan, A. Anqi, Experimental investigation of an evacuated tube solar collector incorporating nano-enhanced PCM as a thermal booster, Appl. Therm. Eng. 180 (2020) 115831, https://doi.org/10.1016/j.applthermaleng.2020.115831.
[132] G. Palanikumar, S. Shanmugan, B. Janarthanan, R. Sangavi, P. Geethanjali, Energy and environment control to box type solar cooker and nanoparticles mixed bar plate coating with effect of thermal image cooking pot, Mater. Today: Proc. 18 (2019) 1243–1255, https://doi.org/10.1016/j.matpr.2019.06.586.
[133] Q.A. Jawad, A.M.J. Mahdy, A.H. Khuder, M.T. Chaichan, Improve the performance of a solar air heater by adding aluminum chip, paraffin wax, and nano-SiC, Case Stud. Therm. Eng. 19 (2020) 100622, https://doi.org/10.1016/j.csite.2020.100622.
[134] M.O. Karaağaç, A. Ergün, Ü. Ağbulut, A.E. Gürel, İ. Ceylan, Experimental analysis of CPV/T solar dryer with nano-enhanced PCM and prediction of drying parameters using ANN and SVM algorithms, Sol. Energy 218 (2021) 57–67, https://doi.org/10.1016/j.solener.2021.02.028.
[135] H. Mousa and A. M. Gujarathi, "Modeling and analysis the productivity of solar desalination units with phase change materials," Renew. Energy, vol. 95, pp. 225–232, 2016/09/01/ 2016, doi:https://doi.org/10.1016/j.renene.2016.04.013.
[136] S. Shoeibi, H. Kargarsharifabad, N. Rahbar, Effects of nano-enhanced phase change material and nano-coated on the performance of solar stills, J. Energy Storage 42 (2021) 103061, https://doi.org/10.1016/j.est.2021.103061.
[137] S. Shoeibi, M. Saemian, M. Khiadani, H. Kargarsharifabad, S. Ali Agha Mirjalily, Influence of PV/T waste heat on water productivity and electricity generation of solar stills using heat pipes and thermoelectric generator: an experimental study and environmental analysis, Energy Convers. Manag. 276 (2023), https://doi.org/10.1016/j.enconman.2022.116504.
[138] S. Shoeibi, H. Kargarsharifabad, S.A.A. Mirjalily, M. Zargarazad, Performance analysis of finned photovoltaic/thermal solar air dryer with using a compound parabolic concentrator, Appl. Energy 304 (2021) 117778, https://doi.org/10.1016/j.apenergy.2021.117778.
[139] S. Shoeibi, N. Rahbar, A. Abedini Esfahlani, H. Kargarsharifabad, A comprehensive review of Enviro-Exergo-economic analysis of solar stills, Renew. Sust. Energ. Rev. 149 (2021) 111404, https://doi.org/10.1016/j.rser.2021.111404.
[140] S.M. Parsa, A. Yazdani, D. Javadi, M. Afrand, N. Karimi, H.M. Ali, Selecting efficient side of thermoelectric in pyramid-shape solar desalination units incorporated phase change material (PCM), nanoparticle, turbulator with battery storage powered by photovoltaic, J. Energy Storage 51 (2022), https://doi.org/10.1016/j.est.2022.104448.
[141] R. Dhivagar, S. Shoeibi, S. M. Parsa, S. Hoseinzadeh, H. Kargarsharifabad, and M. Khiadani, "Performance evaluation of solar still using energy storage biomaterial with porous surface: an experimental study and environmental analysis," Renew. Energy, vol. 206, pp. 879–889, 2023/04/01/ 2023, doi:https://doi.org/10.1016/j.renene.2023.02.097.
[142] Z. Said, M. Ghodbane, A. K. Tiwari, H. M. Ali, B. Boumeddane, and Z. M. Ali, "4E (Energy, Exergy, Economic, and Environment) examination of a small LFR solar water heater: an experimental and numerical study," Case Stud. Therm. Eng., vol. 27, p. 101277, 2021/10/01/ 2021, doi:https://doi.org/10.1016/j.csite.2021.101277.
[143] E.Z. Mahdizade, M. Ameri, Thermodynamic investigation of a semi-open air, humidification dehumidification desalination system using air and water heaters, Desalination 428 (2018) 182–198, https://doi.org/10.1016/j.desal.2017.11.032.
[144] S. Shoeibi, H. Kargarsharifabad, S.A.A. Mirjalily, M. Sadi, A. Arabkoohsar, A comprehensive review of nano-enhanced phase change materials on solar energy applications, J. Energy Storage 50 (2022), https://doi.org/10.1016/j.est.2022.104262.
[145] H. Zhang, C. Xu, and G. Fang, "Encapsulation of inorganic phase change thermal storage materials and its effect on thermophysical properties: a review," Sol. Energy Mater. Sol. Cells, vol. 241, p. 111747, 2022/07/01/ 2022, doi:https://doi.org/10.1016/j.solmat.2022.111747.
[146] A. R. A. Elbar and H. Hassan, "Experimental investigation on the impact of thermal energy storage on the solar still performance coupled with PV module via new integration," Sol. Energy, vol. 184, pp. 584–593, 2019/05/15/ 2019, doi: https://doi.org/10.1016/j.solener.2019.04.042.
[147] H. Hassan, M. S. Yousef, M. S. Ahmed, and M. Fathy, "Energy, exergy, environmental, and economic analysis of natural and forced cooling of solar still with porous media," Environ. Sci. Pollut. Res. Int., vol. 27, no. 30, pp. 38221–38240, Oct 2020, doi: https://doi.org/10.1007/s11356-020-09995-4.
[148] N. M. Shatar, M. F. M. Sabri, M. F. M. Salleh, and M. H. Ani, "Energy, exergy, economic, environmental analysis for solar still using partially coated condensing cover with thermoelectric cover cooling," J. Clean. Prod., vol. 387, p. 135833, 2023/02/10/ 2023, doi:https://doi.org/10.1016/j.jclepro.2022.135833.
[149] P. Liang *et al.*, "A self-floating electrospun nanofiber mat for continuously high-efficiency solar desalination," Chemosphere, vol. 280, p. 130719, Apr 30 2021, doi: https://doi.org/10.1016/j.chemosphere.2021.130719.
[150] B. Praveen kumar, D. Prince Winston, P. Pounraj, A. Muthu Manokar, R. Sathyamurthy, A.E. Kabeel, Experimental investigation on hybrid PV/T active solar still with effective heating and cover cooling method, Desalination 435 (2018) 140–151, https://doi.org/10.1016/j.desal.2017.11.007.
[151] D. De Luca, A. Caldarelli, E. Gaudino, E. Di Gennaro, M. Musto, and R. Russo, "Modeling of energy and exergy efficiencies in high vacuum flat plate photovoltaic–thermal (PV–T) collectors," Energy Rep., vol. 9, pp. 1044–1055, 2023/03/01/ 2023, doi:https://doi.org/10.1016/j.egyr.2022.11.152.
[152] J. Li, S. Wei, Y. Dong, X. Liu, and V. Novakovic, "Technical and economic performance study on winter heating system of air source heat pump assisted solar evacuated tube water heater," Appl. Therm. Eng., vol. 221, p. 119851, 2023/02/25/ 2023, doi:https://doi.org/10.1016/j.applthermaleng.2022.119851.
[153] M. Kumar, Aashish, B. S. Negi, Shimpy, R. Grewal, and H. Manchanda, "Assessment of an ETC based solar water heater at different tilt angles," Mater. Today: Proc., 2023/03/02/ 2023, doi:https://doi.org/10.1016/j.matpr.2023.02.263.
[154] A.E. Kabeel, Performance of solar still with a concave wick evaporation surface, Energy 34 (10) (2009) 1504–1509, https://doi.org/10.1016/j.energy.2009.06.050.
[155] K. V. Modi and A. R. Gamit, "Investigation on performance of square pyramid solar still using nanofluid and thermal energy storage material: an experimental and theoretical study," J. Clean. Prod., vol. 381, p. 135115, 2022/12/25/ 2022, doi:https://doi.org/10.1016/j.jclepro.2022.135115.
[156] N. Wang, L.-L. Ni, A. Wang, H.-S. Shan, H.-Z. Jia, and L. Zuo, "High-efficiency photovoltaic-thermoelectric hybrid energy harvesting system based on functionally multiplexed intelligent thermal management," Energy Convers. Manag., vol. 272, p. 116377, 2022/11/15/ 2022, doi:https://doi.org/10.1016/j.enconman.2022.116377.
[157] M. Nazari, S. Jafarmadar, and S. Khalilarya, "Exergy and thermoeconomic analyses of serpentine tube flat-plate solar water heaters coated with CuO nanostructures," Case Stud. Therm. Eng., vol. 35, p. 102072, 2022/07/01/ 2022, doi:https://doi.org/10.1016/j.csite.2022.102072.
[158] A.H.A. Al-Waeli, et al., Evaluation of the nanofluid and nano-PCM based photovoltaic thermal (PVT) system: an experimental study, Energy Convers. Manag. 151 (2017) 693–708, https://doi.org/10.1016/j.enconman.2017.09.032.
[159] M. Das, M. Catalkaya, O. E. Akay, and E. K. Akpinar, "Impacts of use PID control and artificial intelligence methods for solar air heater energy performance," J. Build. Eng., vol. 65, p. 105809, 2023/04/15/ 2023, doi:https://doi.org/10.1016/j.jobe.2022.105809.
[160] E. Vengadesan and R. Senthil, "Experimental investigation of the thermal performance of a box type solar cooker using a finned cooking vessel," Renew. Energy, vol. 171, pp. 431–446, 2021/06/01/ 2021, doi:https://doi.org/10.1016/j.renene.2021.02.130.
[161] S. M. Parsa, F. Norozpour, A. H. Elsheikh, and A. E. Kabeel, "Solar desalination/purification (solar stills, humidification-dehumidification, solar disinfection) in high altitude during COVID19: insights of gastrointestinal manifestations and

systems' mechanism," J. Hazard. Mater. Adv., vol. 10, p. 100259, 2023/05/01/ 2023, doi:https://doi.org/10.1016/j.hazadv.2023.100259.
[162] A. Rahaei, R. Rafee, and M. R. Zargarabadi, "A photovoltaic thermal system with a complete contact between water and PV modules suitable for district heating and electric power generation," Sustain. Energy Technol. Assess., vol. 47, p. 101325, 2021/10/01/ 2021, doi:https://doi.org/10.1016/j.seta.2021.101325.
[163] S. Mandal and S. K. Ghosh, "Experimental investigation of the performance of a double pass solar water heater with reflector," Renew. Energy, vol. 149, pp. 631–640, 2020/04/01/ 2020, doi:https://doi.org/10.1016/j.renene.2019.11.160.
[164] G. Coccia, A. Aquilanti, S. Tomassetti, G. Comodi, and G. Di Nicola, "Design, realization, and tests of a portable solar box cooker coupled with an erythritol-based PCM thermal energy storage," Sol. Energy, vol. 201, pp. 530–540, 2020/05/01/ 2020, doi:https://doi.org/10.1016/j.solener.2020.03.031.
[165] G. Gasa, C. Prieto, A. Lopez-Roman, and L. F. Cabeza, "Life cycle assessment (LCA) of a concentrating solar power (CSP) plant in tower configuration with different storage capacity in molten salts," J. Energy Storage, vol. 53, p. 105219, 2022/09/01/ 2022, doi:https://doi.org/10.1016/j.est.2022.105219.
[166] C. Yuan *et al.*, "Rapid and stable calcium-looping solar thermochemical energy storage via co-doping binary sulfate and Al–Mn–Fe oxides," Green Energy Environ., 2023/03/02/ 2023, doi:https://doi.org/10.1016/j.gee.2023.02.009.
[167] C. Fu, Q. Shen, and T. Wu, "Exergo-economic comparisons of solar cooling systems coupled to series/parallel absorption chiller types considering the lowest heat transfer area," Case Stud. Therm. Eng., vol. 39, p. 102456, 2022/11/01/ 2022, doi:https://doi.org/10.1016/j.csite.2022.102456.
[168] H. Shakibi, A. Shokri, B. Sobhani, and M. Yari, "Numerical analysis and optimization of a novel photovoltaic thermal solar unit improved by Nano-PCM as an energy storage media and finned collector," Renew. Sust. Energ. Rev., vol. 179, p. 113230, 2023/06/01/ 2023, doi:https://doi.org/10.1016/j.rser.2023.113230.
[169] Z.M. Omara, A.S. Abdullah, A.E. Kabeel, F.A. Essa, The cooling techniques of the solar stills' glass covers – a review, Renew. Sust. Energ. Rev. 78 (2017) 176–193, https://doi.org/10.1016/j.rser.2017.04.085.
[170] K. Sampathkumar, T.V. Arjunan, P. Pitchandi, P. Senthilkumar, Active solar distillation—a detailed review, Renew. Sust. Energ. Rev. 14 (6) (2010) 1503–1526, https://doi.org/10.1016/j.rser.2010.01.023.
[171] A. S. Abdullah *et al.*, "Enhancing trays solar still performance using wick finned absorber, nano-enhanced PCM," Alex. Eng. J., vol. 61, no. 12, pp. 12417–12430, 2022/12/01/ 2022, doi:https://doi.org/10.1016/j.aej.2022.06.033.
[172] S. Shoeibi, S.A.A. Mirjalily, H. Kargarsharifabad, M. Khiadani, H. Panchal, A comprehensive review on performance improvement of solar desalination with applications of heat pipes, Desalination 540 (2022), https://doi.org/10.1016/j.desal.2022.115983.
[173] B. Thamarai Kannan *et al.*, "Improved freshwater generation via hemispherical solar desalination unit using paraffin wax as phase change material encapsulated in waste aluminium cans," Desalination, vol. 538, p. 115907, 2022/09/15/ 2022, doi:https://doi.org/10.1016/j.desal.2022.115907.
[174] M. Al-harahsheh, M. Abu-Arabi, H. Mousa, Z. Alzghoul, Solar desalination using solar still enhanced by external solar collector and PCM, Appl. Therm. Eng. 128 (2018) 1030–1040, https://doi.org/10.1016/j.applthermaleng.2017.09.073.
[175] A. H. Abed, H. A. Hoshi, and M. H. Jabal, "Experimental investigation of modified solar still coupled with high-frequency ultrasonic vaporizer and phase change material capsules," Case Stud. Therm. Eng., vol. 28, p. 101531, 2021/12/01/ 2021, doi:https://doi.org/10.1016/j.csite.2021.101531.
[176] M. Carmona, A. Palacio Bastos, and J. D. García, "Experimental evaluation of a hybrid photovoltaic and thermal solar energy collector with integrated phase change material (PVT-PCM) in comparison with a traditional photovoltaic (PV) module," Renew. Energy, vol. 172, pp. 680–696, 2021/07/01/ 2021, doi:https://doi.org/10.1016/j.renene.2021.03.022.
[177] M. Modjinou *et al.*, "Performance comparison of encapsulated PCM PV/T, microchannel heat pipe PV/T and conventional PV/T systems," Energy, vol. 166, pp. 1249–1266, 2019/01/01/ 2019, doi:https://doi.org/10.1016/j.energy.2018.10.007.
[178] A. T. Hamada, O. Z. Sharaf, and M. F. Orhan, "A novel photovoltaic/thermal (PV/T) solar collector based on a multi-functional nano-encapsulated phase-change material (nano-ePCM) dispersion," Energy Convers. Manag., vol. 280, p. 116797, 2023/03/15/ 2023, doi:https://doi.org/10.1016/j.enconman.2023.116797.
[179] Z. Qiu, X. Ma, X. Zhao, P. Li, and S. Ali, "Experimental investigation of the energy performance of a novel Micro-encapsulated Phase Change Material (MPCM) slurry based PV/T system," Appl. Energy, vol. 165, pp. 260–271, 2016/03/01/ 2016, doi:https://doi.org/10.1016/j.apenergy.2015.11.053.
[180] H. A. Nasef, H. Hassan, S. Mori, and S. A. Nada, "Experimental investigation on the performance of parallel and staggered arrays of PCM energy storage system for PV thermal regulation," Energy Convers. Manag., vol. 254, p. 115143, 2022/02/15/ 2022, doi:https://doi.org/10.1016/j.enconman.2021.115143.
[181] A. Waqas, J. Jie, and L. Xu, "Thermal behavior of a PV panel integrated with PCM-filled metallic tubes: an experimental study," J. Renew. Sustain. Energy, vol. 9, no. 5, p. 053504, 2017/09/01 2017, doi: https://doi.org/10.1063/1.4995022.
[182] M. M. Elsabahy, M. Ahmed, H. Sekiguchi, and M. Emam, "Performance assessment of a novel integrated concentrator photovoltaic system with encapsulated phase change materials," Energy Convers. Manag., vol. 266, p. 115854, 2022/08/15/ 2022, doi:https://doi.org/10.1016/j.enconman.2022.115854.
[183] Y. Su, Y. Zhang, and L. Shu, "Experimental study of using phase change material cooling in a solar tracking concentrated photovoltaic-thermal system," Sol. Energy, vol. 159, pp. 777–785, 2018/01/01/ 2018, doi:https://doi.org/10.1016/j.solener.2017.11.045.
[184] A. Faddouli, et al., Comparative study of a normal solar water heater and smart thermal/thermoelectric hybrid systems, Mater. Today: Proc. 30 (2020) 1039–1042, https://doi.org/10.1016/j.matpr.2020.04.499.
[185] M. Arab, M. Soltanieh, and M. B. Shafii, "Experimental investigation of extra-long pulsating heat pipe application in solar water heaters," Exp. Thermal Fluid Sci., vol. 42, pp. 6–15, 2012/10/01/ 2012, doi:https://doi.org/10.1016/j.expthermflusci.2012.03.006.
[186] H. Yang, Y. Bai, C. Ge, L. He, W. Liang, X. Zhang, Polyethylene glycol-based phase change materials with high photothermal conversion efficiency and shape stability in an aqueous environment for solar water heater, Compos. A: Appl. Sci. Manuf. 154 (2022), https://doi.org/10.1016/j.compositesa.2021.106778.
[187] W. Su, Y. Li, T. Zhou, J. Darkwa, G. Kokogiannakis, Z. Li, Microencapsulation of paraffin with poly (urea methacrylate) shell for solar water heater, Energies 12 (18) (2019), https://doi.org/10.3390/en12183406.
[188] L. Yang, X. Zhang, G. Xu, Thermal performance of a solar storage packed bed using spherical capsules filled with PCM having different melting points, Energy Build. 68 (2014) 639–646, https://doi.org/10.1016/j.enbuild.2013.09.045.
[189] K. Dileep, K.R. Arun, D. Dishnu, M. Srinivas, S. Jayaraj, Numerical studies on the effect of location and number of containers on the phase transition of PCM-integrated evacuated tube solar water heater, J. Therm. Anal. Calorim. 143 (1) (2019) 737–749, https://doi.org/10.1007/s10973-019-09151-2.
[190] M.A. Fazilati, A.A. Alemrajabi, Phase change material for enhancing solar water heater, an experimental approach, Energy Convers. Manag. 71 (2013) 138–145, https://doi.org/10.1016/j.enconman.2013.03.034.
[191] I. Al-Hinti, A. Al-Ghandoor, A. Maaly, I. Abu Naqeera, Z. Al-Khateeb, O. Al-Sheikh, Experimental investigation on the use of water-phase change material storage in conventional solar water heating systems, Energy Convers. Manag. 51 (8) (2010) 1735–1740, https://doi.org/10.1016/j.enconman.2009.08.038.
[192] M.F.I. Al Imam, R.A. Beg, M.J. Haque, M.S. Rahman, Effect of novel phase change material (PCM) encapsulated design on thermal performance of solar collector, Results Mater. 18 (2023), https://doi.org/10.1016/j.rinma.2023.100388.
[193] V. Madadi Avargani, B. Norton, A. Rahimi, H. Karimi, Integrating paraffin phase change material in the storage tank of a solar water heater to maintain a consistent hot water output temperature, Sustain. Energy Technol. Assess. 47 (2021), https://doi.org/10.1016/j.seta.2021.101350.
[194] G. Raju and M. M. J. Kumar, "Experimental study on solar air heater with encapsulated phase change material on its absorber plate," Energy Storage, https://doi.org/10.1002/est2.256 vol. 3, no. 5, p. e256, 2021/10/01 2021, doi:https://doi.org/10.1002/est2.256.
[195] A. K. Singh, N. Agarwal, and A. Saxena, "Effect of extended geometry filled with and without phase change material on the thermal performance of solar air heater," J. Energy Storage, vol. 39, p. 102627, 2021/07/01/ 2021, doi:https://doi.org/10.1016/j.est.2021.102627.
[196] S. Karthikeyan, G. Ravikumar Solomon, V. Kumaresan, and R. Velraj, "Parametric studies on packed bed storage unit filled with PCM encapsulated spherical containers for low temperature solar air heating applications," Energy Convers. Manag., vol. 78, pp. 74–80, 2014/02/01/ 2014, doi:https://doi.org/10.1016/j.enconman.2013.10.042.
[197] P. Sudhakar and M. Cheralathan, "Encapsulated PCM based double pass solar air heater: a comparative experimental study," Chem. Eng. Commun., vol. 208, no. 6, pp. 788–800, 2021/06/03 2021, doi: https://doi.org/10.1080/00986445.2019.1641701.
[198] A. K. Raj, M. Srinivas, and S. Jayaraj, "A cost-effective method to improve the performance of solar air heaters using discrete macro-encapsulated PCM capsules for drying applications," Appl. Therm. Eng., vol. 146, pp. 910–920, 2019/01/05/ 2019, doi:https://doi.org/10.1016/j.applthermaleng.2018.10.055.
[199] M. Sajawal, T.-u. Rehman, H. M. Ali, U. Sajjad, A. Raza, and M. S. Bhatti, "Experimental thermal performance analysis of finned tube-phase change material based double pass solar air heater," Case Stud. Therm. Eng., vol. 15, p. 100543, 2019/11/01/ 2019, doi:https://doi.org/10.1016/j.csite.2019.100543.
[200] G. Madhulatha, M. Mohan Jagadeesh Kumar, and P. Sateesh, "Optimization of tube arrangement and phase change material for enhanced performance of solar air heater - a numerical analysis," J. Energy Storage, vol. 41, p. 102876, 2021/09/01/ 2021, doi:https://doi.org/10.1016/j.est.2021.102876.
[201] N. Arfaoui, S. Bouadila, and A. Guizani, "A highly efficient solution of off-sunshine solar air heating using two packed beds of latent storage energy," Sol. Energy, vol. 155, pp. 1243–1253, 2017/10/01/ 2017, doi:https://doi.org/10.1016/j.solener.2017.07.075.
[202] S. Bouadila, S. Kooli, M. Lazaar, S. Skouri, and A. Farhat, "Performance of a new solar air heater with packed-bed latent storage energy for nocturnal use," Appl. Energy, vol. 110, pp. 267–275, 2013/10/01/ 2013, doi:https://doi.org/10.1016/j.apenergy.2013.04.062.
[203] A. B. Shobo and A. Mawire, "Investigation of aluminum encapsulation of a PCM for domestic cooking," in 2016 International Conference on the Domestic Use of Energy (DUE), 30–31 March 2016 2016, pp. 1–6, doi: https://doi.org/10.1109/DUE.2016.7466715.
[204] A. Kumar, A. Saxena, S. D. Pandey, and A. Gupta, "Cooking performance assessment of a phase change material integrated hot box cooker," Environ. Sci. Pollut. Res., 2023/01/23 2023, doi: https://doi.org/10.1007/s11356-023-25340-x.
[205] A. Kumar, A. Saxena, S. D. Pandey, and S. K. Joshi, "Design and performance characteristics of a solar box cooker with phase change material: a feasibility study for Uttarakhand region, India," Appl. Therm. Eng., vol. 208, p. 118196, 2022/05/25/ 2022, doi:https://doi.org/10.1016/j.applthermaleng.2022.118196.

[206] R. Guédez, M. Arnaudo, M. Topel, R. Zanino, Z. Hassar, B. Laumert, Techno-economic Performance Evaluation of Direct Steam Generation Solar Tower Plants With Thermal Energy Storage Systems Based on High-Temperature Concrete and Encapsulated Phase Change Materials, 2016.
[207] H. Zhang, W. Kong, T. Tan, J. Baeyens, High-efficiency concentrated solar power plants need appropriate materials for high-temperature heat capture, conveying and storage, Energy 139 (2017) 52–64, https://doi.org/10.1016/j.energy.2017.07.129.
[208] S. Cingarapu, D. Singh, E.V. Timofeeva, M.R. Moravek, Use of encapsulated zinc particles in a eutectic chloride salt to enhance thermal energy storage capacity for concentrated solar power, Renew. Energy 80 (2015) 508–516, https://doi.org/10.1016/j.renene.2015.02.026.
[209] S.M. Flueckiger, S.V. Garimella, Latent heat augmentation of thermocline energy storage for concentrating solar power – a system-level assessment, Appl. Energy 116 (2014) 278–287, https://doi.org/10.1016/j.apenergy.2013.11.059.
[210] K. Nithyanandam, R. Pitchumani, Cost and performance analysis of concentrating solar power systems with integrated latent thermal energy storage, Energy 64 (2014) 793–810, https://doi.org/10.1016/j.energy.2013.10.095.
[211] Y. Zheng, et al., Experimental and computational study of thermal energy storage with encapsulated NaNO3 for high temperature applications, Sol. Energy 115 (2015) 180–194, https://doi.org/10.1016/j.solener.2015.02.002.
[212] C. Prieto and L. F. Cabeza, "Thermal energy storage with phase change materials in solar power plants. Economic analysis," Journal of Energy Storage, vol. 43, 2021, doi: https://doi.org/10.1016/j.est.2021.103184.
[213] B.-c. Zhao, M.-s. Cheng, C. Liu, Z.-m. Dai, Cyclic thermal characterization of a molten-salt packed-bed thermal energy storage for concentrating solar power, Appl. Energy 195 (2017) 761–773, https://doi.org/10.1016/j.apenergy.2017.03.110.
[214] B. Muñoz-Sánchez, I. Iparraguirre-Torres, V. Madina-Arrese, U. Izagirre-Etxeberria, A. Unzurrunzaga-Iturbe, A. García-Romero, Encapsulated high temperature PCM as active filler material in a thermocline-based thermal storage system, Energy Procedia 69 (2015) 937–946, https://doi.org/10.1016/j.egypro.2015.03.177.
[215] T. Mehmood, N.u.H. Shah, M. Ali, P.H. Biwole, N.A. Sheikh, Simplified mathematical model and experimental analysis of latent thermal energy storage for concentrated solar power plants, J. Energy Storage 41 (2021), https://doi.org/10.1016/j.est.2021.102871.
[216] K. Nithyanandam, R. Pitchumani, A. Mathur, Analysis of a latent thermocline storage system with encapsulated phase change materials for concentrating solar power, Appl. Energy 113 (2014) 1446–1460, https://doi.org/10.1016/j.apenergy.2013.08.053.
[217] B.-c. Zhao, M.-s. Cheng, C. Liu, Z.-m. Dai, Thermal performance and cost analysis of a multi-layered solid-PCM thermocline thermal energy storage for CSP tower plants, Appl. Energy 178 (2016) 784–799, https://doi.org/10.1016/j.apenergy.2016.06.034.
[218] S.S. Mostafavi Tehrani, Y. Shoraka, K. Nithyanandam, R.A. Taylor, Shell-and-tube or packed bed thermal energy storage systems integrated with a concentrated solar power: a techno-economic comparison of sensible and latent heat systems, Appl. Energy 238 (2019) 887–910, https://doi.org/10.1016/j.apenergy.2019.01.119.
[219] K. Bhagat, S.K. Saha, Numerical analysis of latent heat thermal energy storage using encapsulated phase change material for solar thermal power plant, Renew. Energy 95 (2016) 323–336, https://doi.org/10.1016/j.renene.2016.04.018.
[220] Y. Allouche, C. Bouden, S. Riffat, A solar-driven ejector refrigeration system for Mediterranean climate: experience improvement and new results performed, Energy Procedia 18 (2012) 1115–1124, https://doi.org/10.1016/j.egypro.2012.05.126.
[221] A. Coca-Ortegón, V. Torres-Toledo, J. Müller, A. Coronas Salcedo, Assessment of a solar powered refrigerator equipped with thermal storage for a dairy application, in: Presented at the Proceedings of SWC2017/SHC2017, 2017.
[222] N. Mansour Rezaei Fumani, F. Arabpour Roghabadi, M. Alidaei, S. M. Sadrameli, V. Ahmadi, and F. Najafi, "Prolonged lifetime of perovskite solar cells using a moisture-blocked and temperature-controlled encapsulation system comprising a phase change material as a cooling agent," ACS Omega, vol. 5, no. 13, pp. 7106–7114, Apr 7 2020, doi: https://doi.org/10.1021/acsomega.9b03407.
[223] S. Peng, et al., Solar-driven multifunctional Au/TiO2@PCM towards bio-glycerol photothermal reforming hydrogen production and thermal storage, Int. J. Hydrog. Energy 47 (98) (2022) 41573–41586, https://doi.org/10.1016/j.ijhydene.2022.03.273.
[224] D. Colarossi, P. Principi, Experimental investigation and optical visualization of a salt gradient solar pond integrated with PCM, Sol. Energy Mater. Sol. Cells 234 (2022), https://doi.org/10.1016/j.solmat.2021.111425.
[225] H. Wang, C.Y. Zhang, L.G. Zhang, Effect of steel-wires and paraffin composite phase change materials on the heat exchange and exergetic performance of salt gradient solar pond, Energy Rep. 8 (2022) 5678–5687, https://doi.org/10.1016/j.egyr.2022.04.021.
[226] H. Wang, M. Xiaomeng, Z. Liugang, X. Zhang, Y. Mei, A. Zhang, Numerical and experimental study of effect of paraffin phase change heat storage capsules on the thermal performance of the solar pond, Energy Explor. Exploit. 39 (3) (2020) 1010–1023, https://doi.org/10.1177/0144598720974160.
[227] Z. Ma, M.-J. Li, Y.-L. He, K.M. Zhang, Effects of partly-filled encapsulated phase change material on the performance enhancement of solar thermochemical reactor, J. Clean. Prod. 279 (2021), https://doi.org/10.1016/j.jclepro.2020.123169.
[228] Z. Ma, M.-J. Li, Y.-L. He, K. Max Zhang, Performance analysis and optimization of solar thermochemical reactor by diluting catalyst with encapsulated phase change material, Appl. Energy 266 (2020), https://doi.org/10.1016/j.apenergy.2020.114862.
[229] F. Meng, Q. Chu, Heat storage and release performance experiment of externally hung phase change solar greenhouse in severe cold regions of Northeast China - taking Fuxin City as an example, J. Energy Storage 58 (2023), https://doi.org/10.1016/j.est.2022.106411.
[230] G. Peng *et al.*, "Low-cost high-efficiency solar steam generator by combining thin film evaporation and heat localization: both experimental and theoretical study," Appl. Therm. Eng., vol. 143, pp. 1079–1084, 2018/10/01/ 2018, doi:https://doi.org/10.1016/j.applthermaleng.2018.08.004.
[231] X. Gu, et al., Round-the-clock interfacial solar vapor generator enabled by form-stable phase change materials with enhanced photothermal conversion capacity, Energy Convers. Manag. 277 (2023), https://doi.org/10.1016/j.enconman.2022.116634.
[232] Z. Zheng, H. Liu, D. Wu, X. Wang, Polyimide/MXene hybrid aerogel-based phase-change composites for solar-driven seawater desalination, Chem. Eng. J. 440 (2022), https://doi.org/10.1016/j.cej.2022.135862.
[233] H. Liu, D. Tian, Z. Zheng, X. Wang, Z. Qian, MXene-decorated magnetic phase-change microcapsules for solar-driven continuous seawater desalination with easy salt accumulation elimination, Chem. Eng. J. 458 (2023), https://doi.org/10.1016/j.cej.2023.141395.
[234] Q. Chen, G. Xu, P. Xia, The performance of a solar-driven spray flash evaporation desalination system enhanced by microencapsulated phase change material, Case Stud. Therm. Eng. 27 (2021), https://doi.org/10.1016/j.csite.2021.101267.
[235] M. Zhang, K. Sun, Z. Zheng, H. Liu, X. Wang, Development of MXene-decorated sodium alginate/SiO2@n-docosane hierarchical phase-change microcapsules for solar-driven sustainable seawater desalination, Desalination 550 (2023), https://doi.org/10.1016/j.desal.2023.116380.
[236] M. Tafavogh, A. Zahedi, Design and production of a novel encapsulated nano phase change materials to improve thermal efficiency of a quintuple renewable geothermal/hydro/biomass/solar/wind hybrid system, Renew. Energy 169 (2021) 358–378, https://doi.org/10.1016/j.renene.2020.12.118.
[237] K. Yu, M. Jia, Y. Yang, and Y. Liu, "A clean strategy of concrete curing in cold climate: solar thermal energy storage based on phase change material," Appl. Energy, vol. 331, p. 120375, 2023/02/01/ 2023, doi:https://doi.org/10.1016/j.apenergy.2022.120375.
[238] L. Liu *et al.*, "A foamed cement blocks with paraffin/expanded graphite composite phase change solar thermal absorption material," Sol. Energy Mater. Sol. Cells, vol. 200, p. 110038, 2019/09/15/ 2019, doi:https://doi.org/10.1016/j.solmat.2019.110038.
[239] M. Ren, Y. Liu, and X. Gao, "Incorporation of phase change material and carbon nanofibers into lightweight aggregate concrete for thermal energy regulation in buildings," Energy, vol. 197, p. 117262, 2020/04/15/ 2020, doi:https://doi.org/10.1016/j.energy.2020.117262.
[240] A.S. Abdelrazik, R. Saidur, F.A. Al-Sulaiman, Thermal regulation and performance assessment of a hybrid photovoltaic/thermal system using different combinations of nano-enhanced phase change materials, Sol. Energy Mater. Sol. Cells 215 (2020) 110645, https://doi.org/10.1016/j.solmat.2020.110645.
[241] L. O. Afolabi *et al.*, "Experimental investigation of double slope solar still integrated with PCM nanoadditives microencapsulated thermal energy storage," Desalination, vol. 553, p. 116477, 2023/05/01/ 2023, doi:https://doi.org/10.1016/j.desal.2023.116477.
[242] M. I. Shajahan, D. R. Narayana, N. S. Radha Krishnan, and J. J. Michael, "Evaluation of efficiency of double slope solar still and drinking water yield using silver nanoparticle mixed with phase change material," Energy Sources, Part A, vol. 44, no. 4, pp. 8679–8693, 2022/12/21 2022, doi: https://doi.org/10.1080/15567036.2022.2120572.
[243] S. Shoeibi, H. Kargarsharifabad, S.A.A. Mirjalily, T. Muhammad, Solar district heating with solar desalination using energy storage material for domestic hot water and drinking water – environmental and economic analysis, Sustain. Energy Technol. Assess. 49 (2022), https://doi.org/10.1016/j.seta.2021.101713.
[244] D. Ramya *et al.*, "Investigating the influence of nanoparticle disbanded phase changing material (NDPCM) on the working of solar PV," Mater. Today: Proc., vol. 56, pp. 1341–1346, 2022/01/01/ 2022, doi:https://doi.org/10.1016/j.matpr.2021.11.419.
[245] A. M. Bassam, K. Sopian, A. Ibrahim, M. F. Fauzan, A. B. Al-Aasam, and G. Y. Abusaibaa, "Experimental analysis for the photovoltaic thermal collector (PVT) with nano PCM and micro-fins tube nanofluid," Case Stud. Therm. Eng., vol. 41, p. 102579, 2023/01/01/ 2023, doi:https://doi.org/10.1016/j.csite.2022.102579.
[246] M. L. Rinawa *et al.*, "Analyzing an evacuated tube solar water heating system using twin-nano/paraffin as phase change material," Mater. Today: Proc., vol. 50, pp. 2505–2509, 2022/01/01/ 2022, doi:https://doi.org/10.1016/j.matpr.2021.10.500.
[247] P.M. Kumar, K. Mylsamy, A comprehensive study on thermal storage characteristics of nano-CeO2 embedded phase change material and its influence on the performance of evacuated tube solar water heater, Renew. Energy 162 (2020) 662–676, https://doi.org/10.1016/j.renene.2020.08.122.
[248] M. H. Dhaou, S. Mellouli, F. Alresheedi, and Y. El-Ghoul, "Experimental assessment of a solar water tank integrated with nano-enhanced PCM and a stirrer," Alex. Eng. J., vol. 61, no. 10, pp. 8113–8122, 2022/10/01/ 2022, doi:https://doi.org/10.1016/j.aej.2022.01.040.
[249] B. S. K. Subramaniam, A. K. Sugumaran, and M. M. Athikesavan, "Performance analysis of a solar dryer integrated with thermal energy storage using PCM-Al2O3 nanofluids," Environ. Sci. Pollut. Res., vol. 29, no. 33, pp. 50617–50631, 2022/07/01 2022, doi: https://doi.org/10.1007/s11356-022-19170-6.

[250] R.P. Singh, H. Xu, S.C. Kaushik, D. Rakshit, A. Romagnoli, Charging performance evaluation of finned conical thermal storage system encapsulated with nano-enhanced phase change material, Appl. Therm. Eng. 151 (2019) 176–190, https://doi.org/10.1016/j.applthermaleng.2019.01.072.

[251] P. Sarathkumar, A. R. Sivaram, R. Rajavel, R. Praveen Kumar, and S. K. Krishnakumar, "Experimental investigations on the performance of a solar pond by using encapsulated Pcm with nanoparticles," Materials Today: Proceedings, vol. 4, no. 2, Part A, pp. 2314–2322, 2017/01/01/ 2017, doi:https://doi.org/10.1016/j.matpr.2017.02.080.

[252] D. Dsilva Winfred Rufuss, L. Suganthi, S. Iniyan, P.A. Davies, Effects of nanoparticle-enhanced phase change material (NPCM) on solar still productivity, J. Clean. Prod. 192 (2018) 9–29, https://doi.org/10.1016/j.jclepro.2018.04.201.

[253] S. Nazari, M. Najafzadeh, R. Daghigh, Techno-economic estimation of a non-cover box solar still with thermoelectric and antiseptic nanofluid using machine learning models, Appl. Therm. Eng. 212 (2022), https://doi.org/10.1016/j.applthermaleng.2022.118584.

[254] S. Rastegar, H. Kargarsharifabad, N. Rahbar, M.B. Shafii, Distilled water production with combination of solar still and thermosyphon heat pipe heat exchanger coupled with indirect water bath heater – experimental study and thermoeconomic analysis, Appl. Therm. Eng. 176 (2020) 115437, https://doi.org/10.1016/j.applthermaleng.2020.115437.

[255] S.W. Sharshir, M.A. Eltawil, A.M. Algazzar, R. Sathyamurthy, A.W. Kandeal, Performance enhancement of stepped double slope solar still by using nanoparticles and linen wicks: energy, exergy and economic analysis, Appl. Therm. Eng. 174 (2020) 115278, https://doi.org/10.1016/j.applthermaleng.2020.115278.

[256] H. Panchal *et al.*, "Performance evaluation of using evacuated tubes solar collector, perforated fins, and pebbles in a solar still - experimental study and CO2 mitigation analysis," Environ. Sci. Pollut. Res. Int., Sep 13 2022, doi: https://doi.org/10.1007/s11356-022-22809-z.

[257] N. Rahbar, A. Asadi, E. Fotouhi-Bafghi, Performance evaluation of two solar stills of different geometries: tubular versus triangular: experimental study, numerical simulation, and second law analysis, Desalination 443 (2018) 44–55, https://doi.org/10.1016/j.desal.2018.05.015.

[258] A. Malvika, U. C. Arunachala, and K. Varun, "Sustainable passive cooling strategy for photovoltaic module using burlap fabric-gravity assisted flow: a comparative energy, exergy, economic, and enviroeconomic analysis," Appl. Energy, vol. 326, p. 120036, 2022/11/15/ 2022, doi:https://doi.org/10.1016/j.apenergy.2022.120036.

[259] M. E.A.E. Ahmed, S. Abdo, M. A. Abdelrahman, and O. A. Gaheen, "Finned-encapsulated PCM pyramid solar still – experimental study with economic analysis," J. Energy Storage, vol. 73, p. 108908, 2023/12/01/ 2023, doi:https://doi.org/10.1016/j.est.2023.108908.

[260] V. V. Tyagi, A. K. Pandey, D. Buddhi, and R. Kothari, "Thermal performance assessment of encapsulated PCM based thermal management system to reduce peak energy demand in buildings," Energy Build., vol. 117, pp. 44–52, 2016/04/01/ 2016, doi:https://doi.org/10.1016/j.enbuild.2016.01.042.

[261] K. Faraj, M. Khaled, J. Faraj, F. Hachem, K. Chahine, and C. Castelain, "Energetic and economic analyses of integrating enhanced macro-encapsulated PCM's with active underfloor hydronic heating system," Energy Rep., vol. 8, pp. 848–862, 2022/11/01/ 2022, doi:https://doi.org/10.1016/j.egyr.2022.07.099.

[262] "Techno-Economic Analysis of Phase Change Material Thermal Energy Storage Systems in High Temperature Concentrated Solar Power Plants," 2014.

[263] K. P. Bhandari, J. M. Collier, R. J. Ellingson, and D. S. Apul, "Energy payback time (EPBT) and energy return on energy invested (EROI) of solar photovoltaic systems: a systematic review and meta-analysis," Renew. Sust. Energ. Rev., vol. 47, pp. 133–141, 2015/07/01/ 2015, doi:https://doi.org/10.1016/j.rser.2015.02.057.

[264] O. Ozcan and F. Ersoz, "Project and cost-based evaluation of solar energy performance in three different geographical regions of Turkey: investment analysis application," Eng. Sci. Technol. Int. J., vol. 22, no. 4, pp. 1098–1106, 2019/08/01/ 2019, doi:https://doi.org/10.1016/j.jestch.2019.04.001.

[265] P. Llorach-Massana, J. Peña, J. Rieradevall, and J. I. Montero, "Analysis of the technical, environmental and economic potential of phase change materials (PCM) for root zone heating in Mediterranean greenhouses," Renew. Energy, vol. 103, pp. 570–581, 2017/04/01/ 2017, doi:https://doi.org/10.1016/j.renene.2016.11.040.

[266] C. Cárdenas-Ramírez, F. Jaramillo, and M. Gómez, "Systematic review of encapsulation and shape-stabilization of phase change materials," J. Energy Storage, vol. 30, p. 101495, 2020/08/01/ 2020, doi:https://doi.org/10.1016/j.est.2020.101495.

[267] P. B. Salunkhe and P. S. Shembekar, "A review on effect of phase change material encapsulation on the thermal performance of a system," Renew. Sust. Energ. Rev., vol. 16, no. 8, pp. 5603–5616, 2012/10/01/ 2012, doi:https://doi.org/10.1016/j.rser.2012.05.037.

[268] A. Shahsavar, P. Talebizadehsardari, and M. Arıcı, "Comparative energy, exergy, environmental, exergoeconomic, and enviroeconomic analysis of building integrated photovoltaic/thermal, earth-air heat exchanger, and hybrid systems," J. Clean. Prod., vol. 362, p. 132510, 2022/08/15/ 2022, doi:https://doi.org/10.1016/j.jclepro.2022.132510.

[269] M.S. Yousef, H. Hassan, H. Sekiguchi, Energy, exergy, economic and enviroeconomic (4E) analyses of solar distillation system using different absorbing materials, Appl. Therm. Eng. 150 (2019) 30–41, https://doi.org/10.1016/j.applthermaleng.2019.01.005.

[270] T. Rajaseenivasan and K. Srithar, "Performance investigation on solar still with circular and square fins in basin with CO2 mitigation and economic analysis," Desalination, vol. 380, pp. 66–74, 2016/02/15/ 2016, doi:https://doi.org/10.1016/j.desal.2015.11.025.

[271] A. R. A. Elbar, M. S. Yousef, and H. Hassan, "Energy, exergy, exergoeconomic and enviroeconomic (4E) evaluation of a new integration of solar still with photovoltaic panel," J. Clean. Prod., vol. 233, pp. 665–680, 2019/10/01/ 2019, doi:https://doi.org/10.1016/j.jclepro.2019.06.111.

[272] M. S. Yousef, M. Sharaf, and A. S. Huzayyin, "Energy, exergy, economic, and enviroeconomic assessment of a photovoltaic module incorporated with a paraffin-metal foam composite: an experimental study," Energy, vol. 238, p. 121807, 2022/01/01/ 2022, doi:https://doi.org/10.1016/j.energy.2021.121807.

[273] S. Saadon, L. Gaillard, C. Menezo, and S. Giroux-Julien, "Exergy, exergoeconomic and enviroeconomic analysis of a building integrated semi-transparent photovoltaic/thermal (BISTPV/T) by natural ventilation," Renew. Energy, vol. 150, pp. 981–989, 2020/05/01/ 2020, doi:https://doi.org/10.1016/j.renene.2019.11.122.

[274] A.R. Abd Elbar, H. Hassan, Energy, exergy and environmental assessment of solar still with solar panel enhanced by porous material and saline water preheating, J. Clean. Prod. 277 (2020) 124175, https://doi.org/10.1016/j.jclepro.2020.124175.

[275] P. Azari, A. Mirabdolah Lavasani, N. Rahbar, and M. Eftekhari Yazdi, "Performance enhancement of a solar still using a V-groove solar air collector—experimental study with energy, exergy, enviroeconomic, and exergoeconomic analysis," Environ. Sci. Pollut. Res., 2021/07/28 2021, doi: https://doi.org/10.1007/s11356-021-15290-7.

[276] C. Hernández Moris, C. Felbol, M. T. Cerda, and M. Ibarra, "Theoretical technical–economic comparison of hybrid energy for gas and solar concentration plants in the region of Antofagasta Chile," Sustain. Energy Technol. Assess., vol. 55, p. 102979, 2023/02/01/ 2023, doi:https://doi.org/10.1016/j.seta.2022.102979.

[277] A. Boubault, C. K. Ho, A. Hall, T. N. Lambert, and A. Ambrosini, "Levelized cost of energy (LCOE) metric to characterize solar absorber coatings for the CSP industry," Renew. Energy, vol. 85, pp. 472–483, 2016/01/01/ 2016, doi:https://doi.org/10.1016/j.renene.2015.06.059.

[278] C. Parrado, A. Girard, F. Simon, and E. Fuentealba, "2050 LCOE (Levelized Cost of Energy) projection for a hybrid PV (photovoltaic)-CSP (concentrated solar power) plant in the Atacama Desert, Chile," Energy, vol. 94, pp. 422–430, 2016/01/01/ 2016, doi:https://doi.org/10.1016/j.energy.2015.11.015.

[279] F. Fuso Nerini, et al., Connecting climate action with other Sustainable Development Goals, Nat. Sustain. 2 (8) (2019) 674–680, https://doi.org/10.1038/s41893-019-0334-y.

[280] G.G. Singh, et al., A rapid assessment of co-benefits and trade-offs among Sustainable Development Goals, Mar. Policy 93 (2018) 223–231, https://doi.org/10.1016/j.marpol.2017.05.030.

[281] E.B. Barbier, J.C. Burgess, Sustainable development goal indicators: analyzing trade-offs and complementarities, World Dev. 122 (2019) 295–305, https://doi.org/10.1016/j.worlddev.2019.05.026.

[282] L.M. Fonseca, J.P. Domingues, A.M. Dima, Mapping the sustainable development goals relationships, Sustainability 12 (8) (2020), https://doi.org/10.3390/su12083359.

[283] F. Fuso Nerini, et al., Mapping synergies and trade-offs between energy and the Sustainable Development Goals, Nat. Energy 3 (1) (2017) 10–15, https://doi.org/10.1038/s41560-017-0036-5.

[284] A. Amo-Aidoo, E.N. Kumi, O. Hensel, J.K. Korese, B. Sturm, Solar energy policy implementation in Ghana: a LEAP model analysis, Sci. Afr. 16 (2022), https://doi.org/10.1016/j.sciaf.2022.e01162.

[285] R. Ferguson, W. Wilkinson, and R. Hill, "Electricity use and economic development," Energy Policy, vol. 28, no. 13, pp. 923–934, 2000/11/01/ 2000, doi:https://doi.org/10.1016/S0301-4215(00)00081-1.

[286] N. J. Ashbolt, "Microbial contamination of drinking water and disease outcomes in developing regions," Toxicology, vol. 198, no. 1–3, pp. 229–38, May 20 2004, doi: https://doi.org/10.1016/j.tox.2004.01.030.

[287] P. R. Hunter, D. Zmirou-Navier, and P. Hartemann, "Estimating the impact on health of poor reliability of drinking water interventions in developing countries," Sci. Total Environ., vol. 407, no. 8, pp. 2621–4, Apr 1 2009, doi: https://doi.org/10.1016/j.scitotenv.2009.01.018.

[288] H. Yang, R. Bain, J. Bartram, S. Gundry, S. Pedley, and J. Wright, "Water safety and inequality in access to drinking-water between rich and poor households," Environ. Sci. Technol., vol. 47, no. 3, pp. 1222–30, Feb 5 2013, doi: https://doi.org/10.1021/es303345p.

[289] H.R.a.M. Roser, Clean Water and Sanitation, Our World in Data, 2021.